VESIAC State-of-the-Art Report

THE GENERATION OF THE PRIMARY SEISMIC SIGNAL BY A CONTAINED EXPLOSION

CARL KISSLINGER

ACOUSTICS AND SEISMICS LABORATORY
Institute of Science and Technology
THE UNIVERSITY OF MICHIGAN

April 1963

Contract SD-78

4410-48-X

VESIAC State-of-the-Art Report

THE GENERATION OF THE PRIMARY SEISMIC SIGNAL BY A CONTAINED EXPLOSION

CARL KISSLINGER

Professor
St. Louis University

April 1963

Acoustics and Seismics Laboratory
Institute of Science and Technology
THE UNIVERSITY OF MICHIGAN
Ann Arbor, Michigan

NOTICES

Sponsorship. The work reported herein was conducted by the Institute of Science and Technology for the U. S. Department of Defense under Project SD-78. Contracts and grants to The University of Michigan for the support of sponsored research by the Institute of Science and Technology are administered through the Office of the Vice-President for Research.

ASTIA Availability. Qualified requesters may obtain copies of this document from:

Armed Services Technical Information Agency
Arlington Hall Station
Arlington 12, Virginia

Final Disposition. After this document has served its purpose, it may be destroyed. Please do not return it to the Institute of Science and Technology.

PREFACE

This review is an attempt to summarize the present state of knowledge of the process by which a seismic wave is generated by an underground explosion. An attempt has been made to start with the highly compressed volume of gas formed at the completion of detonation and proceed step by step to the seismic signal. Research investigators in this field will recognize immediately that there are gaps in our knowledge about critical parts of this process that must be bridged by reasonable assumptions about material behavior.

The author is a seismologist, and this report is directed primarily to other seismologists. For this reason, experts in shock-wave physics may find that the sections on the highly stressed region around the explosion contain too much detailed discussion of fundamental principles, without a corresponding coverage in the sections on elastic waves.

The author wishes to acknowledge with gratitude the invaluable assistance given him in the preparation of this report by the staff of VESIAC, Institute of Science and Technology, The University of Michigan. In particular, Mr. Thomas Caless, Mr. Robert Haven, and Mrs. Elaine Medor have provided services without which the completion of this work would have been very difficult.

Finally, the author wishes to express his gratitude to his colleague, Prof. Otto W. Nuttli, Department of Geophysics and Geophysical Engineering, St. Louis University, who read the manuscript during its preparation and offered many helpful suggestions.

CONTENTS

FIGURES

THE GENERATION OF THE PRIMARY SEISMIC SIGNAL BY A CONTAINED EXPLOSION

ABSTRACT

In order to analyze the mechanism by which buried explosions generate seismic waves, the region around the detonation is divided into three zones: (1) a strong-shock (hydrodynamic) zone, (2) a transitional, nonlinear zone, and (3) the elastic region. Experimental equation-of-state data are used in calculating the history of the propagating stress wave, because there is as yet no complete theory of the response of solids to rapidly applied stresses which exceed their yield and crushing strengths. Results indicate that the proper equations of motion are known, as are analytic and numerical methods for solving them. The theory of shock waves in a fluid is applicable to the close-in region, and several failure mechanisms have been postulated for the transition region.

The objective of the analysis is the determination of the stress waveform at the inner boundary of elastic behavior. The peak amplitude and spectral content depend on the yield, the type of medium, and the ambient stress (depth of burial). The experimental determination of the shortest range at which elastic behavior begins is difficult in principle, because solutions valid at great distances are not applicable.

Experimental determinations of the amplitude-yield relationship must take into account (1) the combined effect of the shift of the spectral peak to lower frequencies as the yield increases and (2) the low-pass filtering properties of the earth. Empirical studies of the effect of the shot-point medium are influenced by the properties of the explosive material. The effect of source depth is difficult to isolate because in most test sites the medium changes with depth.

1 INTRODUCTION

> Of the three physical processes involved in seismic exploration, namely the initiation of the seismic waves, their propagation, reflection, refraction, and dispersion, and the recording of some function of the motion of the surface, we possess the least satisfactory understanding of the initiation process.
>
> J. A. Sharpe, 1942

An assumption underlies the entire research program on the identification of underground nuclear explosions by the seismic signal recorded at suitably placed stations; that is, such explosions represent sources having unique properties which are adequate to distinguish them from

all other seismic sources. The discovery of these properties will permit the establishment of criteria for deciding that a particular seismogram or set of seismograms could have been produced only by an explosion.

The theory of wave propagation in the earth has progressed to the point where it would be possible to compute the seismogram resulting from an input of known form at the source, given the detailed properties of the geologic structure between a seismic source and observing point, and the response characteristics of the seismograph. Theoretical seismograms for simplified structures are being computed for a number of applications. Of course, not enough is known of the constitution of the crust or mantle to make this possible at present, but ambitious research efforts now in progress promise to yield the required data eventually.

An excellent example of current ability to derive a particular wave on the seismogram from a detonation of known yield is offered by the computation of P_n arrivals for three nuclear explosions by Werth et al. [1]. Their methods and results indicate both the potential of the analytic tools available and the severe limitations of the data available to perform the computations.

The progress that has been made in the computation of theoretical seismograms makes the question of the properties of the source a pressing one, for we are asking, "What should be the input to our computation?"

All efforts to answer this question have begun by surrounding the source with a sphere with a radius large enough that all processes outside of this sphere can be described by infinitesimal strain theory, either elastic or allowing for frictional losses. Then the question becomes one of the proper loading (or set of stresses) to distribute over this surface to represent the output of the explosion in the form of seismic energy.

This report will summarize present knowledge of the seismic loading from a contained explosion. Of particular interest are the effects on the resulting signal of the yield of the explosive device, the medium in which it is buried, and the depth below the earth's surface. Because small- and large-scale geologic factors, which are not an intrinsic part of the wave-generating process, influence the character of the signal profoundly even at moderate distances, only the close-in effects will be considered—that is, effects at the shortest ranges at which the signal is carried by elastic waves. For example, Adams et al. [2] have found (at the Nevada Test Site) that inhomogeneities in the medium seriously disturb measurements of ground motion at scaled ranges beyond 800 to 1000 feet.[1]

[1] Scaled range = range/[W(kilotons)]$^{1/3}$; see the appendix for discussion of scaling.

A great deal of important work on close-in effects of explosive sources has been done by researchers who are interested primarily in weapons effects and protective construction. For obvious reasons, much of this work has dealt with surface or air bursts. Because the loading due to the intense air blast constitutes an important part of the source mechanism for these shots, the results of this work will not be considered here. Only contained explosions are of interest here, and throughout this paper the term "explosion" will be synonymous with "contained explosion" unless otherwise indicated. Minor venting often occurs when buried explosions are detonated; an explosion will be considered contained as long as the associated air blast has a negligible effect on ground motion. Any treatment of viscous or other losses in the seismic waves during propagation is also outside the scope of this report. There are important, as representing a significant effect of the medium through which the signal travels. This discussion, however, will concern only those loss mechanisms which represent an effect of the medium in which the explosion occurs.

Until very recently, most of the work on the factors affecting the seismic output of an explosion was done by persons who were interested in the use of explosives as controlled energy sources: exploration seismologists, seismologists working with quarry- and mine-blast operations, and, to a lesser extent, demolition experts.

Seismic exploration detonation conditions pertain more closely to the underground nuclear test identification and detection problem than do quarry blasts. Even though the size of a large quarry or construction blast is somewhat closer to the scale of a nuclear explosion, the fact that the shot is always near a free face and is designed to move rock means that a quarry shot is never contained. This fact significantly alters the seismic output. Furthermore, large commercial blasts are always distributed in space and time through the delayed firing of a number of holes. For these reasons, the results of theoretical and experimental research carried out in connection with the use of explosives in exploration are of more value for this study than those based on observations of quarry blasts. However, some excellent basic work on the mechanism of rock breakage, especially that carried out by the U. S. Bureau of Mines, bears directly on the subject of this report.

Because of the differences between chemical and nuclear detonations, research based on the study of high explosives alone cannot possibly solve this problem. Consequently, only very recent or in-progress research (theoretical and experimental) on nuclear sources will aid in elucidating the wave-generating processes. Most of the important information on the behavior of earth materials in the highly stressed region around the explosion is still to be gathered. As this report was being written, an extensive series of underground explosions is in progress under the sponsorship of the U. S. Atomic Energy Commission; it is very likely that analysis of data from these

experiments will provide numerical values to be used in the theoretical results outlined here, at least for the selected materials at the test sites.

2
THE MODEL OF AN EXPLOSION AS A SEISMIC SOURCE

If it were possible to surround an explosion with a surface of known shape on which the complete stress history at each point was known as a function of the parameters describing the explosion (yield, type of explosive, medium around the charge, depth of burial), and if this surface were so chosen that only elastic processes took place outside of it, the differential equations describing elastic wave propagation could be integrated to give the ground motion at any point in the neighborhood outside this source region.

The theory of wave generation by explosions has advanced through a succession of efforts to get an increasingly accurate picture of the loading function. The earliest efforts [3, 4, 5] simply ignored the complex processes inside the hypothetical surface, and proceeded from an intelligent conjecture of the nature of the loading. This approach made it impossible to relate actual amplitudes and waveforms of ground motion, stress, or strain to the yield, but made possible a qualitative picture of the manner in which the explosion parameters affect the results to be obtained.

The next stage was to discuss qualitatively the effects of the nonlinear, irreversible region [6, 7, 8, 9]. Some early studies have been followed up by the present concerted efforts to treat in detail the processes occurring in the highly stressed region. Authorities generally agree on how to handle the "strong" shock zone immediately around a nuclear detonation; and, as mentioned above, there is no serious problem in the elastic zone. It is true that loss mechanisms at infinitesimal strains must be taken into account if the seismic waveform is to be accurately predicted [10]. The greatest uncertainty lies in the transition zone, where stresses are falling to the neighborhood of the crushing strength and then the yield strength of the medium. However, as pointed out by Fugelso [11, p. 1], the unknown factors in the identification of a seismic event as a blast lie in this region. The various approaches outlined in this report can almost be categorized by the number of subregions into which this zone of transition is divided.

Cushing and Reily [12] suggest a useful coarse division of the zones around the shot. They refer to the close-in nonlinear region, in which shock pressure far exceeds the crushing strength and shear stresses are negligible compared to compressive stresses, and to the terminal nonlinear region, in which the shock pressures are at or above the elastic limit of the medium, and are generally comparable to the medium's crushing stress, and in which the shear strength must be considered. It is possible and desirable to define the limits of these regions quantitatively, and to further subdivide the terminal nonlinear region [13].

This report will present the theory of wave generation, starting from the immediate neighborhood of the explosion and proceeding outward. The main features of the close-in nonlinear region will be discussed first. Then the various viewpoints on the transition region will be reviewed, and finally the character of the seismic signal at the beginning of elastic-wave propagation will be described. Present knowledge of the waveform (time history) or spectrum (frequency content) of the input seismic signal will be summarized. The report will also review field data from chemical and nuclear explosions, and will present the various empirical scaling rules that have been developed, compared with the theoretical results.

The physics of the explosion itself will not be discussed. Detailed discussion of the detonation process for chemical explosions may be found in Cole [14], Cook [15], and Jones and Miller [16]. It will be assumed that the detonation results in an initial spherically symmetric intense shock front. Evidence of departures from symmetry of the seismic signal from an explosion will be discussed in Section 6.4.

3
SHOCK WAVE PROPAGATION AND THE HUGONIOT EQUATION OF STATE

3.1. THE RANKINE-HUGONIOT EQUATIONS

Stresses in the immediate vicinity of the explosion reach levels of hundreds of kilobars or megabars, and exceed the strength of any earth material enough that the rigidity is completely negligible and the phenomena may be described by treating the medium as a perfect fluid. Studies that attempt to work in detail from the explosion outward treat the shock wave as propagating in a fluid. The phenomena in this case are governed by the Rankine-Hugoniot equations for a shock wave in a fluid. These equations will be reviewed here because they are basic to much that follows. More detailed treatments of these relations may be found in works devoted to the present problem [13, 18, 20].

The Rankine-Hugoniot relationships are derived from the principles of conservation of mass, momentum, and energy across a steep front at which pressure, density, and particle velocity are discontinuous. If the shock front is advancing with a speed U into an undisturbed region of fluid in which the density is ρ_o and the ambient pressure p_o, conservation of mass across the front requires that the particle velocity u and the density ρ_s immediately behind the front satisfy the equation $\rho_s(U - u) = \rho_o U$, which may be written as

$$\frac{u}{U} = 1 - \frac{\rho_o}{\rho_s} = 1 - \frac{v_s}{v_o} \qquad (1)$$

where $v = 1/\rho$ is the specific volume.

Conservation of momentum is used to relate the pressure jump across the front to the other parameters: $p_s - p_o = \rho_o U^2 - \rho_s (U - u)^2$. If ρ_s is eliminated by using Equation 1 and calling the overpressure $p_s - p_o = p$, then

$$p = \rho_o U u \tag{2}$$

Conservation of energy requires that the work done by the pressures at the front equals the change in the total energy of the fluid. Referred to a unit mass where I_o represents the initial internal energy and $I_s - I_o$ the change at the front, the total change in energy per unit mass (internal and kinetic), assuming an adiabatic process, is $(I_s - I_o) + \frac{1}{2}\left[(U - u)^2 - U^2\right]$. Equating this to work per unit mass, $\frac{p_o U - p_s (U - u)}{\rho_o U}$, yields $\frac{p_o}{\rho_o} + I_o + \frac{1}{2}U^2 = \frac{p_s}{\rho_s} + I_s + \frac{1}{2}(U - u)^2$. This can be rewritten, using Equation 2:

$$(I_s - I_o) + \frac{1}{2}u^2 = \frac{p_s}{\rho_o}\frac{u}{U} \tag{3}$$

$$= p_s\left(\frac{1}{\rho_o} - \frac{1}{\rho_s}\right) = p_s (v_o - v_s) \tag{3a}$$

These three basic relations can be combined in various ways to obtain the desired shock parameters in terms of those that are more easily measured. The velocity of shock propagation and the particle velocity in terms of pressure and specific volume are found from Equations 1 and 2:

$$U^2 = \frac{p_s - p_o}{v_o - v_s} v_o^2 \tag{4}$$

$$u^2 = (p_s - p_o)(v_o - v_s) \tag{5}$$

From Equations 5 and 3a, the change in internal energy is

$$(I_s - I_o) = \frac{1}{2}(p_s + p_o)(v_o - v_s) \tag{6}$$

Equation 6 is called the Hugoniot equation of the fluid [17]. It is the locus of all final states p_s, v_s that can be attained from an initial state p_o, v_o by passing a shock through the fluid.

The significance of the various expressions derived above can be visualized through the pressure-volume diagram in Figure 1 (see Reference 13, Figure 4.1, Reference 18, Figure 1, and Reference 19, Figure 3.3). From Equation 3a, the total energy per unit mass behind the shock is $p_s (v_o - v_s)$, the area of the rectangle bounded by $p = p_s$, $v = v_o$, and $v = v_s$. From

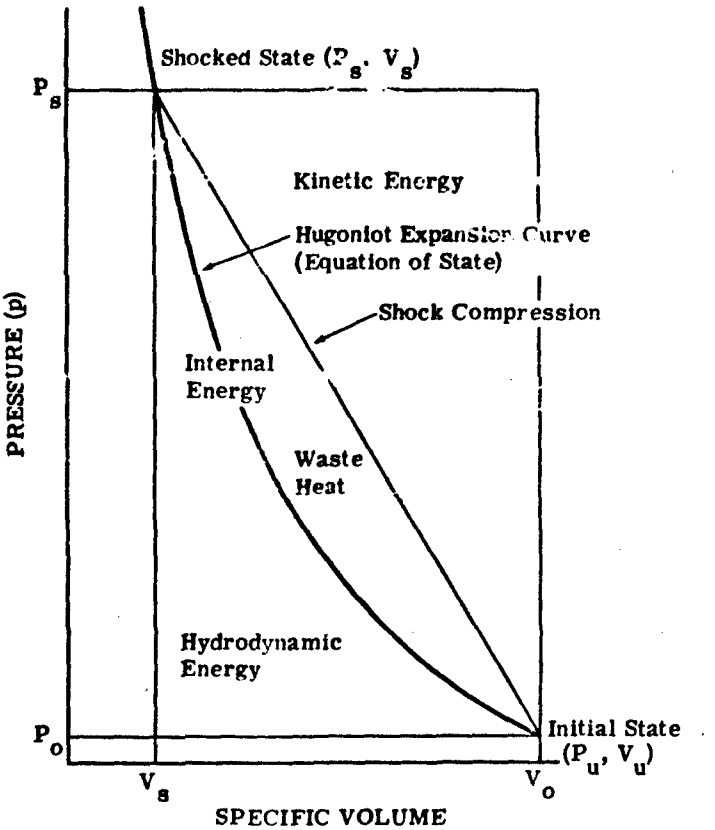

FIGURE 1. ENERGY RELATIONS ON THE GRAPH OF THE EQUATION OF STATE (After Bishop, Chaszeyka, and Porzel)

Equation 5, the kinetic energy per unit mass is $\frac{1}{2}(p_s - p_o)(v_o - v_s)$, the area of the triangle above the line of shock compression. From Equation 6, the area of the trapezoid $\frac{1}{2}(p_o + p_s)(v_o - v_s)$ represents the internal energy. The area under the expansion curve back to the initial state represents $\int p\,dv$ work, and is available as potential or hydrodynamic energy which is given up during expansion. The area between the compression line and the expansion curve represents energy lost from the shock by the increase in entropy across the steep shock front. Because it is no longer available to support the propagation of the shock, this energy has been called waste heat. It appears as a final rise in the temperature of the medium [19]. Heat conduction occurs so slowly that the deposition of waste heat is permanent as far as the shock wave is concerned. For solids, and less exactly for fluids, the coefficient of thermal expansion is small enough that the final volume is close to v_o [13]. The equation of state or Hugoniot curve is, of course, a property of the material and at present is based on empirical values of p vs v.

3.2. THE VARIATION OF U WITH p

A useful property of shock wave propagation can be derived from Equation 4 by differentiating with respect to p_s:

$$\frac{dU}{dp_s} = \frac{v_o}{2} \frac{1 + \left(\frac{p_s - p_o}{v_o - v_s}\right)\frac{1}{\frac{dp_s}{dv_s}}}{(v_o - v_s)^{1/2}(p_s - p_o)^{1/2}}$$

The quantity $\frac{dp_s}{dv_s}$ is obtained from the Hugoniot equation of state for the medium and is a function of v_s. The shock velocity U will increase with increasing pressure as long as

$$\frac{p_s - p_o}{v_o - v_s} < -\frac{dp_s}{dv_s} \tag{7}$$

For all materials, both sides of the inequality as written are positive (pressure decreases with increasing specific volume), and the inequality is satisfied if the line joining the shocked state to the initial state makes a smaller angle with the negative v-axis than does the tangent to the equation of state at the point (p_s, v_s). As shown by Rice et al. [17] and discussed by Cushing and Reilly [12], if the equation of state has a cusp (as it will in any solid with a non-zero yield stress), and a somewhat greater crushing stress, there will be a region in which shock velocity increases with decreasing pressure, and in place of a stable single shock front, a two-wave structure forms. This will occur when the shock-front pressure has decayed to the neighborhood of the crushing stress of the medium in the terminal nonlinear region. The shock front velocity can become less than the velocity of the elastic compressional wave, so that an elastic precursor runs ahead of the shock front.

3.3. INTRODUCTION OF ADIABATIC LAW [13, 20]

The internal energy can be eliminated from the equation of state (Equation 6) by introducing the law for adiabatic expansion of an ideal gas. The change in internal energy of the system in going from an initial to a final state is $I_f - I_i = \int_{v_i}^{v_f} p\,dv$, where the integration is taken along an adiabat, $pv^\gamma = \text{const.}$; γ = ratio of specific heats. Integrating,

$$I_f - I_i = \frac{p_f v_f - p_i v_i}{\gamma - 1} \tag{7a}$$

Bishop takes the value of $I_s - I_o$ for the adiabat connecting the ambient and shocked states and equates it, as an approximation, to the right hand side of Equation 6, obtaining

$$(\gamma_s - 1)^{-1} (p_s v_s - p_o v_o) \simeq \frac{1}{2} (p_s + p_o)(v_o - v_s) \tag{8}$$

He shows that this approximation holds for strong shocks in which $p_s >> p_o$ by obtaining for this case $\frac{\rho_s}{\rho_o} = \frac{\gamma_s + 1}{\gamma_s - 1}$, a result given by Taylor [21]. He also shows that Equation 8 is valid for very low pressures (acoustic case), by demonstrating that $\gamma_s = -\frac{v_o}{p_o}\frac{\Delta p}{\Delta v}$, which is the differential form of the equation of the adiabat.

Therefore, there is justification for proceeding to use an "effective-average" adiabatic exponent, γ_s, in any "hydrodynamic" medium. Other authors have proceeded to use this γ without explicitly examining the approximation involved in Equation 8. By replacing γ_s, the exponent at p_s, with γ, a value for states in the neighborhood of p_s, and using the Rankine-Hugoniot relations, several results given by Taylor are readily obtained.

First, from Equation 8,

$$\frac{\rho_s}{\rho_o} = \frac{(\gamma - 1) + (\gamma + 1)\frac{p_s}{p_o}}{(\gamma + 1) + (\gamma - 1)\frac{p_s}{p_o}} \tag{9}$$

Introducing $c_o^2 = \frac{\gamma p_o}{\rho_o}$ (the acoustic velocity in the undisturbed medium) and Equation 9 into Equations 4 and 5 gives

$$\frac{U^2}{c_o^2} = \frac{1}{2\gamma}\left[\gamma - 1 + (\gamma + 1)\frac{p_s}{p_o}\right] \tag{10}$$

$$\frac{u_s}{U} = \frac{2\left(\frac{p_s}{p_o} - 1\right)}{\gamma - 1 + (\gamma + 1)\frac{p_s}{p_o}} \tag{11}$$

Bishop considers a medium to be in a "hydrodynamic" state if γ is a slowly varying function of pressure.

A shock is considered "strong" if p_s is sufficiently greater than p_o so that Equations 9 through 11 take the form [21]:

$$\frac{\rho_s}{\rho_o} = \frac{\gamma + 1}{\gamma - 1} \tag{9a}$$

$$\frac{U^2}{c_o^2} = \frac{\gamma + 1}{2\gamma} \frac{p_s}{p_o} \tag{10a}$$

$$\frac{u_s}{U} = \frac{2}{\gamma + 1} \tag{11a}$$

A very useful form of the equation of state is obtained by introducing $v_h = v_o - v_s$ (the change in specific volume) and $p = p_s - p_o$ (the overpressure) into Equation 9.

Then $\frac{\rho_s}{\rho_o} = \left(1 - \frac{v_h}{v_o}\right)^{-1}$, and Equation 9 becomes

$$\frac{v_h}{v_o} = \frac{2\left(\frac{p_s}{p_o} - 1\right)}{(\gamma - 1) + (\gamma + 1)\frac{p_s}{p_o}} = \frac{2\left(\frac{p_s}{p_o} - 1\right)}{2\gamma + (\gamma + 1)\frac{p_s - 1}{p_o}}$$

$$= \frac{2\frac{p}{p_o}}{2\gamma + (\gamma + 1)\frac{p}{p_o}}$$

or

$$\frac{v_o}{v_h} = \frac{\gamma + 1}{2} + \frac{\gamma p_o}{p} \tag{12}$$

Bishop interprets γp_o as the adiabatic elastic modulus for a condensed medium, where γ is at the ambient state. If c_o is the ambient compressional wave velocity, then $\frac{\gamma p_o}{\rho_o} = c_o^2$, so that $\gamma p_o = \rho_o c_o^2 = K_o$, an elastic modulus. Therefore, Equation 12 becomes

$$\frac{v_o}{v_h} = \frac{1}{2}(\gamma + 1) + \frac{K_o}{p} \tag{13}$$

Dividing through by $\frac{K_o}{p}$, $$\frac{p/K_o}{v_h/v_o} = 1 + 1/2\ (\gamma + 1)\left(\frac{p}{K_o}\right) \tag{14}$$

If the overpressure p is small compared to the elastic constant K_o, v_h is small, and Equation 13 becomes

$$\frac{p/K_o}{v_h/v_o} = 1, \text{ or } K_o = \frac{p}{v_h/v_o} = \frac{p}{-\Delta v/v}$$

This merely confirms the interpretation of K_o as an elastic modulus, i.e., the ratio of small stress to small strain. Then, for large stresses,

$$\frac{p}{v_h/v_o} = K_o\ (1 + x) = K_s \tag{15}$$

where

$$x = 1/2\ (\gamma + 1)\frac{p}{K_o} = (K_s/K_o)^{-1} \tag{16}$$

and K_s is the elastic modulus for finite strains. The quantity x is a factor to correct the infinitesimal strain modulus to a finite strain modulus, and is a function of the stress.

In notation more familiar to seismologists, c_o is the P-wave velocity, $K_o = k + \frac{4}{3}\mu = \lambda + 2\mu$, in which k is the bulk modulus, μ the rigidity modulus, and λ is Lamé's constant. If the velocity of propagation of elastic shear waves is designated by c_s, then

$$\mu = \rho_o c_s^2,\ K_o = \mu\left(\frac{c_o}{c_s}\right)^2,\ \frac{k}{K_o} = 1 - \frac{4}{3}\frac{\mu}{K_o} = 1 - \frac{4}{3}\left(\frac{c_s}{c_o}\right)^2$$

From Equations 1 and 2, Equation 13 becomes

$$1/2\ (\gamma + 1) = \left(\frac{U}{u}\right) - c_o^2\ (uU)^{-1} \tag{17}$$

γ can then be determined from the experimental propagation data, U, u, and c_o. From Equations 16 and 17, another form for x is $x = \frac{U^2}{c_o^2} - 1$.

Following Bishop, we shall use the value of x to describe the regime in which the processes are taking place; i.e., when x is very large, the shock is strong, and when x is very small, the behavior is elastic. Thus transitional states can be specified for a given medium by values of x,

if observational data are available. If overpressure is used to specify the regime, Equation 12 can be expressed as

$$\frac{p}{p_o} = \frac{2\gamma}{\gamma + 1}\left[\frac{U^2}{c_o^2} - 1\right] = \frac{2\gamma x}{\gamma + 1} \tag{18}$$

Bishop has assembled values for γ, based on Equation 17, for various media from data collected by several investigators. These values are presented in Table I.

For x greater than 1, γ is generally found to be a slowly varying function of p and, from Equation 18, overpressure varies linearly with x.

The equations of state for tuff and halite, taken from Bishop, are shown in Figures 2 and 3. These summarize his analysis, and will be discussed in detail below. On these figures $p_1 = p_o$, the ambient pressure.

TABLE I. ADIABATIC EXPONENTS FOR SOME GEOLOGIC MATERIALS AND FOR WATER [13]

Material	Density ρ_o	Adiabatic Exponent γ	Acoustic Velocity c_o
Granite and Basalt	2.67 (gm/cm^3)	1.7	4.9 (km/sec)
Halite	2.15	2.1	4.40
Wet tuff	1.85	3.2	2.44
Dry tuff	1.7	2.1	2.44
Alluvium	1.6	2.7	1.22
Water	p = 30 kb	5	1.5
Water	p = 100 kb	3.8	1.5
Water	p = 400 kb	2.8	1.5

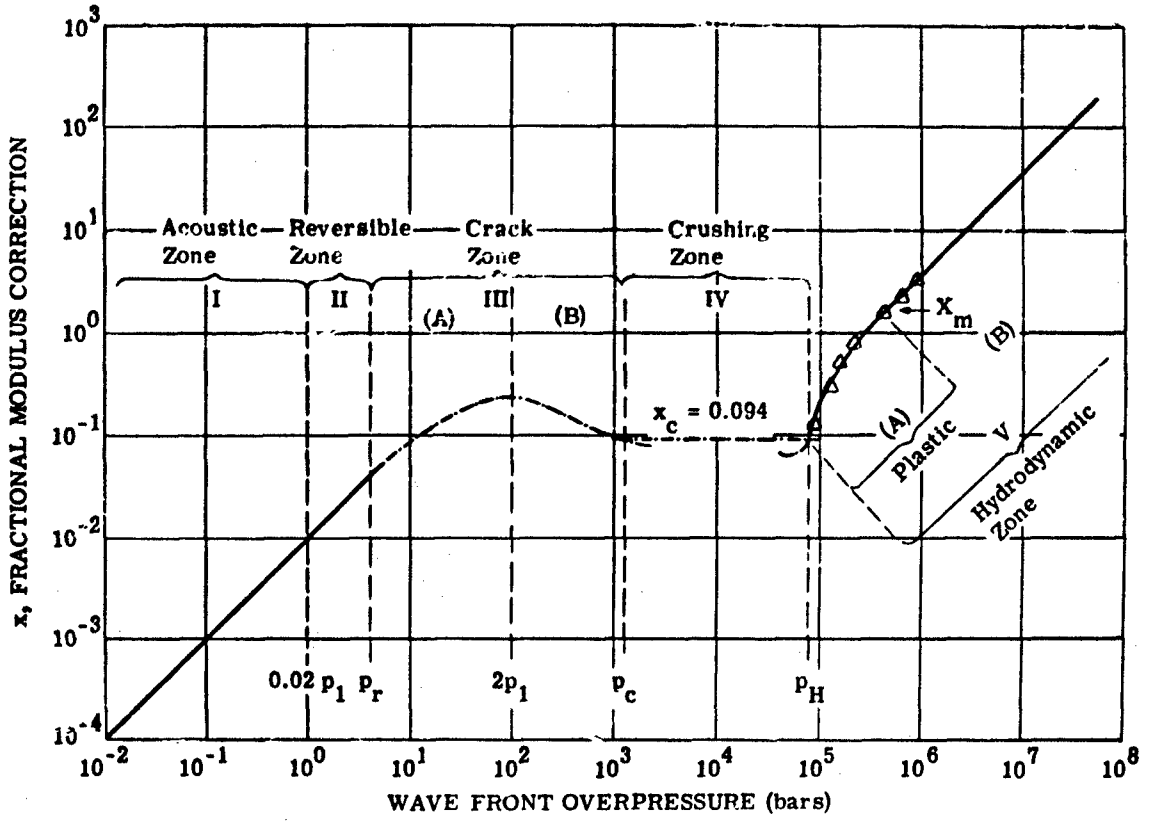

FIGURE 2. EQUATION OF STATE FOR HALITE ($p_1 \equiv p_0$ = 50 bars) (After Bishop)

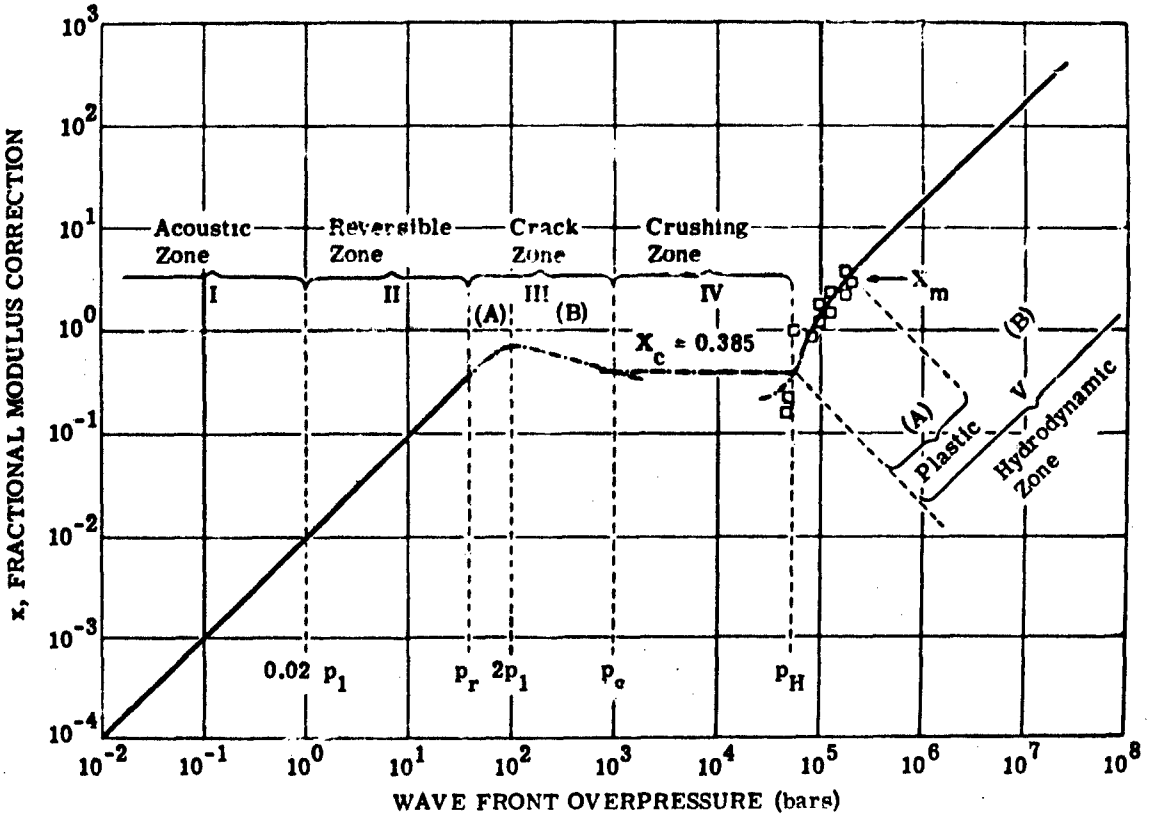

FIGURE 3. EQUATION OF STATE FOR VOLCANIC TUFF ($p_1 \equiv p_0 \approx 50$ bars) (After Bishop)

4
THE STRONG SHOCK REGION

According to the qualitative classification of Cushing and Reily [12], the close-in nonlinear region is that in which a hydrodynamic shock-wave analysis is valid. As stated above, this requires that shock pressures greatly exceed crushing pressure and that shear stresses be negligible. The formidable task of determining the thermodynamic properties of the strongly shocked material must then be accomplished. The objective, from the viewpoint of this report, is to determine where the transition to the terminal nonlinear region occurs and how much energy remains in the shock wave at that radius [22, p. 75].

The Rankine-Hugoniot equation of state is required for the medium; at present, this information is primarily empirical. The equation-of-state work on metals gives useful insight into the problem, but little has been done on porous materials. The work of Chaszeyka [22] and Chaszeyka and Porzel [18] seems to be the best available on materials resembling earth materials; work is in progress, however, by Fugelso [11] and Bishop [13].

Fugelso points out that, owing to the characteristics of earth materials (i.e., inhomogeneity, complex mineralogical structure, porosity, and small-scale structural defects), there is no hope of finding an analytic equation of state to fit the experimental data over the entire range of interest.

Bishop defines the hydrodynamic region as that in which the effective adiabatic exponent γ varies slowly with pressure. The lower limit of the hydrodynamic range is a critical pressure at which crushing ends and hydrodynamic flow begins. Because this pressure falls in a region of plastic flow, it is somewhat indeterminate. Bishop approximates this critical value p_H, the hydrodynamic termination pressure, with a value p_2 which corresponds to a value of $x = x_2 = 0.5$. For $p > p_2$, the x - p curve (see Figures 2 and 3) is almost a straight line ($\gamma \simeq$ constant), except for values close to p_2, where a transition zone of large plastic deformations occurs.

A shock is then defined as being "strong" initially if $x \geq 100$ for any radial distance. This occurs for nuclear explosions, but never for chemical detonations. Figure 3 shows that $x = 100$ for tuff at about 1.5 megabars.

Porzel [19] maintains that the waste heat is the controlling mechanism for a well contained spherically symmetric explosion, such as the RAINIER event. This viewpoint is supported by analysis of soil-like mixtures of air and solid particles [18, 22]. Waste heat was defined above as heat which remains in the material after it expands adiabatically back to the ambient pressure following the passage of the shock wave. Chaszeyka has shown [22] that for even small amounts of air included in the soil or rock-like material, virtually all of the energy of shock compression goes into waste heat.

For all materials, there is some pressure value high enough to heat and vaporize the material irreversibly, and leave it in a gaseous state even after expansion to the ambient pressure. All of the material inside the shock radius corresponding to this "vaporization pressure" becomes part of the cavity. For very strong shocks, there will be energy in the waste-heat part of the p-v diagram in excess of that required to vaporize the material: this will appear as superheat in the gas. Since this energy is available by expansion of the gas, it is not part of the waste heat defined above. Thus, for pressures far in excess of the vaporization pressure, all materials are good transmitters of shock energy [19]. Nuckolls [23] used a value of 1.0 megabar as the peak shock pressure required to deposit enough heat to vaporize the tuff in his calculation of the phenomena associated with the RAINIER event.

Bishop handles the question of the energy available to the shock at any radius by defining an "effective shell thickness." The concept is based on the fact that a spherical shell carrying some fraction of the original energy of the explosion eventually breaks away from the hot gas core, and once this has happened, no energy to support the shock can be received from the core. In the strong shock region with which the discussion is presently concerned, the shell is still in complete contact with the core.

Peet [24, p. 526] points out that Sharpe's calculations of the seismic signal from a spherical cavity show that the shape of the radial pressure profile away from the front has only a minor effect on the results. Both theory and observations indicate that the total pulse duration is short in the close-in region [23]. Basic communication theory asserts that if 100 cps is taken as the upper limit of useful energy for seismic observations, the record of the seismic signal from a pulse shorter than 0.01 second can reveal nothing about the wave shape or spectral content of the input [12, 23]. Therefore, no recoverable information is lost if the shock energy in the source region is considered to be confined to a thin shell.

The effective thickness of the shell is defined as having a volume equal to the total energy in the shock divided by the energy per unit volume at the shock front, taken to be the kinetic energy portion of Figure 1. The thickness, y, of this shell in the strong shock region is given by Bishop [13, p. 48]:

$$\left[1 - \frac{y}{R} + \frac{1}{3}\left(\frac{y}{R}\right)^2\right]\frac{y}{R} = \int_0^1 \left(\frac{\rho}{\rho_f}\right)\left(\frac{u}{u_f}\right)^2 \eta^2 \, d\eta \qquad (19)$$

in which the subscript f refers to the shock front

$$\eta = \frac{r}{R}$$

and R is the radius of the front. The radial profile of density ρ and particle velocity u must be known to apply this relationship.

In the case of a TNT detonation wave, $y/R = 0.064$, which means that most of the kinetic energy is confined to a shell bounded by the front and an inner radius only 6% smaller than the radius of the front.

Taylor's theory of strong shocks [21] provides the required radial variation of ρ and u. These profiles are a function of γ, the adiabatic exponent. The shell thickness is then only a function of γ, which, of course, is a property of the medium.

The analysis for the strong shock and hydrodynamic regions will be summarized on the basis of Bishop's procedure. After a nuclear explosion, there will be an initial zone in which the parameter $x \geq 100$. Taylor's theory of very intense shocks gives the following equations:

$$p_1 = 2(\gamma + 1)^{-1} \rho_o c_o^2 x_1 \tag{20}$$

$$R_1 = \left[p_1^{-1} W_t B(\gamma)\right]^{1/3} \tag{21}$$

where p_1 is the shock front pressure for $x_1 \geq 100$ and R_1 is the radius of the front for this pressure. W_t is the explosion energy release, and $B(\gamma)$ is a function of γ graphed in Figure 4. γ is calculated from Equation 17.

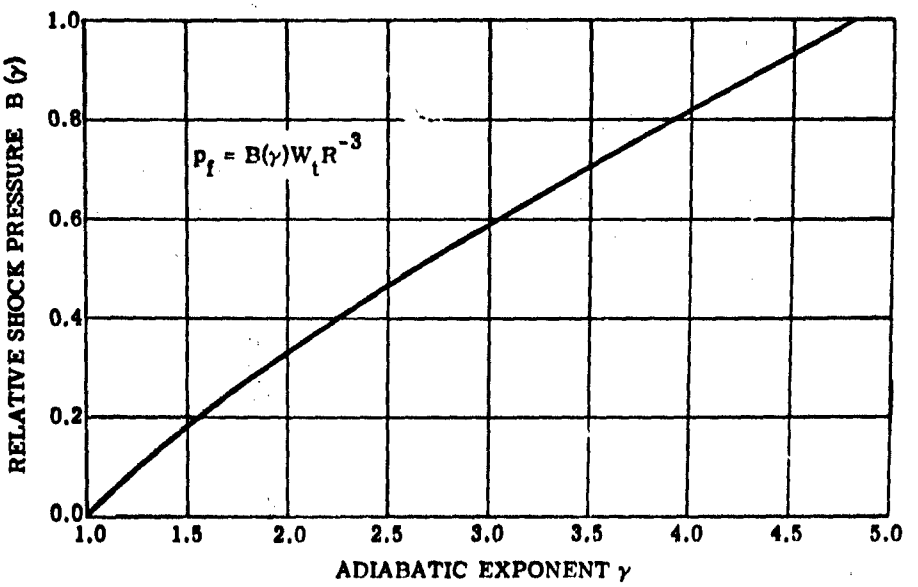

FIGURE 4. RELATIVE SHOCK PRESSURE VS. ADIABATIC EXPONENT (After Bishop)

As the pressure falls below the "strong shock" level (in the sense that Taylor's equations no longer give good results), but is still hydrodynamic ($p_s > p_2$), the following equations may be used to follow the shock history:

$$p = p_1\left(\frac{x}{x_1}\right) \tag{22}$$

$$3 \log\left(\frac{R}{R_1}\right) = \log\frac{x_1}{x} + (2b^{-1} - 1) \log\left[\frac{1 + \frac{b}{x}}{1 + \frac{b}{x_1}}\right] \tag{23}$$

where p = overpressure at radius R in the hydrodynamic range, and b = a heat loss parameter given by

$$b = 1/3\ (2 + q_a) \tag{24}$$

where

$$q_a = 0.4z_1\ (1 + x_m)\ [1 - 1.82\ (1 + \gamma)]^{-1} \tag{25}$$

The plastic flow limit, x_m, is determined from experimental Hugoniot data as the smallest value of x for which the log x - log p graph is a straight line (for tuff this value is about 3.5; see Figure 3); $z = \frac{R}{y}$ is the ratio of shock front radius tc effective shell thickness, given in Figure 5, and z_1 is the value at R_1.

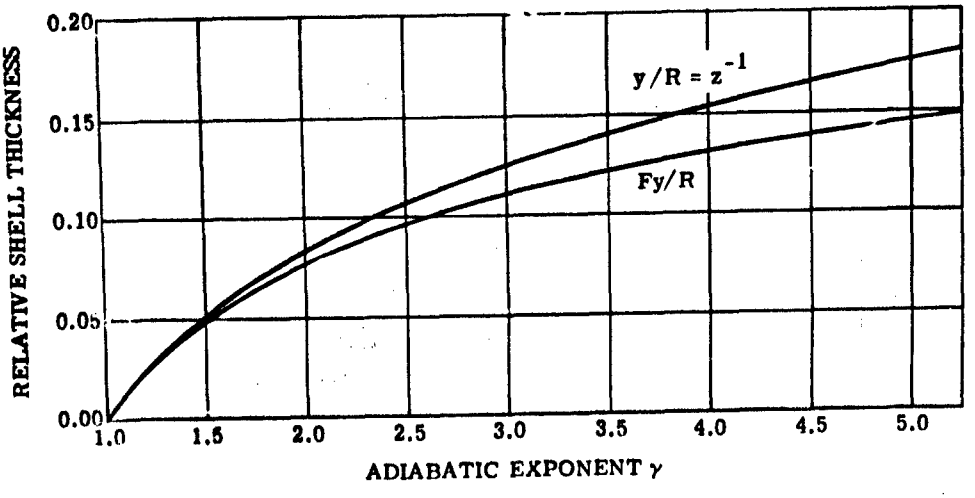

FIGURE 5. SHELL THICKNESS VS. ADIABATIC EXPONENT (After Bishop)

The shell thickness ratio in the hydrodynamic region is given by

$$3 \log\left(\frac{z}{z_1}\right) = \left[(b-1)^{-1} \log\left(\frac{1+\frac{1}{x}}{1+\frac{1}{x_1}}\right) + 2b^{-1} - (b-1)^{-1}\right] \log\left[\frac{1+\frac{b}{x}}{1+\frac{b}{x_1}}\right] \qquad (26)$$

Chaszeyka [22] describes the behavior of an aggregate of silica beads and air intended to simulate some actual earth materials under strong shock conditions. When a shock passes through an aggregate, the solid particles undergo compression, bending, and shear. When sizable voids exist in the aggregate, the compression of the included air causes the temperature of the mixture to increase beyond that which would occur if a uniform sample of the solid were shocked. The resulting thermal stresses in the solid add to the destructive effect of the shock on the solid component. The result is that the aggregate crushes down to its solid fraction at a pressure that is low compared to its static crushing pressure.

Even though the shock propagates faster in a gas than a solid, the braking effect of the surrounding solid tends to hold back the shock through the air, resulting in an essentially uniform shock front.

The heat-transfer process from the compressed air to the solid particles is complex. In developing the Rankine-Hugoniot equation of state for the aggregate, Chaszeyka assumes that as the particles are crushed down (filling the voids), they break up into very small fragments which are thoroughly intermixed with the air so that temperature equilibrium occurs in about one microsecond. His equation of state will not be repeated here, but the resulting cycle for a strong shock is shown in Figure 6. The equation of state is derived by shocking the air and the aggregate to the peak pressure, and then letting them reach an equilibrium temperature.

Results of an earlier study of equations of state and blast-wave properties by Chaszeyka and Porzel [18] are shown in Figures 7 through 10. The materials selected were two types of tuff, sand, clay, sandstone, granite, and ice. The overpressure-distance curves are for a 1-kt explosion.

This discussion requires an additional note on chemical explosions in solids. The shock is never strong (in the quantitative sense of $x > 100$ [13, p. 128]), and it is known [22, p. 53-54] that shock waves from nuclear explosions do not scale directly to those produced by chemical explosions. Bishop explains how the initial shell thickness ratio, z_1, at the boundary between the detonation wave in the explosion and the medium can be calculated in terms of the detonation velocity in the explosive and the pressure at the boundary between explosive and medium. This input pressure may not be great enough to make the process hydrodynamic; if it is high enough,

however, then it is a straightforward calculation to use the value of z_1 to get the other input quantities needed to apply Equations 22 through 25 for the hydrodynamic region. If it is not, the values are used as input to the equations in the crushing and cracking zone to be developed in the next section.

Brode [26] provides a complete example of the calculation of the pressures on the wall of a cavity enclosing a chemical explosion. His calculations indicate that the cavity pressure is affected by the loading density of the explosive, the equation of state of the explosion products, the presence of air in the cavity, and the details of the detonation of the explosive material. It is of greatest importance to the present discussion that he was able to calculate cavity pressures which, when used as inputs to the calculation of elastic waves [27], gave results agreeing closely with observed values.

Nicholls [28] has also done recent work on the manner in which the properties of the explosive affect the energy appearing in the form of seismic waves. He concludes that the maximum seismic energy is generated when the characteristic impedance of the explosive (product of loading density and detonation velocity) is equal to the impedance of the medium (product of density and compressional wave velocity).

All investigators agree that progress in the analysis of strong shocks depends on additional experimental data on the behavior of earth materials at the pressures involved. As we have seen, the pressure-vs.-specific-volume curve over the entire range of pressures from ambient to the highest value of peak shock pressure enters into the calculation of the response of the medium.

Cushing and Reily [12] point out the fact that available data are based on: (1) static tests, (2) dynamic tests using small amplitude elastic waves, and (3) dynamic tests using shock waves. Consequently, there is a lack of information about the behavior of soils and rocks at pressures in the neighborhood of the crushing strength. The result is that the response in the terminal nonlinear region (discussed in the following section) is the greatest source of uncertainty in the sequence of events from the explosion to the seismic signal.

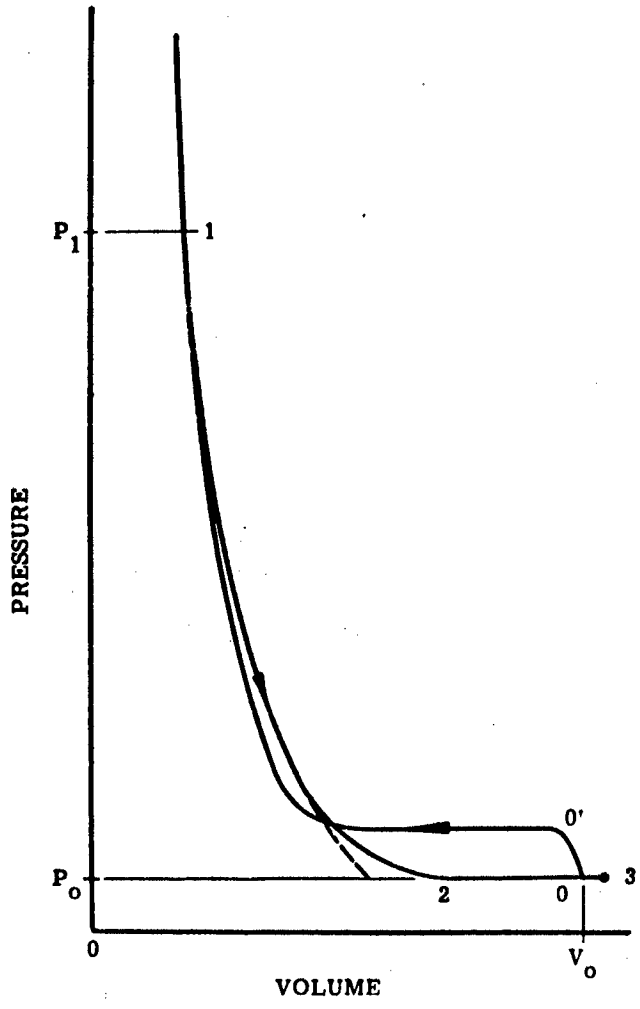

FIGURE 6. PRESSURE-VOLUME CURVE: SILICA-AIR (After Chaszeyka)

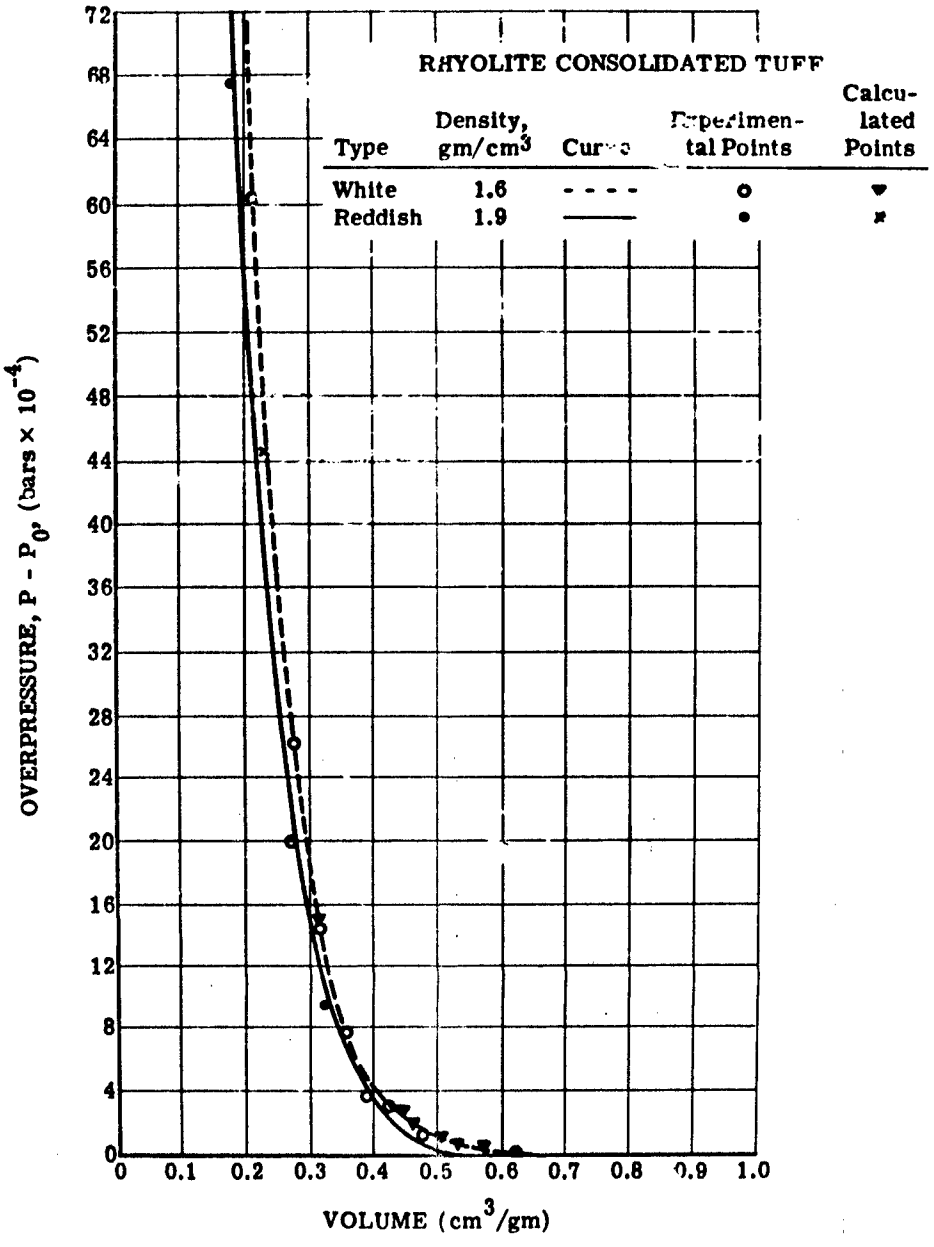

FIGURE 7. PRESSURE-VOLUME CURVE FOR TUFFS (After Chaszeyka and Porzel)

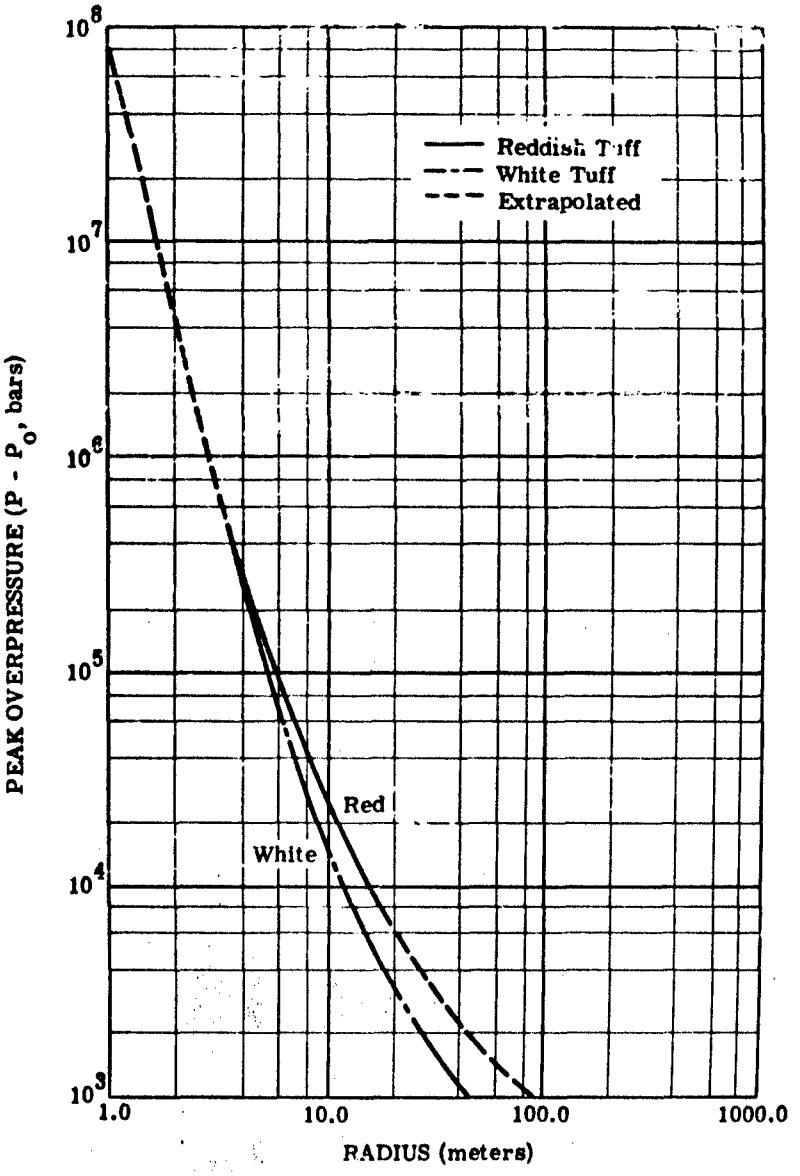

FIGURE 8. PEAK OVERPRESSURE VS. DISTANCE FOR TUFFS (1 kiloton yield)
(After Chaszcyka and Porzel)

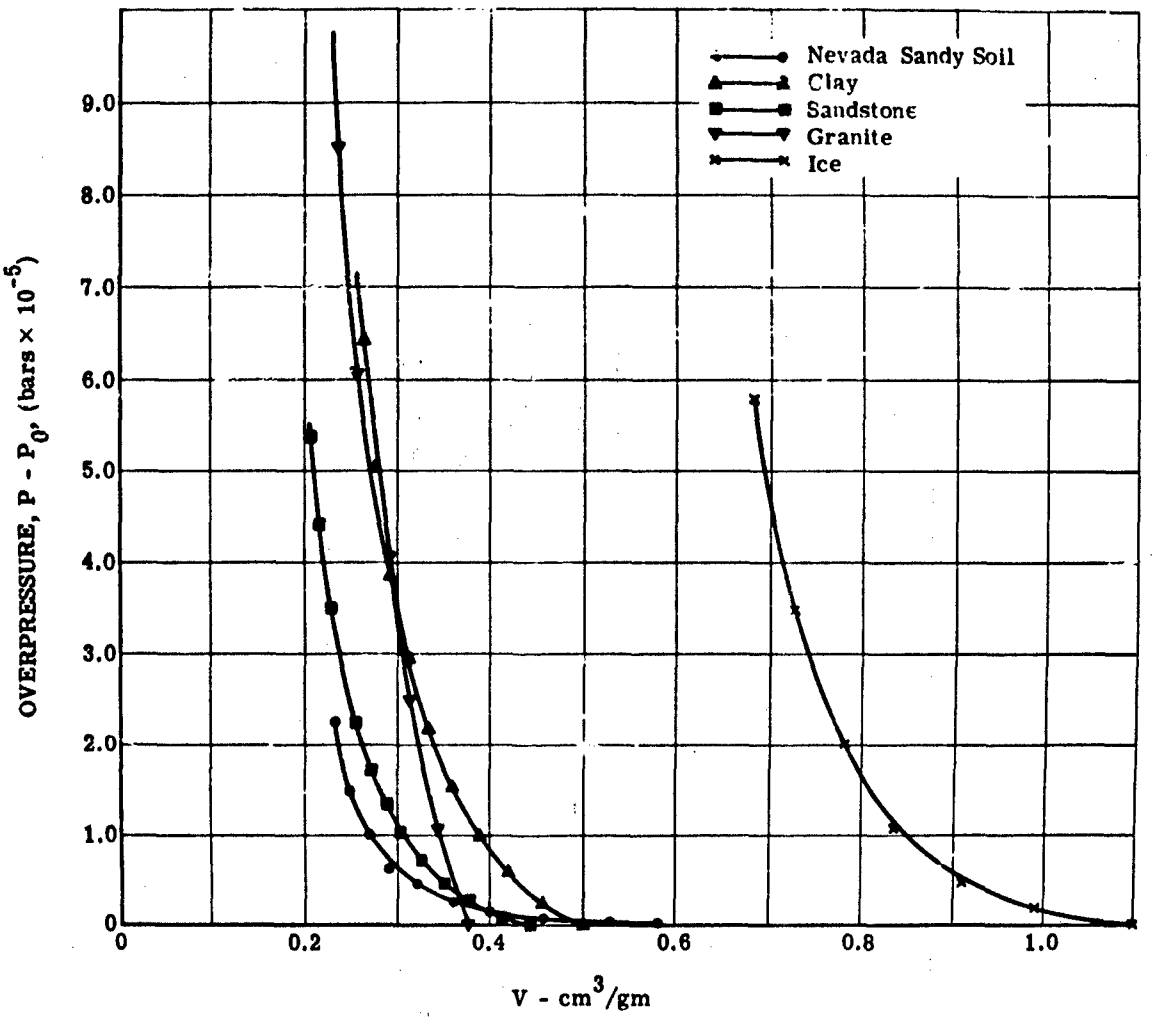

FIGURE 9. PRESSURE-VOLUME CURVES FOR VARIOUS MATERIALS (After Chaszeyka and Porzel)

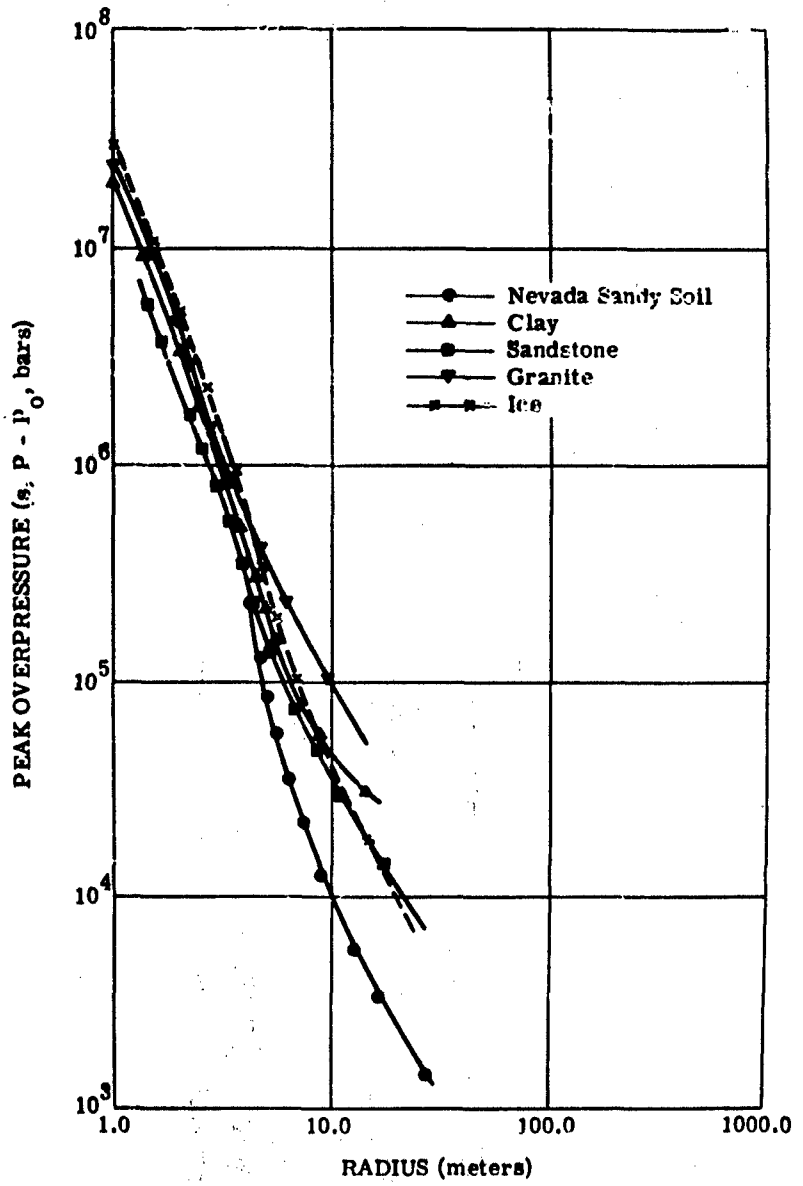

FIGURE 10. PEAK OVERPRESSURE VS. DISTANCE FOR VARIOUS MATERIALS (1 kiloton yield) (After Chaszeyka and Porzel)

5
THE TERMINAL NONLINEAR REGION: THE TRANSITION FROM A SHOCK WAVE TO AN ELASTIC WAVE

In the region discussed here, the material no longer behaves hydrodynamically because the shear strength cannot be neglected, but the stresses still exceed the elastic limit. The processes taking place in this region hold the key to many of the most important questions within the scope of this report. The actual transition from a shock wave to a seismic wave occurs at an overpressure less than the crushing strength of the medium. The limits of this region of transition and the characteristics of shock propagation within it are controlled by the crushing stress, the yield stress, and the elastic limit. These properties may be the best parameters to use in describing quantitatively the effect of the medium on the seismic output of an explosion. Furthermore, the entire pressure-volume curve for the pressure range corresponding to the zone of transition will determine the waste heat deposited in it, and thereby determines the energy available to the seismic waves. Many investigators retain the term "pressure" for this region, using it synonymously with "mean stress," one third the sum of the principal stresses.

It was stated above that there is no hope of recovering information on the short-duration pulse in the initial shock from seismic waves with the periods usually observed. If there are processes which tend to lengthen the pulse, however, they must occur in this zone of transition, and it may be possible to deduce the character of the pulse at the output of this region from the recorded elastic waves [12]. This pulse lengthening is not an apparent increase in the predominant period because of selective transmission of low frequencies by the earth.

The pressure range of interest here is almost unexplored both theoretically and experimentally, except for work on metals [13, p. 69]. Theoretical analyses of waves in this region are very difficult and have been approached through the application of theories of plastic flow, fracture, and compaction.

The significance of this region's existence has long been recognized by exploration seismologists, but apparently no workers in this field have seriously attempted to determine the effects quantitatively. Clewell and Simon [29] recognized that the rise time of the input seismic signal is very much lengthened relative to the detonation pulse from a high explosive because of inelastic processes in this region. The result is a limitation on the power of reflected waves to resolve thin beds in the sedimentary section.

Morris [6] also discusses the types of effects to be expected in this region. He recognizes that earth materials are much weaker in tension than in compression, and points out that the growth of cracks will accompany tensile stresses and that energy from the compressive shock will be required to replace the strain energy released through cracking. He also indicates the

change in pulse shape to be expected because large stresses undergo greater attenuation than small ones in many earth media.

This last point is made clear by an examination of the dynamic stress-strain curve for silty clay, Figure 11 [30]. Because the unloading curve is almost vertical, considerable compaction results from a stress cycle. The area between the loading and unloading curves represents energy lost from the stress wave. Lampson [30] comments that large stresses not only undergo greater attenuation, but also propagate with a lower velocity, so that the waveform is spread out in time and diminished in amplitude. The seismic wave velocity ordinarily observed is determined by the slope of the curve for very low stresses.

Peet, in discussing seismic waves from a shock, assumes an abrupt transition from a hydrodynamic region to elastic behavior [24]. He states that the nonlinear effects may be confined to a small region between the two zones, or the region may scale with charge weight in the same way the shock wave region does, so that his model of the source does not change. The boundary between the two types of behavior is specified in terms of "a certain yield stress," and is not further defined. Peet's results will be discussed in more detail in the section on elastic wave propagation.

Aoki [10] has obtained expressions for the seismic waves generated in this region and for the wave form at its termination. His analysis is based on Tresca's yield condition for plastic flow [31]. He defines a plastic wave as any kind of wave with a propagation velocity less than an elastic wave. But since these intermediate stress level phenomena may propagate in the form

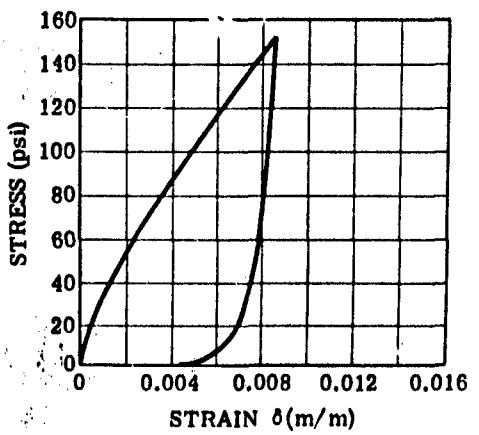

FIGURE 11. EXPERIMENTAL DYNAMIC STRESS-STRAIN CURVE FOR FREE EARTH (SILTY CLAY) (After Lampson)

of cracks produced by brittle fracture, Aoki states that the term "fracture wave" may be more appropriate than "plastic wave." He considers the cases of waves traveling behind the elastic wave with speeds given by $(k/\rho)^{1/2}$ and $(\mu/\rho)^{1/2}$, where k and μ are the incompressibility and rigidity, respectively. In either case, an elastic precursor runs ahead of the main shock, and as the pressure decreases, the two merge to form the elastic pulse.

Cushing and Reily [12] have established an elastic-plastic static model using a procedure very similar to Aoki's. They do, however, devote more attention to the equation of state in the region. They have also started work on a dynamic model in which the previous stress-strain history of the medium is taken into account, and have set up a statistical model of a porous medium.

Zvolinskii [52] assumes a medium in which there is an abrupt change from linear elastic behavior to an incompressible compacted state. Since plastic flow in the compacted state is irreversible, he proposes a model in which the plastic work is proportional to the change in the greatest shear, with the proportionality constant depending on the mean stress. Essentially, he generalizes the work of Aoki and Cushing and Reily by using a more general yield condition, in which the difference between the maximum compressional and tensile stresses is a function of the mean stress rather than a constant. He is one of several authors who model this region by allowing the material to crush to an incompressible state.

Haskell [33] has also developed a static theory for the transition zone, using an incoherent granular aggregate rather than a plastic as a model of the material. Then the stress in the zone of failure is determined by the Coulomb-Mohr criterion [31] instead of a Tresca or von Mises yield condition. Haskell compares his final results with data from chemical explosions in halite and from the RAINIER event. He finds that he can match the data to his theory, but to do so he must use values for the internal friction parameter that are much lower than those obtained from compression tests on unconsolidated materials. He suggests that plastic flow and fracturing both may occur in the zone, giving this result.

Fugelso [11] points out several shortcomings of any application of present plastic deformation theories to cases in which the loads are applied very rapidly, or for a very short time. The inherent difficulties in developing a theory of dynamic plastic deformation result from the nonlinearity of the equations and the fact that the stress-strain curve itself is a function of the loading rate. Fugelso has developed a theory of plastic deformation based on the theory of dislocations within a crystalline body, and applied it to the problem of impact loading of a rod, combining the effects of elastic distortion and the movement of dislocations.

Fugelso's conclusions include the following:

1. The deformation resulting from the arrival of the stress wave occurs in two steps: an instantaneous elastic deformation and a time-dependent plastic deformation.
2. The elastic wave propagates as a distinct wave, but there is no distinct plastic wave.
3. The stress-strain curve for any material is not unique, but is dependent on the strain rate and the duration and magnitude of the stress.

In view of the work done also by Aoki and Zvolinskii (above), the conclusion reached here is important: that the solution gives no forward propagating wave that moves with a velocity lower than that of the elastic compressional wave. The solution is valid, of course, only for the one type of nonelastic deformation mechanism assumed. Fugelso states that his model is intended for crystalline bodies, and soils are specifically mentioned among media for which more complicated mechanisms may be involved.

An examination of the pressure-volume diagram for a soil-like material (see Figure 12) in terms of Equation 4 indicates part of the reason for the complicated nature of the transitional processes [12, 17, 19]. The velocity of shock propagation is proportional to square root of $(p - p_0)/(v_0 - v)$. The linear portion of the pressure-volume curve, with p_e as the elastic limit, fixes a slope which divides the curve into two parts. For a pressure p_1, $(p_1 - p_0)/(v_0 - v_1) > (p_e - p_0)/(v_0 - v_1)$, the shock is "superseismic," and the conditions for a single stable shock are satisfied [17]. However, for a pressure p_2 below the intersection of the elastic portion (extended) with the pressure-volume curve, the inequality is reversed and the shock breaks up into a two-wave structure. Figure 13, taken from Cushing and Reily [12, p.16], shows the radial profile of the resulting pressure pulse. The arrival of the front, traveling at the seismic compressional-wave velocity, is accompanied by a steep rise in stress to the elastic limit. The pressure then increases gradually to an intermediate value, p_1, determined by the tangent to the equation-of-state curve through p_2, v_2. Relative to the p_1, v_1 state, conditions for a stable shock exist, so that the steep rise to the peak pressure p_2 occurs.

Some important consequences of this behavior are (1) a zone for which the peak stress is well above the crushing strength, but for which the peak stress moves subseismically, so that elastic precursors result; and (2) a mechanism for lengthening the pulse in time. A computed pressure-time history for a point in the transition zone of the RAINIER event is seen in Figure 14 [23].

Chaszeyka [22] conducted a systematic investigation of the first stages of the transition process both in hard, low-porosity material, and in dry, unconsolidated, noncohesive soils, such

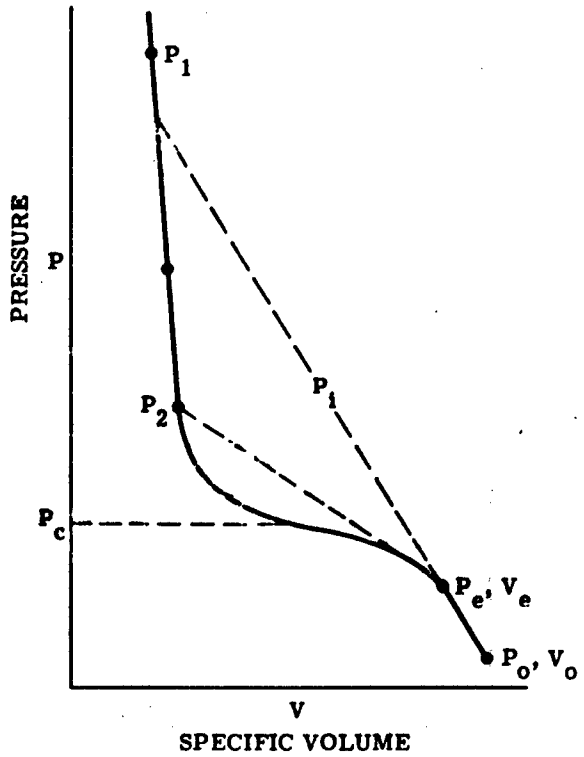

FIGURE 12. TYPICAL PRESSURE-VOLUME CURVE

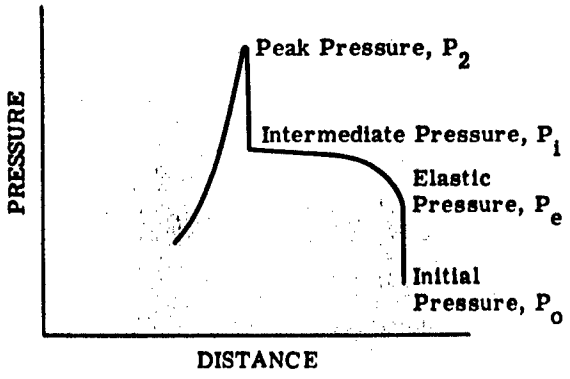

FIGURE 13. PRESSURE-DISTANCE WAVE SHAPE FOR NON-SIMPLE SHOCK CONDITIONS (After Cushing and Reily)

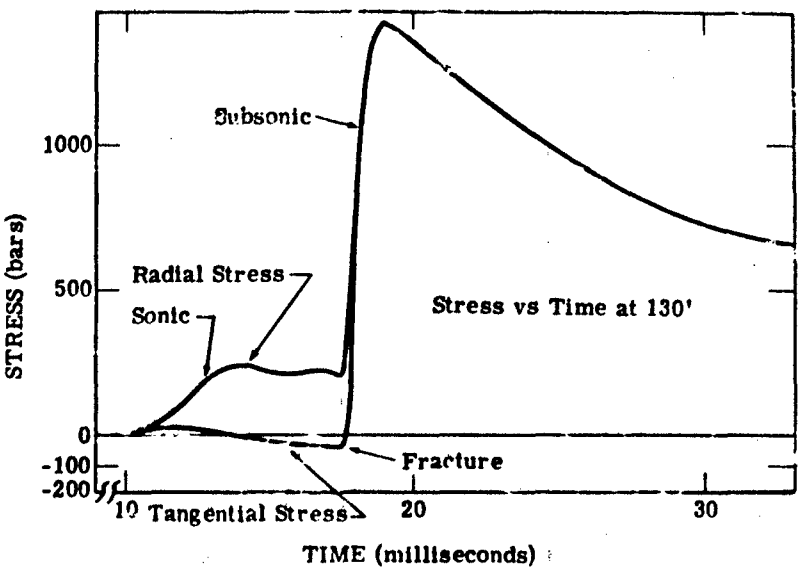

FIGURE 14. COMPUTED STRESS WAVE IN NONLINEAR REGION, RAINER EVENT (After Nuckolls)

as dry sand. His study partially supports the assumption made by Peet: nonelastic processes do not greatly affect the generation of seismic waves in the case of a porous, sandy-type soil. For a granite-like rock, however, a seismic wave of considerable amplitude is generated when the pressure in the shock front is at or above the crushing strength. The zone of crushing and compaction is examined in this work.

For a solid which is malleable and nearly isotropic and has a negligible air content, the shock weakens through gradual decrease of the deformation until it becomes an elastic wave. The transition is not sharp. If the solid is porous or if it is equivalent to an aggregate of solid particles and air, the propagation changes considerably during the transition.

A porous, aggregate-type medium will have a lower crushing limit, p_{cl}, at which the solid grains must begin to fracture, and an upper crushing limit, p_{cu}, at which the interstices are filled with crushed material (see Figure 15). If hydrodynamic behavior is defined as occurring above the crushing strength, the transition begins near p_{cu}. Between p_{cu} and p_{cl} is a region of invariant reduced volume (Chaszeyka's terminology), or compaction. The pressure in the shock drops from p_{cu} because of thermal losses and work on the medium. At a pressure p_c between the two crushing limits, the volume is reduced to a fixed value v_c. This behavior is indicated by the vertical dashed lines on Figure 15. The transition from compacting to plastic behavior

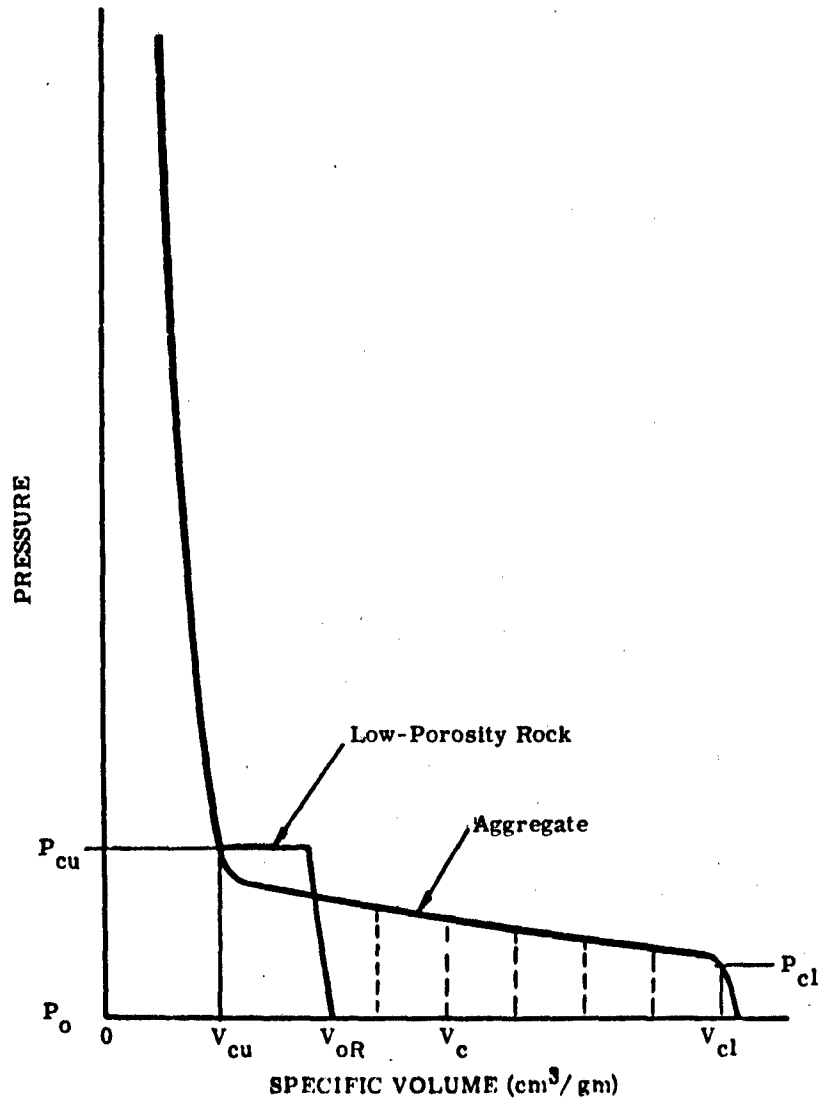

FIGURE 15. TRANSITION REGIONS (After Chaszeyka)

occurs near p_{cl}; the final transition to a seismic pulse occurs at an overpressure below the limit for plastic flow.

The solid particles are compressed during the compacting process, but the change in volume from this cause is negligible compared to that arising from fracturing of the grains. The air shock in this region is low. The energy loss that attenuates the shock from p_{cu} to p_{cl} is nearly all due to work done in crushing the solid portion of the aggregate.

The behavior of a hard low-porosity rock is indicated by the step on Figure 15. Here a definite value of the crushing stress exists at which the material crushes to hydrodynamic behavior; below this value it behaves nearly elastically.

Chaszeyka gives a form for the variation in density, particle velocity, and pressure through the transition zone. Since the density to which the material is compacted decreases as the peak pressure drops with increasing radial distance, the density will be lower at the shock front than behind it. A density-distance relation of the form

$$\rho = \rho_s (R/r)^q \tag{27}$$

is assumed, in which r is the distance to a point behind the front ($r \leq R$), and $q = -\frac{\partial \log \rho}{\partial \log r}$.

By conservation of mass (and using the fact that ρ is constant behind the shock in the compacted zone), the following expression for q is obtained:

$$q = 3\left[1 - \frac{\rho_s}{\rho_o}\frac{1 - (R/R_u)^q (R_u/R)^3}{1 - (R_u/R)^3}\right] \tag{28}$$

in which R_u is the radius corresponding to p_{cu}, and is the smallest radius at which compaction to constant density occurs.

For a particle velocity u_s at the front, the velocity at a point in the zone is

$$u = \frac{u_s \rho_s R^2}{\rho r^2} \tag{29}$$

The pressure distribution is found from conservation of momentum. In terms of quantities already defined,

$$p - p_o = (p_s - p_o)\left(1 + \left(\frac{\rho_s}{\rho_o} - 1\right) R^q \left\{ \frac{(\rho_s/\rho_o)^2 R^4}{4+q}\left[\frac{1}{R^{4+q}}(2 - q) + \frac{1}{r^{4+q}}(q - 2)\right] + \frac{(\rho_s/\rho_o)^2}{\rho_s/\rho_{o-1}} \frac{R}{1+q}\left[\frac{d \log u_s}{d \log (p - p_o)}\left(\frac{-d \log (p_s - p_o)}{d \log R}\right) - 2\right]\left(\frac{1}{R^{1+q}} - \frac{1}{r^{1+q}}\right)\right\}\right) \quad (30)$$

This equation shows that for an aggregate the pressure decreases toward the origin from the shock front.

The decrease of peak pressure with radius of the shock is found by the technique of blast wave integration developed by Chaszeyka and Porzel [18]. The computed result for an aggregate of 69% silica and 31% air is shown in Figure 16; p falls off at about R^{-6}. Comparison with Figures 2 and 3 shows that the pressure range covers the region of the crushing zone designated by Bishop. The radius at which the upper crushing limit occurs can be found for any material from a curve like the one shown in Figure 16 if adequate experimental information is available.

For a porous medium in the zone $R > R_u$, the value of q in Equation 27 varies from about 1.5 (when R is 10% greater than R_u) to zero (as R approaches infinity). In this case, the small part of the original energy from the explosion still remaining (less than 3%) is dissipated in crushing the solid particles; the shock weakens as a result of both this crushing work and spherical spreading.

For a hard rock, ρ_s approaches ρ_o rapidly as the stress drops below the sharply defined crushing limit. The exponent q has a low value and approaches zero quickly, being about 0.02 when R is 10% greater than R_u. The result is a relatively small energy decrease, and a strong seismic pulse will be generated at a pressure only slightly below the crushing limit.

The transition discussed here is only the first in the sequence leading to the seismic pulse [22, p. 144]. For later transitions, associated with lower overpressures, we return to Bishop's treatment. He divided the equation of state into five regions, with several subregions (see Figures 2 and 3). Starting from the high pressure end, Region V is the previously discussed hydrodynamic region for which $x > 1$, and γ is nearly constant. A subrange in which large plastic deformations occur is seen just above the hydrodynamic termination pressure, p_H.

The pressure p_H is approximated by p_2, corresponding to $x = 0.5$, and marks the upper limit of Region IV, the zone of crushing. The crushing pressure p_c determines the lower boundary of

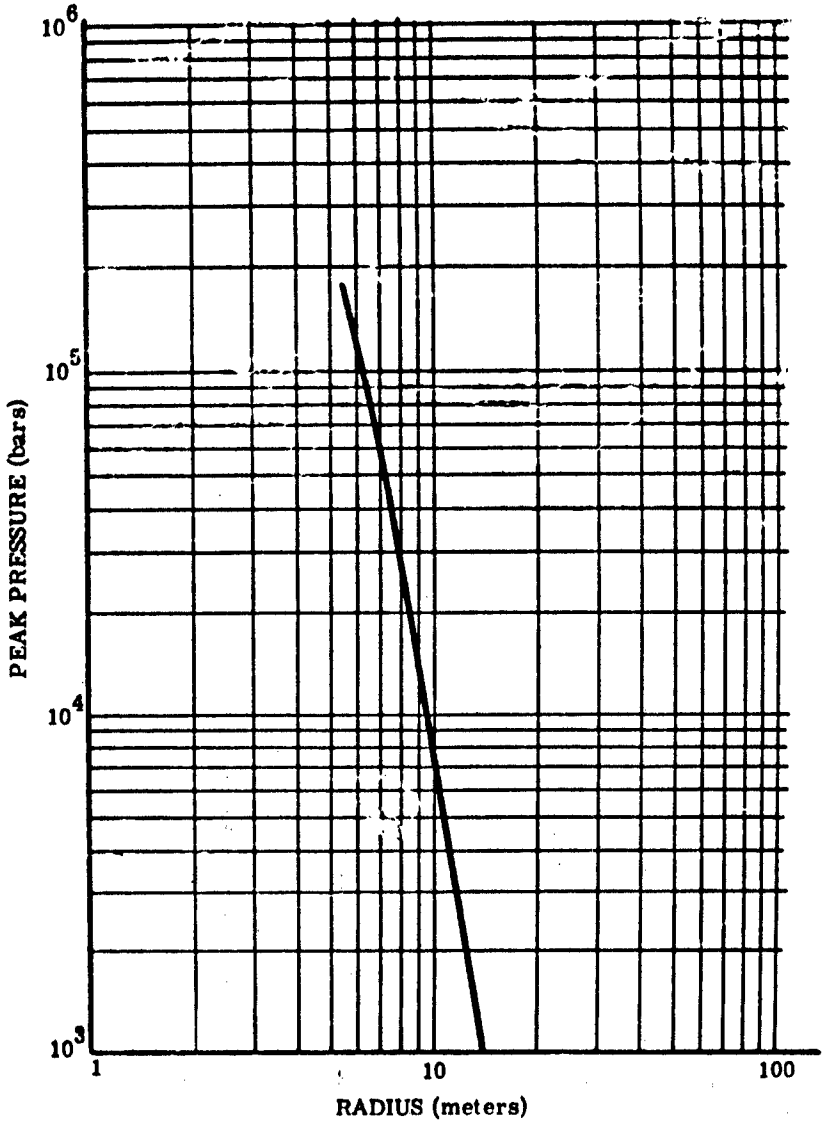

FIGURE 16. PRESSURE VS. DISTANCE FOR A 1-KILOTON EXPLOSION IN AN AGGREGATE (After Chaszeyka)

crushing. The crack zone, Region III, is subdivided into two parts: IIIa, a region of hoop-stress tensile cracks, IIIb, in which shear stress cracks occur. The lower limit of the crack zone is designated p_r, which denotes the highest pressure in the stress wave for which processes are reversible. The boundary between the two types of crack occurs at the maximum in the x - p curve, at a pressure near twice the ambient pressure. Regions III and IV represent irreversible, nonhydrodynamic behavior.

Region II is that in which processes are reversible, but strains are finite; Region I is the zone of elastic waves. Region II (called the "semiacoustic zone" by Bishop) begins at an overpressure of about 0.02 p_o.

The low-pressure end of the x - p diagram will be considered in detail first. For strictly infinitesimal strains, the adiabatic exponent is $\gamma_o = \rho_o c_o^2/p_o$ (see derivation of Equation 13). For condensed media (liquids or solids), γ_o is large compared to one for p_o near one bar. For small but finite strains, the transition across the shock will be nearly reversible. As Porzel [19, p. 41] states, all materials are excellent transmitters of shock energy at low pressures. Bishop postulates a form for γ for the finite-strain, nearly reversible case that is analogous to that for γ_o above:

$$\gamma_{rev} = \rho_o \frac{U^2}{p_o} \tag{31}$$

in which γ_{rev} is the semiacoustic exponent, and the compressional wave velocity c_o has been replaced by the shock velocity U. γ_{rev} is also a large number, so that the value of x for reversible processes is approximated by

$$x_r = 1/2 \ (p/p_o) \tag{32}$$

where p is small enough for the assumption of reversibility to hold. It follows that x_r must be small compared to one. In order to carry on without experimental data, Bishop assumes 0.5 as the maximum value of x for the semiacoustic region. From Equation 32, this requires that p_r, the reversible limit in terms of pressure, be less than or equal to p_o, the ambient pressure.

This choice of the reversible limit is based on the fact that most earth materials have very low tensile strengths. They will fail in tension as soon as the tensile hoop stresses associated with the radial compressive stress overcome the lithostatic compression. This will occur at an overpressure close to the ambient pressure.

By analogy with the elastic case, dynamic bulk and shear moduli can be defined such that $K_s = K_o (1 + x) = k_s + 4/3 \mu_s$. In the semiacoustic region, it is not unreasonable to take $k_s/\mu_s = k/\mu$, and Bishop postulates that this relation may be approximately true up to $p = 2p_o$, the maximum point shown on Figures 2 and 3.

The behavior in crushing has been discussed in the review of Chaszeyka's work; Bishop's treatment, however, will be summarized here for the sake of continuity. In the crushing region, the dynamic bulk modulus k_s is almost constant, while the dynamic shear modulus μ_s is very small. The x - p curve is nearly flat, with a constant value of x given by

$$x_c = -1 + 2k/K_o = 1 - (c_s/c_o)^2 \tag{33}$$

(see the discussion following Equation 16). Bishop concludes that no equation of state can be established for the crushing zone except by measurements on specific materials.

The onset of Region III (coming up from the low pressure end) occurs when the medium is first broken up into large fragments by radial cracks from the hoop stresses. This occurs when the tensile stress exceeds the resultant of the ambient stress and the tensile strength of the medium. It is not possible to assign a precise value to p_r at which cracking begins because of the imperfect nature of earth materials. The value p_o seems to be a reasonable estimate.

As the stress increases above p_r, the fragments are broken into smaller and smaller pieces until the medium is reduced to an almost homogeneous aggregate of particles of relatively high strength; crushing then begins at pressure p_c. Radial cracking predominates up to a pressure of about $2p_o$; above this pressure, circumferential cracks produced by shear stresses combine with the radial cracks to make the smaller pieces. In the zone of shear stress cracks (see Figures 2 and 3) the x - p curve has a negative slope, the shock velocity decreases with increasing pressure, and the previously discussed elastic precursors result.

Bishop has developed equations, on the basis of numerous assumptions and approximations necessitated by the lack of experimental data, which make it possible to follow the history of the shock through the transition zone. He discusses these equations thoroughly; no attempt to justify them fully will be made here.

The output of the hydrodynamic zone is the input to the crushing zone. Therefore, the calculations start by finding R_2 and p_2, the approximate radius and pressure of the shock at hydrodynamic termination, from Equations 22 through 25. The effective shell thickness ratio z_2 is found from Equation 26. Then, for $p_c < p < p_2$:

$$\log \frac{z}{z_2} = (1 + x_c)^{-1} \log \frac{R}{R_2} \tag{34}$$

$$\log \frac{p_2}{p} = \left\{ (1 + 1.5x_c) \log \frac{z}{z_2} + \frac{1}{6} z_2 x_c \left(\frac{z}{z_2} - 1 \right) \right\} \tag{35}$$

where x_c is given by Equation 33.

Some assumption about losses from the shock as it passes over the medium is essential to the development of these equations. The blast-wave integration procedure developed by Chaszeyka and Porzel [18] is a method of keeping track of the waste heat deposited during propagation of the shock. Bishop treats the problem in the following manner.

The heat loss per unit mass from the shell Q_s is found in terms of the waste heat Q (defined above) by $Q_s = G_m G_x Q$, in which G_x is a shock-strength factor which is zero for very strong shocks, and G_m is a factor which depends on the medium. By assuming that $G_x = (1 + x)^{-1}$, it is possible to write $G_m = (1 + x)\, Q_s/Q$. A value of $G_m = 2.0$ was found to agree well with experimental data in the crushing zone for halite, tuff, and alluvium, the only earth materials investigated. Equations 34 and 35 are based on this value.

In the cracking zone, with the overpressure between the crushing and reversible pressure, good results were obtained by the use of an inverse square law for overpressure decay:

$$\log (p_c/p) = 2 \log (R/R_c) \tag{36}$$

where R_c is the shock radius at which p_c occurs.

In the semi-acoustic zone, $p < p_r$,

$$\log\left(\frac{R}{R_r}\right) = \left[\frac{1}{3}\log\left(\frac{p_r}{p}\right) + \frac{2}{3}\log\left(\frac{1 + \frac{4}{3}\frac{p_o}{p}}{1 + \frac{4}{3}\frac{p_o}{p_r}}\right)\right] \tag{37}$$

The results of applying the theory to available data from explosions in halite (COWBOY and GNOME events) and volcanic tuff (HOBO and RAINIER projects) are shown in Figures 17 and 18. Equation-of-state data were taken from Lombard [34], and ambient stress values are taken from Adams and Swift [35]. The COWBOY data are taken from Murphey [36]; the GNOME values are from preliminary results obtained by the Sandia Corporation.

On these figures, R_l is the radius in feet of a sphere of pelletol TNT. With the pelletol density taken as 1.0 gm/cm^3, $R/R_l = 6.38\ R\ W^{-1/3}$, where W is the charge weight in pounds. The value of R_l for the GNOME nuclear event was taken as 28.5 ft, the radius of a pelletol sphere with the same energy release, 3 kilotons. The cube-root scaling brings the nuclear and small chemical explosion data into good agreement.

Using the properties of pelletol and halite, Bishop shows that the input pressure of 100 kilobars corresponds to the upper limit of the zone of crushing. There is consequently no hydro-

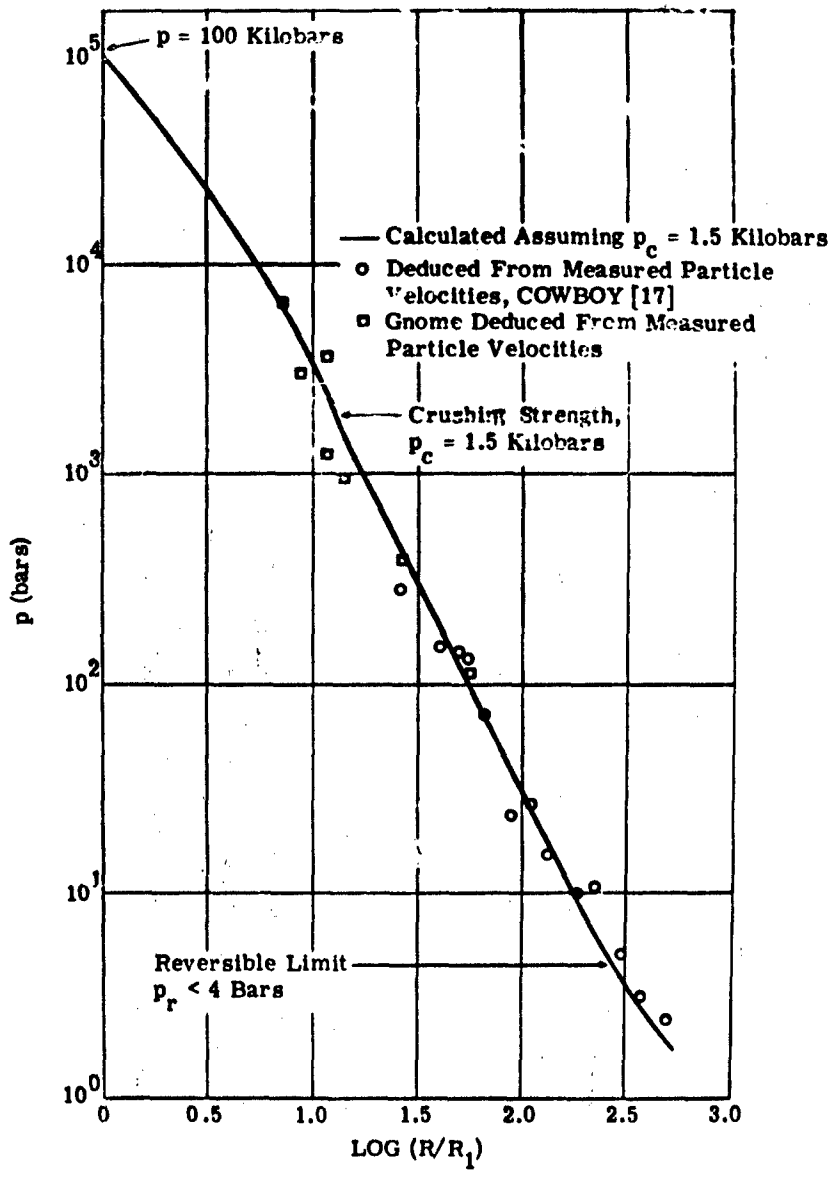

FIGURE 17. PRESSURE VS. DISTANCE CURVE FOR HALITE (After Bishop)

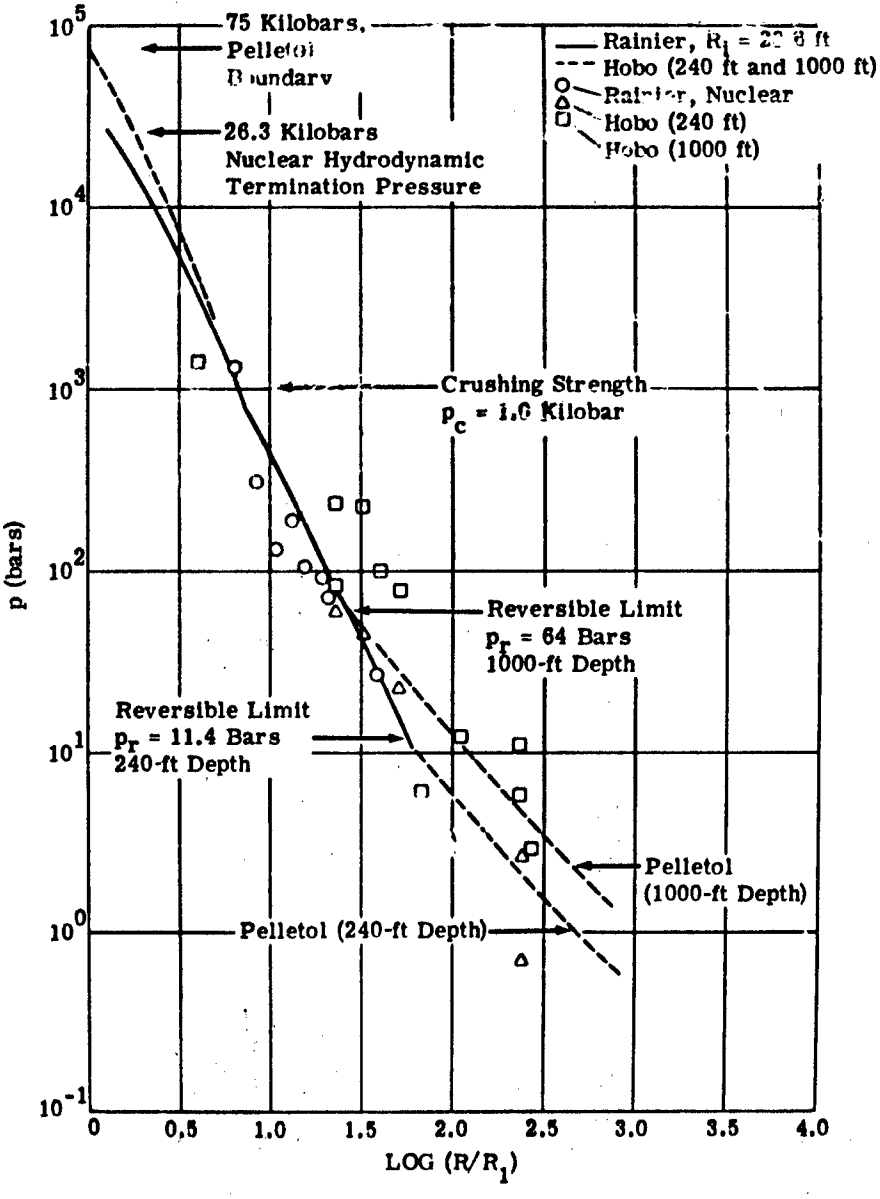

FIGURE 18. PRESSURE VS. DISTANCE CURVE FOR VOLCANIC TUFF (After Bishop)

dynamic region, and all pressures from the COWBOY series are in the cracking region. The plotted pressures in the figures were not measured, but were calculated from observed particle velocities, using equations developed in the theory.

For tuff, the input pressure for pelletol is 75 kilobars. Values derived from Equations 34 and 35 are shown on Figure 18. The first quantitative results on the effect of source depth encountered in this review can be seen in the HOBO data. The reversible limit p_r is seen to increase significantly as the depth of the shot (and therefore the ambient stress) increases. The maximum value this limit can attain has been set as the resultant of the ambient stress and the tensile strength of the medium. The actual value may be smaller than this because of preexisting cracks or other departures from uniformity of the medium. For the tuff, the reversible limit is near the maximum, but it appears to be much less than the maximum of 59 bars for the COWBOY data on Figure 17.

The two methods of analysis, Chaszeyka's and Bishop's, can be compared by the results presented on Figures 8 and 18 for explosions in tuff. The abscissas of Figure 8 are to be divided by 6.0 (the value of R_1 in meters) for one kiloton, and the logarithm taken. Thus six meters on Figure 8 corresponds to 0.0 on Figure 18, 30 meters to 0.7, and 60 meters to 1.0. The region of overlap is therefore limited, but within this region the agreement is very good. The tendency for the pressure-distance curve to be slightly concave to the distance axis shown on Figure 18 is not seen on Figure 8. It is concluded that both methods of analysis are sound, and the principal need is for more experimental data.

Although the nonlinear processes have been analyzed for the manner in which they absorb energy from the shock pulse, no analysis has been made of the seismic signal proceeding from these disturbances directly. Only the radial compressional pulse is followed. A growing crack is a source of seismic waves, and experimental evidence has been accumulated that these waves can be observed [37]. It has been suggested also that the boundary between the expanding explosion products and the surrounding medium may be unstable, developing wave-like perturbations so that the output from the source may not be spherically symmetrical [38].

Propagation in the elastic region will be reviewed next on the assumption that the source is spherically symmetrical; the evidence of asymmetry will be discussed subsequently.

6
THE ELASTIC-WAVE REGION

The entire earth, outside of the hydrodynamic and nonlinear regions discussed in the previous sections, constitutes the region of elastic wave propagation. This report does not consider

the details of the effects of departures from ideal elasticity in this region on the shape and amplitude of the seismic signal. Also omitted are the details of the structure of the crust and upper mantle, which must be taken into account in determining the actual amplitude of the various seismic waves as observed at distant points [1]. Attention is directed to the signal at short ranges, and at long ranges if the medium is homogeneous and infinite in extent.

Theoretical and experimental studies of explosion-generated elastic waves have been carried out for many years, starting with the early work in exploration seismology, somewhat later extending to quarry and mine-blast observations, and most recently to nuclear explosions. Some of the experimental work has been designed to test theoretical results, but most of it has been directed to empirical correlations of maximum seismic wave amplitude with various parameters characterizing the explosion and observation conditions. Results of the search for empirical scaling relations are covered in a later section of this report. The early theoretical papers made no attempt to determine numerical values of amplitude in terms of charge weight.

In a classic paper, Sharpe [3] attempted to explain certain facts known from experience to exploration seismologists. Referring specifically to seismic reflections from horizons in the sedimentary section, he summarized these observations as follows:

1. A given amount of explosive detonated in a clay or water-saturated sand formation results in a greater amplitude of reflected motion than an equal charge detonated in a dense, rigid formation such as limestone.

2. If a hole is sprung by an initial large charge in order to form a sizable cavity, later small charges will result in a larger amplitude of reflected motion than would be produced in the absence of springing.

3. The frequency spectrum of reflected motion is a function of the formation in which the charge is fired: shots fired in the low velocity zone result in very low frequency motion compared to shots fired below the low velocity zone; shots fired in a rigid material (such as a limestone) result in a much higher frequency motion than shots made in, for example, a shale; in a general way, the high frequency content of reflected motion increases with an increase in shooting depths.

4. The frequency spectrum of reflected motion is a function of charge size; a large charge has a tendency to increase the proportion of low frequencies in the reflected motion.

5. The amplitude of reflected motion produced by a given quantity of a high explosive is much greater than that produced by a quantity of low-speed explosive, even when the maximum pressure is the same.

These statements touch upon every point of concern within this present report: i.e., the effect on the amplitude and spectral content of the seismic signal of the medium around the shot, the depth of burial, the yield, the coupling, and the properties of the explosive material.

6.1. THE WAVEFORM OF EXPLOSION-GENERATED P WAVES

Sharpe took as his source model a spherical cavity around the shot having a radius, a, large enough so that only elastic processes took place at or outside the surface. This cavity is designated the "equivalent cavity" or the "equivalent radiator" by various authors. An exponentially decaying pressure pulse, with the pressure equal at all points of the spherical surface, was postulated as the loading equivalent to the explosion: $p(a, t) = p_m e^{-\alpha t}$.

No attempt was made to relate a, p_m, or α to the size of the charge and the properties of the medium.

Although Sharpe obtained his results for the special case in which Poisson's ratio $\sigma = 0.25$, or $\lambda = \mu$, it is useful to generalize the result for an arbitrary elastic medium. This has been done by Blake [5], but the solution will be given in a slightly different notation. The ratio of shear modulus to Lamé's constant, $\mu/\lambda = m$, will be used in place of the parameter K introduced by Blake. Thus, $\sigma = \frac{1}{2(1+m)}$, and $m = 1$ for $\sigma = 0.25$.

The displacement potential for the exponential pressure on the cavity wall is given by

$$\phi = \frac{a p_m}{\rho r} \frac{1}{\omega_o^2 + \left(\frac{m\omega_o}{\sqrt{m + m^2}} - \alpha\right)^2} \left\{ - \exp(-\alpha\tau) + \exp\left(-\frac{m\omega_o\tau}{\sqrt{m + m^2}}\right) \left[\cos \omega_o\tau + \left(\frac{m}{\sqrt{m + m^2}} - \frac{\alpha}{\omega_o}\right) \sin \omega_o\tau\right]\right\} \tag{38}$$

in which ρ = density

r = distance from center of cavity

$\omega_o = \frac{2c\sqrt{m + m^2}}{a(1 + 2m)}$

$c = \sqrt{\frac{\lambda + 2\mu}{\rho}}$ = compressional wave velocity in the medium

$\tau = t - \frac{r - a}{c}$

The displacement, which is purely radial under the assumptions, is the derivative of the potential in Equation 38. For the important special case of a step in pressure, $\sigma = 0$, and the displacement[2] is

$$\mu = \frac{ap_m}{4\mu}\left\{\left(\frac{a}{r}\right)^2 - \sqrt{\frac{1+2m}{1+m}}\left(\frac{a}{r}\right)^2 \exp\left(-\frac{m\omega_o^2}{\sqrt{m+m^2}}\right)\right.$$

$$\left.\sin\left[\omega_o\tau + \tan^{-1}\left(\frac{\sqrt{m+m^2}}{m}\right)\right] + 2\sqrt{\frac{m}{1+m}}\left(\frac{a}{r}\right)\exp\left(-\frac{m\omega_o\tau}{\sqrt{m+m^2}}\right)\sin\omega_o\tau\right\} \qquad (39)$$

The first term represents the permanent displacement resulting from the fact that the pressure p_m continues to act on the cavity forever. At large ranges ($r >> a$), the last term in Equation 39 predominates.

$$u = \frac{p_m a^2}{2\mu r}\sqrt{\frac{m}{1+m}}\exp\left(-\frac{m\omega_o\tau}{\sqrt{m+m^2}}\right)\sin\omega_o t \qquad (40)$$

The displacement is thus a damped sinusoid with angular frequency ω_o, which varies directly as the compressional wave velocity and inversely as cavity radius, and becomes low for small values of m, characteristic of soils.

For small values of m, the amplitude becomes large (and μ becomes small), assuming that the peak pressure and radius at the inner boundary of the elastic region are unchanged.

The damping factor (fraction of critical damping) ζ is a function of the properties of the medium:

$$\zeta = \left(\frac{m}{1+2m}\right)^{1/2} = \left(\frac{\mu}{\lambda+2}\right)^{1/2} \qquad (41)$$

The motion in rock (for which m is near 1.0) will be more highly damped, or less oscillatory, than in soil. Aoki [10] presents waveforms for particle velocity which illustrate this for m = 1.0 and 1/75 (see Figures 19 and 20). The effect of including elastic precursors from the nonlinear region, as Aoki does, is to increase the rise time of the signal. The following notation applies to these two figures:

[2] The symbol "u" is widely used for particle velocity in hydrodynamics and particle displacement in elasticity theory. Rather than introduce a new symbol, the same symbol is used for both in different parts of this report. From this point, "u" is displacement, "v" is velocity.

v = particle velocity

b = radius of beginning elastic zone (≡ a)

k = constant from von Mises' yield condition: $\sigma_{rr} - \sigma_{\theta\theta} = \sqrt{3}k$

$\tau = \frac{c(t - t_o)}{b} - \frac{r - b}{b}$, t_o is time at which shock reaches the radial distance b

αc = propagation velocity of "plastic" or "fracture" waves, taken as $\sqrt{\frac{E}{\rho}}$, where E is the bulk modulus for "plastic" waves and the rigidity modulus for "fracture" waves

c = compressional wave velocity

s = decay exponent in pressure pulse ($\equiv \frac{a\alpha}{c}$ in notation of this report)

In Figure 19, where $\lambda = \mu$, m = 1, the two velocities of inelastic wave propagation are $\sqrt{\frac{5}{3}}c$ and $\sqrt{\frac{1}{3}}c$ for the "plastic" and "fracture" waves, respectively. In Figure 19, s = 0, corresponding to a step function in pressure.

The results for a clay-like material ($\lambda = 75\mu$; see Figure 20) are based on a velocity of the elastic-plastic boundary of 0.9 c and four rates of pressure decay. The initial spike (corresponding to rapid pressure decay, or large values of s) will be highly attenuated at a distance because of the transmission characteristics of the earth, discussed below.

The response to arbitrary forcing functions can be obtained by superposition of solutions of the forms given above. Duvall [4], working with radial strain data, was able to arrive at waveforms closely resembling his field records by adding the responses to two exponential pressure functions with different rates of decay. He found that at short ranges the non-oscilla-

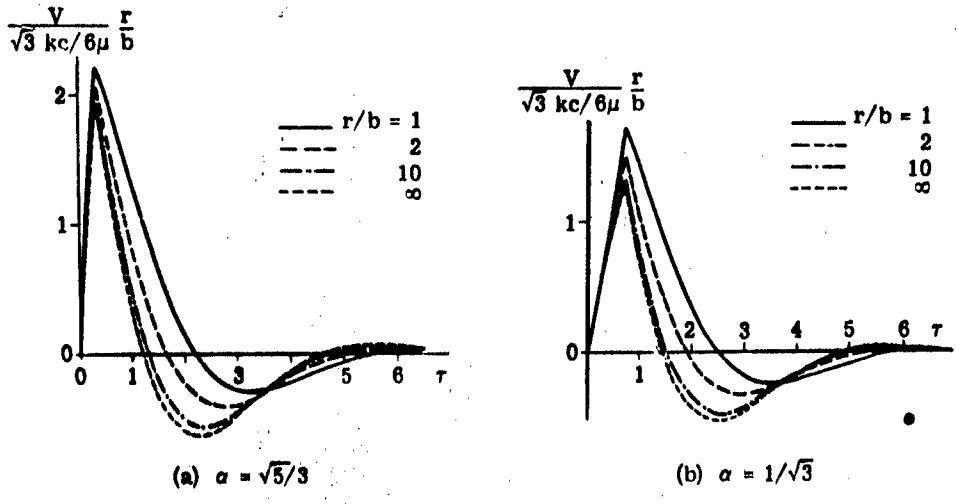

FIGURE 19. WAVEFORMS CALCULATED FOR $\lambda = \mu$ STEP FUNCTION INPUT PRESSURE (After Aoki)

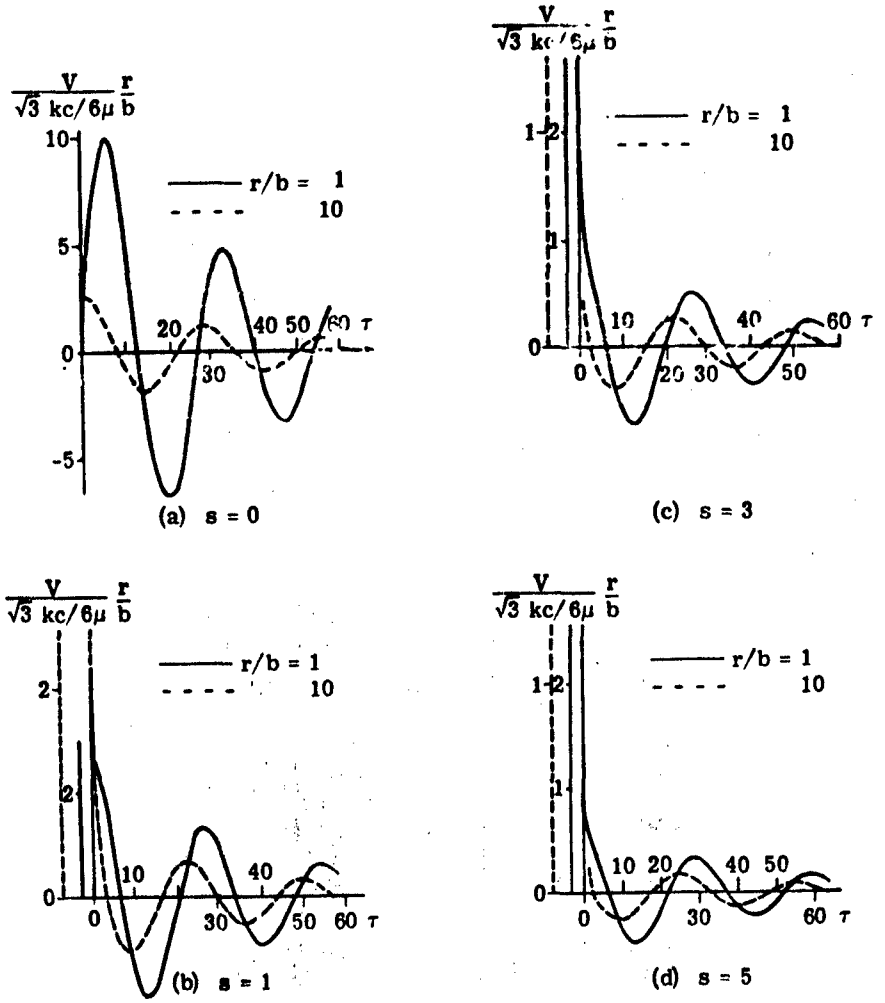

FIGURE 20. WAVEFORMS CALCULATED FOR λ = 75 μ, α = 0.9 (After Aoki)

tory part of the solution predominates, and the time of the first zero crossing is not accurately predicted by taking a half period corresponding to ω_o. He also points out that the range at which elastic behavior begins cannot be determined by locating the limit of non-oscillatory wave shapes.

Vaněk [39, 40, 41] has examined the effect of the higher power terms in 1/r in solutions like Equation 39. These terms produce a region two or three times the radius a in which the peak amplitude of the spherical compressional waves decays faster than r^{-1}. Since the material is assumed to respond in a perfect elastic manner, this requires an abnormal attenuation due to geometric spreading. Vaněk concludes that the peak amplitude propagates faster than the wave front in this zone, the more rapid propagation yielding the faster attenuation. This conclusion implies that the beginning of the elastic zone cannot be determined experimentally by finding the shortest range at which the peak displacement decays as the inverse first power of the distance.

An excellent opportunity to test this entire approach to the theory of explosion-generated seismic waves was offered by the Project COWBOY experimental series. The objective of the program was to test the use of cavities to decouple underground explosions [36, 42, 43, 44]. The subject of decoupling itself is outside of the scope of this report, but the results of some of the investigations carried out in connection with COWBOY are directly related to the topic.

Data obtained from some of the shots in this series apply directly to this discussion; the shots were fired in cavities of sufficient size that the response of the salt was nearly elastic, if not exactly so. The conditions of the theory outlined above were therefore satisfied at the cavity boundary. Comparisons of theoretical waveforms (based on elastic response) with observed ones are presented by Parkin [27] and by Herbst, Werth, and Springer [43].

Parkin used the theoretical pressures on the cavity boundaries calculated by Brode [26] as the input to his computation of displacement and other motion parameters as functions of range and time. The results for the decoupled shots were excellent; those for the "overdriven" cavities showed departures which could be ascribed to plastic deformation. Parkin obtained his results by the direct numerical evaluation of the integral solution for the displacement for an arbitrary pressure waveform on the cavity wall.

Herbst et al. [43] present a theoretical waveform for one of the cavity shots in the COWBOY series which agrees very closely with that observed. The technique used here also was numerical integration of the equations for elastic response.

As shown earlier in this report, the smallest radial distance at which the stress is low enough for the response to be elastic is a function of the medium, the depth of the source, and the yield. For a given medium and depth, the peak pressure, p_m, at the boundary between the

elastic region and the nonlinear zone is a constant. The basis of decoupling a shot is that the radius at which the pressure is down to p_m is much smaller for a cavity shot than for one tightly tamped in the medium [44], and therefore the radiated amplitude is found to be smaller from solutions like Equation 40.

6.2. THE SPECTRAL CONTENT OF EXPLOSION-GENERATED P WAVES

Solutions of the form of Equations 39 or 40 suggest that a natural frequency ω_o, determined by the properties of the medium and the size of the charge, will characterize the compressional wave. However, this conclusion ignores the fact that the earth acts as a low-pass filter upon elastic waves [29, 44]. Using numbers suggested by O'Brien [7] for a 100 lb shot in a medium with a P-wave velocity of 5000 fps and Poisson's ratio of 0.25, we find that ω_o is 471 rad/sec, corresponding to a frequency of 75 cps. Frequencies in this range are commonly observed in the reflection method of seismic prospecting, but they are not encountered in observations at larger distances. Even if they are transmitted, most of the instrumentation used for recording at distances of more than a few km will not pass frequencies higher than about 10 cps.

Therefore it is necessary to examine the amplitude spectrum corresponding to the solution above, and attempt to determine the effect on the observed amplitude of the low-pass character of the transmission-recording system. This has been done by several investigators, all of whom arrive at similar conclusions [7, 24, 45, 46, 47].

Peet has developed a theory in his attempt to relate amplitude to yield, in which the shock-wave and elastic-wave regions are in juxtaposition. The validity of his results for the elastic-wave region is not in any way affected by the fact the terminal nonlinear region has been neglected, as long as the actual radial distance to the elastic zone increases as the cube root of the yield. Only the numerical value radius of the equivalent cavity in terms of the yield may be incorrect. In turn, this affects only the numerical values of amplitude.

On the basis of the output from the hydrodynamic region, Peet finds the following relations at the input to the elastic wave region, r = a:

$$p(a, t) = p_m \exp\left(-c_2 t / W^{1/3}\right) \tag{42}$$

where $a = \left(c_1/p_m\right)^{1/n} W^{1/3}$

p_m = radial stress at which elastic behavior begins (a property of the medium)

t = time from start of shock wave

c_1, c_2 = constants

n = empirical quantity = 1.16

The pressure given by Equation 42 is a very much simplified version of all that was covered in the first two sections of this report.

Because the stress pulse maintains its shape as it propagates for perfect elasticity while the various kinematic quantities (e.g., particle velocity) do not, Peet works with the spectrum of the mean stress.

If the displacement potential, such that $u(r, t) = \frac{\phi}{r}$, is taken to be $\phi = \frac{c^2}{r} f\left(t - \frac{r}{c}\right)$, the mean stress ("pressure") is $p = \frac{\lambda + 2\mu}{r} f''\left(t - \frac{r}{c}\right)$. For the pressure function of Equation 42, it follows (for a linear elastic medium) that the stress scales in both time and amplitude as $W^{1/3}$: $p(r, t) = \frac{B}{r} W^{1/3} g\left(\frac{t}{kW^{1/3}}\right)$. The scaling of the pressure waveform is shown in Figure 21, on which $Q = W$.

The behavior of the amplitude spectrum [24, Equation A.II.13] is given in Figure 22. The spectrum has a single maximum at a frequency $f = cW^{-1/3}$, at which the amplitude is proportional to $W^{2/3}$. (The negative sign in the exponent is omitted from Peet's Equations A.II.12 and A.II.21, but should be there from his Equation A.II.20; see Figure 23.) If the radius "a" increases as $W^{1/3}$ (as is required by similitude considerations [46]), the spectral maximum varies as a^2, in agreement with the pulse amplitude in Equation 40. For low frequencies, the spectral amplitude is proportional to $f^2 W^{4/3}$, while at very high frequencies, the amplitude varies as $f^{-1} W^{1/3}$.

The effect of charge size on the shape of the spectrum is demonstrated by Figure 23. Small charges give a flat spectrum with the maximum at a high frequency. The difficulty in comparing

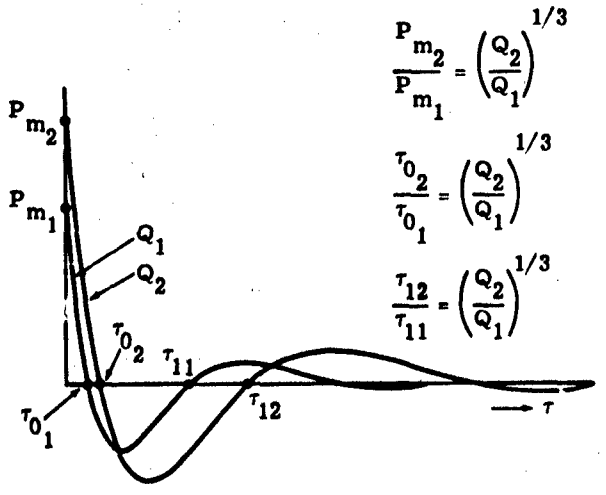

FIGURE 21. SCALING OF THE WAVEFORM (After Peet)

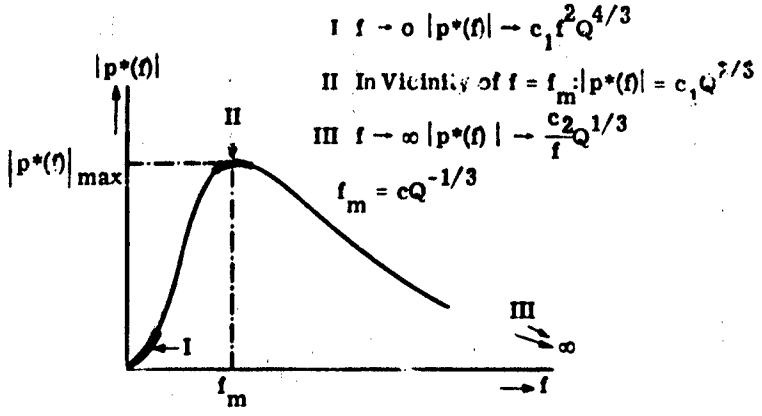

FIGURE 22. GENERAL PLOT OF THE FREQUENCY SPECTRUM OF p(r, t) (After Peet)

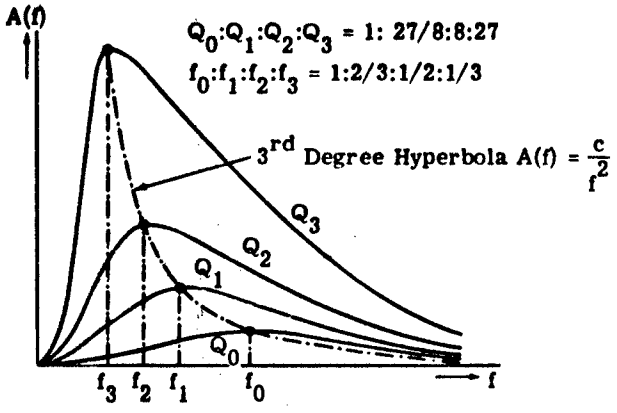

FIGURE 23. THE FREQUENCY SPECTRUM OF p(r, t) FOR SEVERAL CHARGES (After Peet)

amplitude-yield data for small and large yields, brought on by the low-pass character of the earth-instrument system, is illustrated in Figure 24. For small charges, the portion of the spectrum which would be recorded is that for which the dependence on yield is near the first power; e.g. from $W^{4/3}$ to $W^{2/3}$. For the large charge, however, the spectrum falls almost entirely within the pass band, and the exponent of the yield will be smaller.

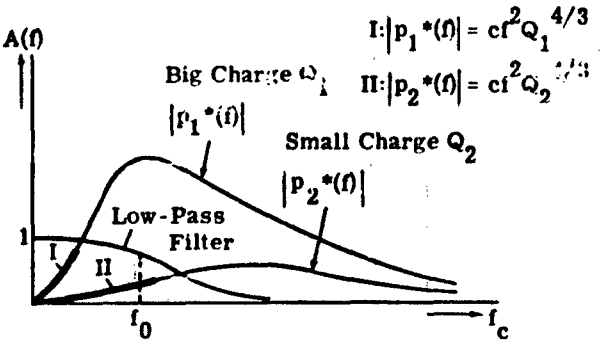

FIGURE 24. THE POSITION OF THE FREQUENCY SPECTRA OF BIG AND SMALL CHARGES WITH RESPECT TO THE PASSBAND OF A LOW-PASS FILTER (After Peet)

Werth and Herbst [48] have found a first-power dependence of head-wave amplitude on yield for low yields and a two-thirds power dependence for high yields. The yield at which the dependence changes is higher for hard media (salt and granite) than for soft ones (alluvium and tuff).

Latter, Martinelli, and Teller [46] have also analyzed the low-frequency part of the spectrum, and concluded that the signal at a distance will vary as the first or 4/3 power of the yield depending on whether the pressure at the elastic-inelastic boundary decays slowly or rapidly compared to the cutoff frequency of the earth-instrument system. Data precise enough to permit these two scaling laws to be distinguished are difficult to obtain.

Rather than work from the spectrum for the exponentially decaying pressure wave, O'Brien [7] uses Blake's result [5] for radiation of a steady-state sinusoid from the cavity. He finds that the criterion for determining the type of yield dependence is whether $\omega a/c$ is less than or greater than 1.0. For low frequencies, the signal amplitude (particle velocity) should vary directly as the charge weight. However, for very large charges (a is large), or for very high frequencies, the signal amplitude will increase as the cube root of the yield. For the first case, all frequencies will increase in the same manner, so that the pulse shape does not change with charge size. For the second, the pulse will lengthen somewhat with charge size.

As pointed out by Herbst et al. [43] and Carpenter et al. [45], O'Brien assumes that the radius of the equivalent cavity increases as the cube root of the charge weight, but that this cavity is determined by a limiting condition for the medium of impulse per unit area equal to a fixed value. Since impulse scales as $W^{1/3}$ (see appendix), these assumptions are inconsistent. However, as shown by

Carpenter et al., the step function approximation for the stress at the boundary also gives a first-power dependence on yield for low frequencies.

Proceeding from very general considerations of the relation between pulse shape and the slope of the spectrum, Weston [47] points out that for most disturbances, the total impulse at distances more than a few wavelengths is close to zero, and the amplitude spectrum of the pressure at low frequencies varies as f. Under conditions that length- and time-scale as $W^{1/3}$, he then shows that the low-frequency amplitude is proportional to W. The variation of the low-frequency amplitude spectrum with the first power of the frequency and yield results from the particular pulse shape, one for which $\int p\,dt = 0$ at infinite time, but $\iint p\,dt\,dt$ does not. In the case of a pulse for which the integral of the impulse is also zero at infinity, the low-frequency spectral amplitude varies as f^2 and $W^{4/3}$, as in Peet's result. Other exponents for f and W are appropriate for other pulse shapes.

In applying these general results to underground explosions, Weston looks for the type of source conditions that would be consistent with these relations, for the equivalent cavity model of an explosion. A step in pressure is the simplest loading that will give the prescribed first-power dependence of amplitude on frequency at a distance. The actual decay in pressure in the cavity will not affect the results as long as it is slow compared to the longest waves of interest. For a fast pressure decay, spherical elastic-wave theory may not apply right up to the radius at which elastic behavior begins, and the cavity model may have to be abandoned. Weston states, in conclusion, that the first-power dependence of amplitude on yield applies for frequencies much less than 1000 $W^{-1/3}$ cps, and for ranges greater than about 700 $W^{1/3}$ ft (W in lb).

Carpenter, Savill, and Wright [45] have recently examined the amplitude-yield relation in terms of $W^{1/3}$ scaling. After considering the results for a single frequency (which would correspond to the response of a very sharply tuned seismograph), they conclude that the bandwidth of the instrument must be taken into account when determining this relation from field data. As they point out, and as was seen above, different results can be obtained for different passbands of the earth-instrument system. They conclude that a simple $W^{1.0}$ dependence is likely to apply to any particular frequency band up to some limiting value of W, beyond which the increase is less rapid.

These authors also point out an inherent difficulty in applying any kind of scaling laws to wave generation and propagation in the real earth. Scaling is assumed for wave generation; for transmission, however, a constant geometry is assumed, and these are incompatible except for an infinite homogeneous medium. The opinion held by Carpenter et al. is that this conflict is not of primary importance in many practical situations.

6.3. ENERGY AVAILABLE FOR ELASTIC WAVES

The fraction of energy originally released that is available at the beginning of the elastic zone can be calculated by the methods outlined for the high-pressure regions, once adequate data on the pertinent properties of the medium have been collected. The actual energy that is transmitted to long distances can only be determined by including effects of absorption and scattering.

Parkin [27] presents a table of calculated values of released and radiated energy for TNT shots of 20 lb to 2000 lb fired in various sized cavities in salt. The values are based on Brode's results [26]. The fraction of the energy radiated varies from 4×10^{-5} (for a completely decoupled shot) to 8×10^{-4} (for an overdriven cavity). No estimates for tamped shots are given.

Howell and Budenstein [49] performed energy calculations for seismic waves generated by explosive charges of about 1.0 lb at depths of about 10 ft in unconsolidated material tamped with water. Their result for the total energy in the wave train (not the P wave alone) for a surface distance of 10 ft indicates that about 5% of the source energy is present in the frequency range of six to 120 cps. O'Brien [7] estimates that the energy in the low frequencies is no more than 3% of the source energy for an underground explosion, and may be much less. In view of the fact that the low-frequency amplitude spectrum increases as the first or second power of the frequency (energy as the second or fourth power), the energy reaching large distances is likely to be much less than 1% of the yield.

Berg and Cook [50] calculated the total energy in the wave trains recorded at distances of 6.78 to 22 km from two very large quarry blasts; by extrapolation back to the source, they estimated that 2.7% of the total energy content of the explosive charge appeared in the form of elastic waves.

Nicholls [28] used the known properties of the explosive material to determine yield energy, and calculated the energy transmitted into the medium from strain measurements. His calculations indicate that 2% to 4% of the chemical energy is coupled to the rock, but he believes that values of 10% to 20% may be more realistic. The measurements were made from experiments using three different types of dynamite and granular TNT, tightly tamped in salt. He quotes the results of earlier Bureau of Mines investigations for granite, in which 10% to 18% of the explosive energy is coupled to the earth. These values seem far higher than any others reported.

Working with the RAINIER event, Porzel [19] finds that only 3% of the original energy was left at the termination of the crushing stage (130 ft), and concludes that roughly 99% of the energy is deposited as heat in the cavity and in a thin shell of compressed material near the source.

These figures are in general agreement with estimates given above. Porzel concludes also that the energy available to produce seismic waves "bears no direct relation with the original energy release," but is determined by the geometry of the charge and hole in which the charge is placed, and the properties of the medium (vaporization pressure and dynamic crushing strength). At long distances the "apparent energy" will be of the order of 10^{-3} of the original yield. This value agrees with that cited by Griggs and Press [51] for a 20-kt underground nuclear explosion (presumably the BLANCA event).

Although the statements above are in full accord with the concepts that have been developed in this report, Porzel arrives at some additional conclusions that are somewhat startling. He doubts that the acoustic approximation ever applies (in the sense of constant energy in the wave) and that it is a misnomer to talk about partition of energy between the source region and the radiated signal. The available energy decreases constantly with distance and rapidly approaches zero, because of known departures from homogeneity and linear elasticity. His conclusion is that even the 1% of the explosion energy available at the termination of the nonlinear zone became insignificant. He suggests that the seismic signals "alleged to be observed as a result of the RAINIER event" are the result of minor earthquakes triggered by the passage of the shock wave through jointed and faulted material. By this reasoning, the energy observed on the seismogram is principally tectonic strain energy accumulated in the test site through geologic time.

Press and Archambeau [52] have examined this hypothesis, and present convincing arguments that, although an explosion will release accumulated strain, the magnitude of the energy involved is too small to affect the resulting seismic waves.

Porzel's argument that the duration of the pressure pulse is too short to be resolved by seismic instruments overlooks (1) mechanisms in the terminal nonlinear region which act to lengthen the pulse somewhat, and (2) the fact that the observed seismogram will not be the pulse incident on the elastic wave region, but the response of the earth-instrument system to this pulse. In fact, a nuclear explosion, because of its short duration, is valuable to seismologists in that it provides a direct observation of the impulse response of the transmission path and seismograph, which in turn can be used to study earthquake focal mechanisms [51, 53].

The energy radiated in the form of seismic waves depends upon many factors besides the yield of the explosion; Parkin's recent work [27] on correlation of various parameters characterizing elastic waves, therefore, merits careful consideration. He correlates the theoretical peak values of displacement, particle velocity, acceleration, and stress in salt with scaled range by employing a variation on established scaling procedures. In the following discussion, it is assumed that the medium behaves elastically.

Parkin first correlates the calculated values of radiated energy with the energy released by the explosion. He finds a good correlation of radiated energy with the ratio of released energy to cavity radius. The mechanism of energy release enters as a parameter. Certainly a generalized law, in which the elastic constants of the medium are included, would be of great value.

Parkin next suggests that even though radiated and released energy can be correlated, these two quantities are of such greatly different magnitudes that it is worthwhile to consider two different scale factors. For those effects directly related to the explosion, $W^{1/3}$, the cube root of the yield is to be used, as in conventional procedures; for quantities associated with propagation in the elastic medium, $W'^{1/3}$, the cube root of the radiated energy is introduced.

He presents correlations of the various quantities mentioned above. Only the peak displacement gave a good correlation in dimensionless form. By testing various combinations of dimensionless velocity, acceleration, and stress with the scale factor for the elastic medium, he was able to get quite satisfactory correlations; the poorest was for the acceleration. He finds that if the dimensionless quantities $\frac{u}{W^{1/3}}$, $\frac{\partial u}{\partial t}/c$, and $\frac{\partial^2 u}{\partial t^2}\frac{W^{1/3}}{c^2}$ are multiplied by $\left(W^{1/3}\right)^{-n}$, $n = 0, 1, 2$ for displacement, velocity, or acceleration, respectively, the resulting quantities are inversely proportional to the scaled range $r/W^{1/3}$. Dimensionless radial stress, σ_{rr}/E, when multiplied by $W^{-1/3}$ also is inversely proportional to $r/W^{1/3}$. E is Young's modulus.

This theory was tested by using experimental values of peak particle velocity from the COWBOY cavity shots. The exponent of scaled range turned out to be -1.3, rather than 1.0. He suggests that the disagreement can be explained by dissipation of energy due to plasticity and other inelastic effects in the salt at small strains.

6.4. SYMMETRY OF THE SOURCE

The entire development of the theory of explosion-generated waves has proceeded on the assumption that the source produces a spherically symmetrical stress wave. Very few observations of the azimuthal distribution of wave amplitudes have been published, and some of these are difficult to interpret because of known variations in geological structure between the source and various observing points and differences in the geology at the various recording sites.

The vertical and longitudinal components of motion recorded at short range from small explosions in soil have been found to show negligible variation with azimuth [10, 31]. On the other hand, marked variations in amplitude are found for all components for similar experiments in rock [31].

Denoyer et al. [54] report observations of asymmetrical radiation of P and S waves as recorded at distances of 190 to 285 km in two different directions. They postulate that this variation is caused at least in part by the fact that the source was located in low-velocity basin fill bordered by high-velocity material. The two azimuths (~150° apart) at which the data were available were not oriented in any special way with respect to the axes of the basin. The authors recognized that the differences in local geology at the recording sites and the presence of complicated structure between the source and these sites add to the difficulty of evaluating the hypothesis.

Additional evidence on the extent to which the source is asymmetrical is that underground explosions always generate prominent SH- or Love-type waves [9, 37, 38, 52, 55]. If the source were completely symmetric, horizontally polarized shear waves could not be generated in an isotropic, homogeneous, or horizontally stratified medium. Such motion can be explained by mode conversion at geologic or topographic irregularities along the transmission path and by reflection of P or SV waves from nonhorizontal boundaries. However, insistence that the source is symmetrical requires the introduction of a variety of ad hoc assumptions to explain a regularly observed phenomenon.

Processes in the nonlinear region around the explosion (discussed in earlier parts of this report) seem to be an adequate source of SH-wave generation, and even nonsymmetric P- and Rayleigh-wave generation. Wright and Carpenter [38] suggest cracking in hard rock and instability of the gas-soil boundary in unconsolidated material as possible sources. Kisslinger et al. [37] have suggested radial crack production as the source of SH motion that they have observed.

Apparently no one but Aoki has attempted to calculate the elastic waves proceeding from the nonlinear region, and he starts with the assumption of spherical symmetry. Short has observed that cracking in salt does not occur equally in all directions, but that large cracks extend in a few directions [56]. If this is generally true, it would seem difficult but not impossible to attempt an analysis of the wave motion generated by cracking. The distribution of first-motion amplitude of P and S waves around a growing crack is given by Knopoff and Gilbert [57]. It is necessary to estimate the number and direction of cracks, their rate of growth in terms of the properties of the medium, and the amplitude of displacement normal to the crack.

7
EXPERIMENTAL STUDIES OF WAVE GENERATION BY EXPLOSIONS

Knowledge concerning the characteristics of explosion-generated seismic waves is based primarily on observations, because of the many uncertainties involved in the behavior of the explosion, the coupling to the earth, and the properties of the medium. In preceding sections

some empirical relations have been included along with the theoretical development presented in order to illustrate particular points. This section presents a brief, systematic review of published observations.

It is not practical to discuss each published paper on this subject in detail, owing to the large number in existence. Fortunately, a number of review papers consolidate information from several investigations; such reviews will be the primary source of the material presented herein. Each review paper contains an appropriate bibliography, and the reader interested in the details of experimental methods and conditions will find it advisable to go back to the original papers.

Experimental studies are valuable for gaining insight into the phenomena involved and for predicting the results of further experiments. In the absence of a complete theory, it is important to be able to treat a given experiment as a model of all experiments. This requires an understanding of how the effects of the explosion scale with the various parameters that characterize the experiment. Some scaling relations have been presented in the previous section. A brief discussion of the principles of scaling is presented in the appendix.

The following discussion covers effects of depth of burial, medium, and the combination of yield and distance.

7.1. THE EFFECT OF SOURCE DEPTH

When the effect of the depth of burial on the resulting seismic signal is considered, it is necessary to distinguish between effects on body waves (the P wave in particular) and effects on surface waves. By their very nature, surface waves depend for their existence on the presence of a free surface, and are strongly affected by the distance of the source from this surface [58, 59]. Several studies of surface-wave generation and propagation have been published, but they will not be reviewed here [59, 60, 61, 62].

There is no such direct effect for body waves. It is apparent from the theory presented above, however, that the radial distance at which elastic behavior begins is a function of the lithostatic (or ambient) pressure. In turn, this radius has been shown to directly affect the signal amplitude. Bigger "equivalent cavities" give bigger signals. In a homogeneous medium, the P-wave amplitude can be expected to increase rather sharply as the depth of the charge is increased from zero to that required for complete containment, and then decrease gradually for greater shot depths (increased ambient stress). At most test sites, it is very likely that beds of rock of differing properties are encountered as the shot depth is increased, so that depth alone is not the controlling factor.

Experiments on the effect of source depth on the P wave are subject to some inherent difficulties. If the observations are made at short ranges with fixed detector positions, the effects of source-detector distance may overwhelm the effect of depth. Since absorption losses are imperfectly known, corrections for variations in distance are uncertain. If a seismometer is located on the surface, another problem arises. As is well known, the surface displacement is not the same as the incident displacement, but is a resultant of the incident and reflected waves. The observed displacement is a complicated function of the angle of incidence and the elastic properties of the medium [63]. At short ranges for which the angle of incidence decreases rapidly with increasing depth, therefore, the data must be interpreted with care. The use of deeply buried detectors eliminates this problem.

On the other hand, when observations are made at distances great enough so that the angle of incidence is not greatly affected by the depth, normal geologic conditions will usually result in the first arrival being a head wave from some subsurface boundary. Of course, the effect of depth on this head wave may be of interest, but examination of the direct P wave becomes difficult.

Stengel has studied shot-depth effect for 1.5-lb charges of dynamite [64]; the principal results are reported in a more easily accessible paper by Howell [65]. The depth was varied from 7 to 102 ft, and the media were dolomite, weathered dolomite, and gravel and sand near the surface. A close-in instrument was moved as the depth changed to keep the angle of incidence roughly the same, and an instrument at 200 ft from the shot hole was kept fixed. Relative energy in the wave train was calculated from particle velocity records.

The energy-depth data for the close seismometer oscillate through an order of magnitude for changes in depth of about 10 ft. The extreme excursions are bounded by parallel trends corresponding to an exponential increase of energy with depth, given by $E_d = E_o \exp(0.047\, d)$. The total relative energy at 200 ft is described quite well by the same relation. For the deeper shots a strong refraction arrival increased in energy at a slightly higher rate. Obviously, an exponential increase of relative energy with depth can be valid only for relatively shallow depths.

In his pioneering study of blast effects in soil, Lampson [30] found that at scaled ranges of $r/W^{1/3}$ between 2 and 15, both pressure and positive impulse per unit area were linearly dependent on a coupling factor which depended on depth. This factor for one of the soils in which he worked is presented in Figure 25. The factor has a maximum at a depth of about $2W^{1/3}$ (W in pounds); it falls off rapidly for shallower depths, and more slowly for great depths.

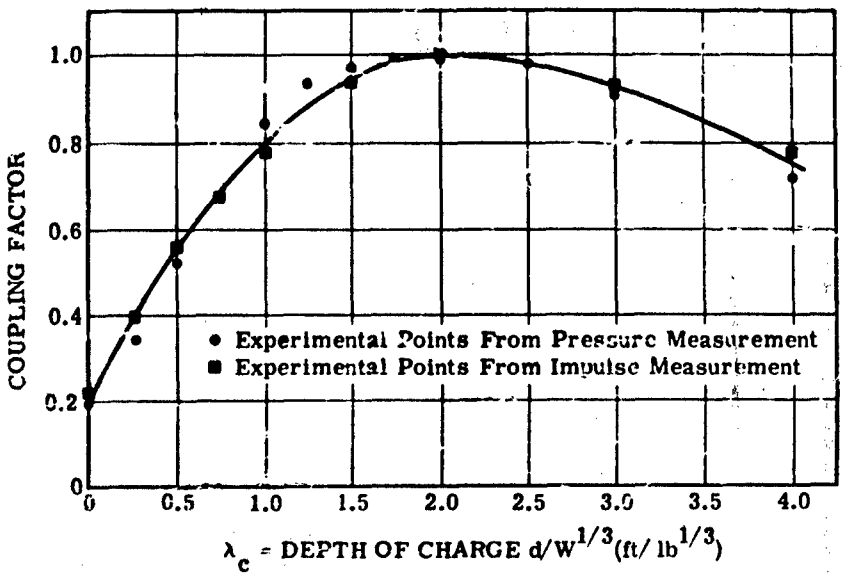

FIGURE 25. EXPLOSIVE COUPLING FACTOR AS A FUNCTION OF DEPTH OF CHARGE: CLAYEY SILT SOIL (After Lampson)

Rocard [66] has recently published results of a preliminary attempt to combine data from a wide variety of sources into a single curve of relative seismic amplitude at long ranges as a function of depth (see Figure 26). The data points b are from numerous small charges recorded at 5 km; n indicates nuclear explosions of the HARDTACK II series; m represents underwater explosions recorded at 110 and 300 km; and g means submarine grenades recorded at 160 to 190 km. All data were scaled to a charge weight of 1.0 kg by dividing the depth by the cube root of the charge weight in kilograms. The curve was developed from pairs of data points corresponding to similar recording conditions and different scaled depths.

The unit of "seismic effect" on this curve was taken as the signal from a half-buried charge. Rocard suggests (private communication) that an explosion that is just deep enough to be contained is a better experimental standard. Such an explosion has a value of about 5 on the curve, so the abscissas should be divided by 5 to give the relative seismic effect in terms of this revised unit. The curve shows an increase by a factor of ~6 at great depth relative to the barely contained charge.

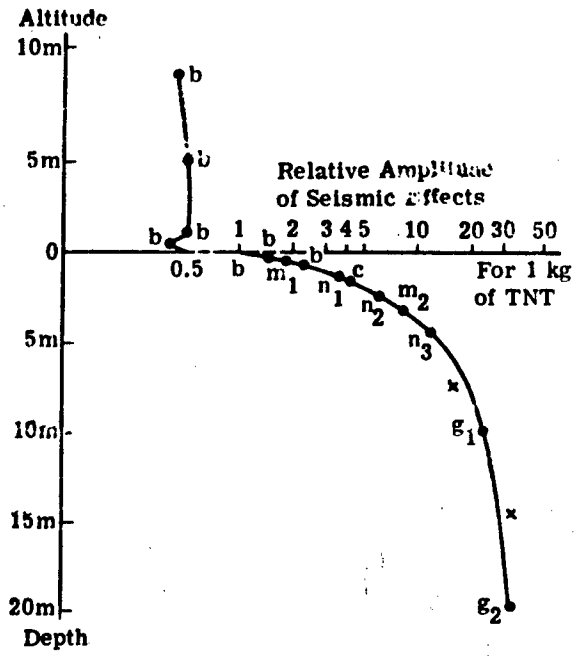

FIGURE 26. RELATIVE AMPLITUDE OF SEISMIC SIGNAL AS A FUNCTION OF DEPTH OR ALTITUDE (After Rocard)

The vertical curve for surface and above-ground detonations of small charges and the discontinuity at depths just below the surface agree roughly, at least, with recent unpublished observations of the present author.

Ricker [67] found an increase in the seismic efficiency of buried charges to a depth of about 100 ft for 1.0-lb charges of dynamite from his experiments in the Pierre shale. Scaled to 1.0 kg, this maximum is at a depth of 40 meters, a result not discordant with Rocard's curve.

Rocard has pointed out (private communication) that the data on the curve (Figure 26) for the deeper shots were obtained from tests in the Mediterranean Sea that were deep compared to the barely contained expolosion, but well above the sea bottom. No data are included from shots so near the bottom that interference from that boundary might alter the results.

Adams and Swift [35] found, for two TNT shots in tuff, that the radiated elastic energy for a shot at a depth of 1010 ft was roughly four times that for a shot at 240 ft. The measured ambient stress was five times as great for the deeper explosions. When scaled to 1.0 kg,

these depths are 44 and 9.4 meters, and an amplitude increase by a factor of 2 is concordant with an extension of Rocard's curve.

7.2. THE EFFECT OF THE MEDIUM

The manner in which the properties of the medium enter into the wave-generation process was indicated in the sections concerning theoretical development. The Hugoniot equation of state, the crushing strength, elastic limit, porosity, fluid content, and brittleness all play roles implied by the equations describing the progress of the pressure pulse.

The value of Poisson's ratio plays a key role in the elastic-wave region at short range, determining whether the pulse is highly oscillatory or pulse-like. The size of the inelastic region and the peak pressure at its boundary (both dependent on the medium) determine the amplitude for a given yield. The predominant period in the P wave depends on the size of the equivalent cavity, the compressional wave velocity, and Poisson's ratio.

As suggested by the quotation from Sharpe at the beginning of this section, a shot in weathered material produces a broader pulse than one in unweathered material, and a shot in hard rock produces a sharper pulse than one in softer material. This has been confirmed experimentally [68]. Field records illustrating the effect of the medium at short ranges are shown in Figure 27 [69]. The limestone records are characterized by much higher frequencies than the other media. At distances over 100 meters, the P wave is attenuated below the level of sensitivity of the instrumentation and the records are dominated by surface waves, which are of much greater amplitude in the soil than in rock.

Although every experimental study of explosion-generated seismic waves includes the effect of the medium, only a few have been devoted specifically to this problem. Lampson [30, p. 26] concludes that the type of soil is the most important single variable governing the transmission of the stress wave from an underground explosion. His work pertains only to soil, of which five different types were included. He defines a soil constant (with dimensions of an elastic modulus) which was found to vary from an average value of 800 for loess to 100,000 for saturated clay. The pressure at a given scaled range was found to depend linearly on this constant. This "constant" is variable over a rather wide range for a given soil, depending on the moisture content and the compaction. A reasonably good correlation of the soil constant and the compressional seismic-wave velocity was found. This is a bit unexpected, since the seismic wave velocity pertains to small strains and the soil constant the entire (nonlinear) stress-strain curve up to the peak stress.

A recent set of experiments, specifically designed to test the effect of the medium on coupling, was carried out for the two media which have received the greatest attention in this

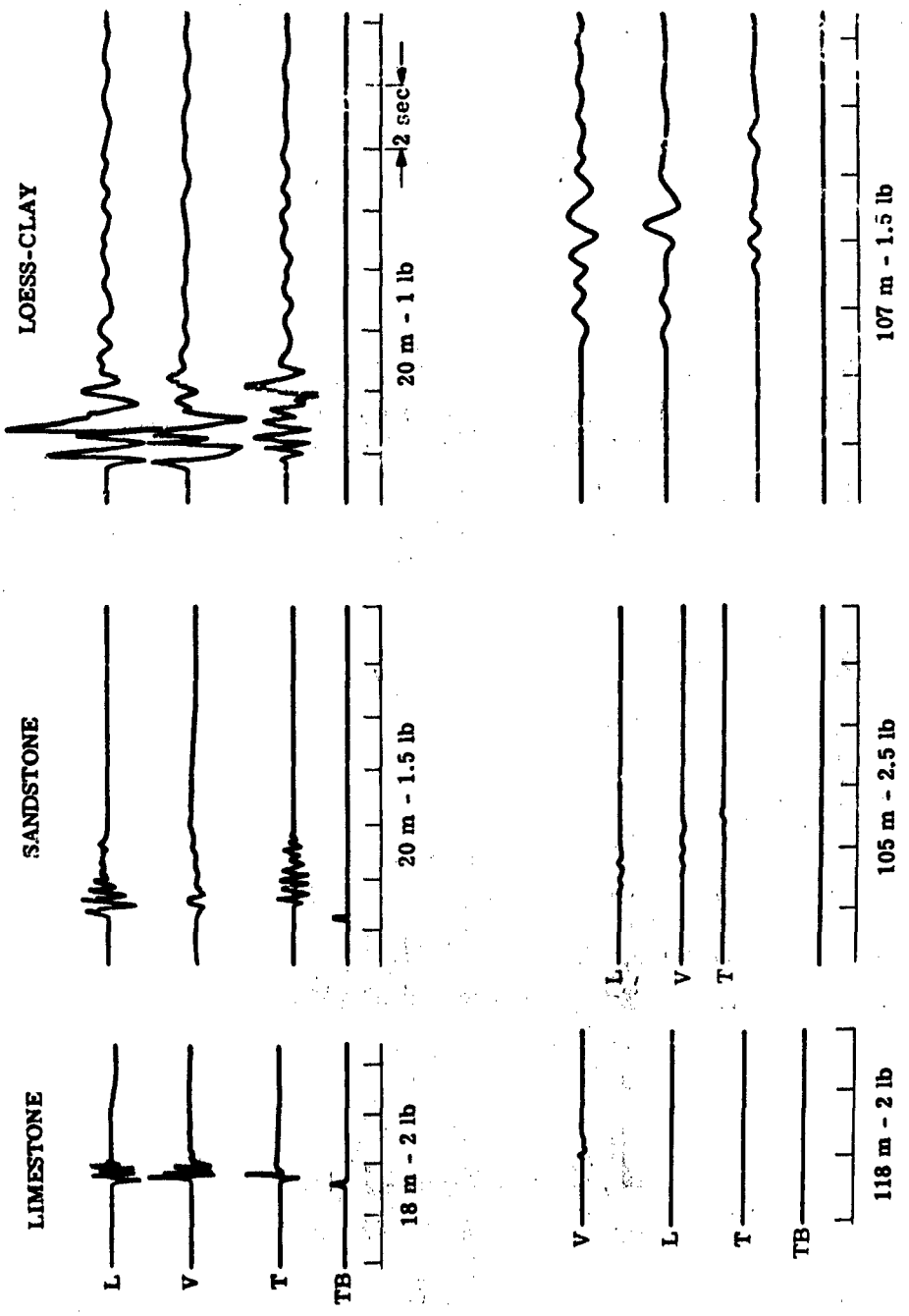

FIGURE 27. RECORDS ILLUSTRATING THE EFFECT OF THE MEDIUM ON THE CLOSE-IN SEISMIC SIGNAL (After Kisslinger)

report: tuff and salt [35]. Charges of granular TNT of 100 to 1000 lb were tamped in holes at depths such that the ambient stress levels were similar. Only the relative strengths of the signals in the two media are investigated, with no attempt to get an absolute coupling coefficient for either. The result, showing the frequency dependence of the medium effect, is presented in Figure 28. The authors (Adams and Swift) conclude that the ratio of signal strength in tuff to that in salt is 1.6 ± 0.4 for the frequency range of 30 to 60 cps. This corresponds to a ratio of energies of roughly 2.6 to 1.

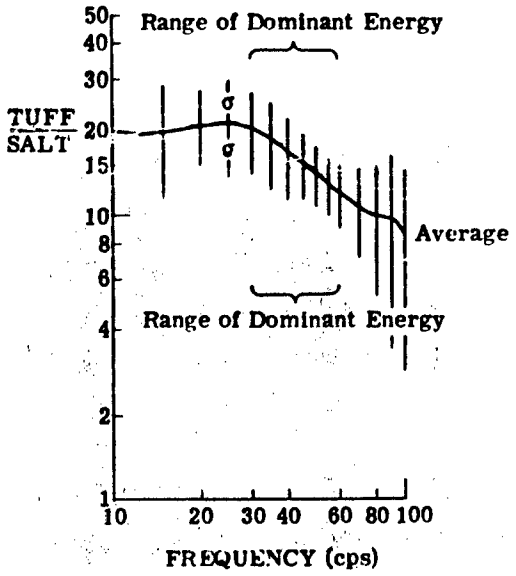

FIGURE 28. MEDIUM COUPLING FOR TUFF TO SALT AS A FUNCTION OF FREQUENCY (After Adams and Swift)

It should be noted that this result is at least partly explained by Nicholl's findings for the effect of the ratio of impedance of the explosive to that of the rock [28]. Nicholl's gives a value for the characteristic impedance of granular TNT of 16.7 lb-sec/in^3 and for salt of 35 lb-sec/in^3. From the density and compressional velocity for tuff at a depth of 1000 ft from Adams and Swift, the impedance of the tuff is 16.5 lb-sec/in^3. Thus, the impedance ratios are 0.48 for salt and 0.99 for tuff. Applying these values to the average curve in Figure 11 of Nicholl's paper, a ratio of energy coupled into the tuff to that in the salt is about 1.4, or a tuff-to-salt signal amplitude ratio of 1.2.

Though the result given by Adams and Swift is a true medium effect, it is valid only for the particular explosive. It even seems possible to reverse the result by using high-velocity

dynamite (impedance of 32.3 lb-sec/in^3), although Nicholls gives no discussion of behavior for impedance ratios greater than 1.0. It would seem that future experiments on the effect of the medium, using chemical charges, should employ several types of explosives.

Werth and Herbst [48] have studied amplitudes of seismic waves generated by nuclear explosions in tuff, salt, granite, and alluvium. They isolate the effect of the medium at the source by including in their analysis the effects of coupling out of the source region and of the crustal structure between the source and the recording site. The theory developed in Reference 1 is applied. All results are scaled to a yield of 5 kt by the $W^{1/3}$ relationship. The amplitudes, at distances of the order of 500 km relative to tuff, are: tuff, 1; alluvium, 0.25; granite, 1.11; and salt, 1.61. If realistic models of the crustal structure are included, the amplitude ratios for the first half-cycle of the head wave from the Mohorovicic discontinuity are: tuff, 1; alluvium, 0.18; granite, 2.26; and salt, 2.11. The result of Adams and Swift for the tuff-to-salt ratio is seen to be reversed.

Although the experimental work under discussion is primarily field work, worthwhile information on the wave-generating process can be gained from laboratory experiments. Such tests lend themselves especially well to work on the properties of the medium, since there is an obvious limit to the range of yields and effective source depths that is practical to investigate.

The basic principles of shock-wave propagation, as outlined in the discussion of the Rankine-Hugoniot equations, have been used directly by Hughes and McQueen [70] to measure rock densities at pressures from 150 to 750 kilobars. Although their objective was to obtain information of direct importance to geophysical studies of the earth's interior, it is obvious from the many comments on the lack of data pertaining to rock properties at high pressures that experiments of this type are highly important to the solution of the present problem.

Ito, Terada, and Sukurai [71] used similar techniques in their investigation of wave generation in sandstone and marble. Shock waves produced by blasting caps and 300-gram high-explosive charges were used to load the specimens. Stress was measured by shock-wave techniques, and strain was directly recorded by suitable gauges.

The stress wave showed a decrease in rise time with increasing peak pressure for marble, but not for sandstone. These conclusions are based on peak pressures from blasting caps of about 0.3 to 1.6 kilobars. Dynamic values of Young's modulus were determined to be two or three times greater than static values; dynamic strength is also greater than static strength. Evidence of plastic flow was found for the explosive charges, but not for the caps.

The internal structure of the marble specimen was altered much more than that of the sandstone for the same loading. This conclusion was reached by running static compression tests on the samples after the shock wave tests. Direct evidence of the low velocity of shock propagation in certain parts of the nonlinear region was found.

The peak pressure was found to decrease very rapidly with distance from the source, and differences in peak pressures for different kinds of explosive materials were evident only in a narrow range close to the source.

7.3. RELATION OF SIGNAL STRENGTH TO RANGE AND YIELD

Whether an investigator is interested in explosion-generated waves from the viewpoint of quarry blasting, seismic exploration, or detection, he obviously is concerned with the manner in which the various parameters associated with the stress wave vary with the yield and the distance from the source. Consequently, the published studies on this aspect of the problem are numerous, and a complete review of all the literature on this subject will not be undertaken.

The effects of the medium around the shot and the depth of the source enter into all of these studies. The results presented herein are empirical relations pertaining to the particular conditions of the test on which they are based, and extrapolation to other situations must be approached cautiously.

A large number of reports have been published covering individual projects connected with the explosion program of the U. S. Atomic Energy Commission. Most of these are in the form of project reports that are not widely accessible. However, papers reviewing large parts of this work have recently appeared in the regular scientific periodicals, and these will be used as the primary references.

The work of the U. S. Coast and Geodetic Survey and several other individuals and organizations on the measurements of surface motion is summarized by Carder and Mickey [72]. Surface displacements and accelerations produced by yields of 180 lb to 19.2 kilotons (equivalent) of TNT have been measured at distances from 0.1 to 900 km. These shots have been fired in salt, tuff, alluvium, limestone, quartzite, and basalt. It will be noted that these measurements are outside of the free-field region, and are influenced by geologic structure and the resulting reflections and refractions. The results are entirely concerned with maximum values of dispalcement and acceleration, without regard to the particular wave type or path with which the values are associated. In a sense, the results do not directly relate to the principal subject of this report, the initial P wave. These results are included, however, because they are certainly a measure of the effectiveness of the explosion as a seismic source.

Peak acceleration data for all shots fired in the Rainier Mesa at the Nevada Test Site are summarized in Figure 29. The ground acceleration prediction formula is

$$a = (2.4 \pm 1.0)\ (W^{0.75}/r^2) \qquad (43)$$

where a = peak acceleration in units of gravity

W = yield in kilotons

r = range in thousands of feet

The data on Figure 29 have been normalized to 1.0 kt by the $W^{0.75}$ law. The formula is intended to be used from outside the free field zone to 5 or 6 km.

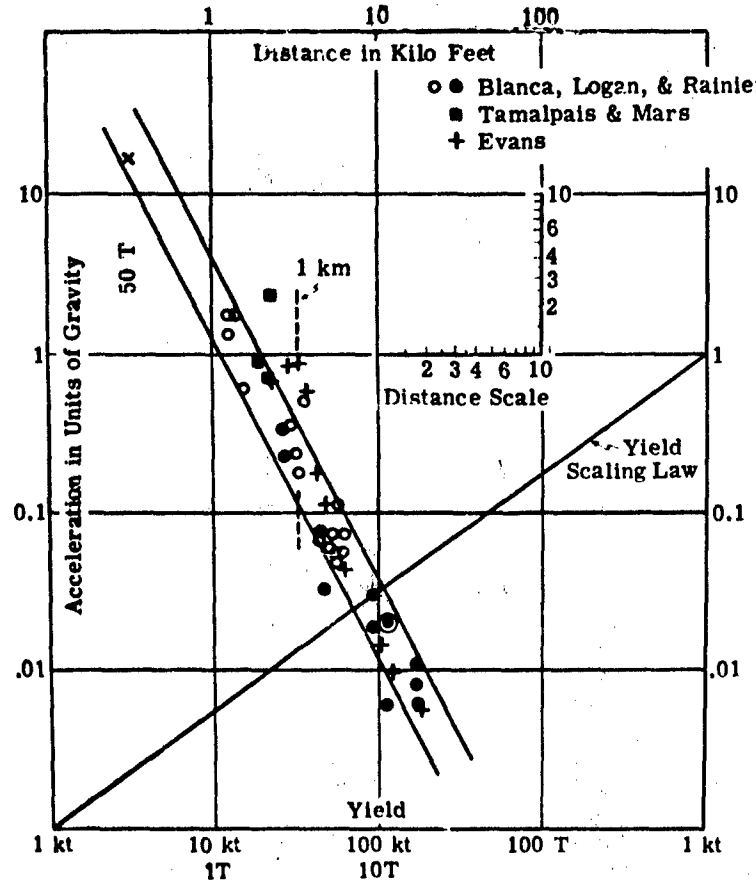

FIGURE 29. ACCELERATION VS. DISTANCE NORMALIZED TO A 1-KILOTON YIELD (After Carder and Mickey)

A general scaling law for maximum earth displacement has gone through a number of revisions. The form offered by Carder and Mickey is

$$A = CW^{0.75}r^{-n} \times 10^{-kf^{0.8}r}$$

where A = maximum surface displacement (cm)

C = a constant

r = source-to-detector distance (ft)

n, k are constants

f = dominant frequency by visual examination (cps)

The values of the constants have been found to depend upon the distance range. With reference to the 300- to 9800-ft range in Figure 30, C is $10^{4/57}$, n is 2, and k is 1.75×10^{-6}; in the 9800-ft to 100-mi range, C is $10^{0.6}$, n is 1, and k is 1.83×10^{-6}. From 100 to 600 mi, C is $10^{-2.82}$, n is 0.5, and k is 7.6×10^{-7}. These amplitudes are multiplied by about 3 for instruments mounted on alluvium.

The work conducted by several agencies on strong motion from underground nuclear shots is summarized in the report by Adams et al. [2]. Since these data were taken in the free-field zone, they pertain directly to the present report. The largest amplitude of acceleration or displacement in the direct wave is used in the studies of surface motion.

Subsurface peak radial acceleration was found to decrease as the cube or fourth power of the slant range. A tendency toward a second or first power dependence is indicated at larger ranges, but is masked by effects produced by local geology. Adams et al. point out that acceleration data, especially those collected at the surface, are greatly affected by the presence of bedding planes or other surfaces of discontinuity in the medium. They also point out that particle velocity may prove to be a better parameter than acceleration to use as a reference, because it is closer in waveform to the stress pulse.

Vertical, radial, and tangential components of surface acceleration were all found to follow the same formula with satisfactory precision:

$$a = W^{0.7}/r^{-2.1} \times 10^{6.5}$$

where a = units of gravity

W = kilotons

r = slant range (ft)

This formula may be compared with that of the Coast and Geodetic Survey by expressing r in thousands of ft. The coefficient in Equation 43 becomes 1.6, near the lower limit of the Coast

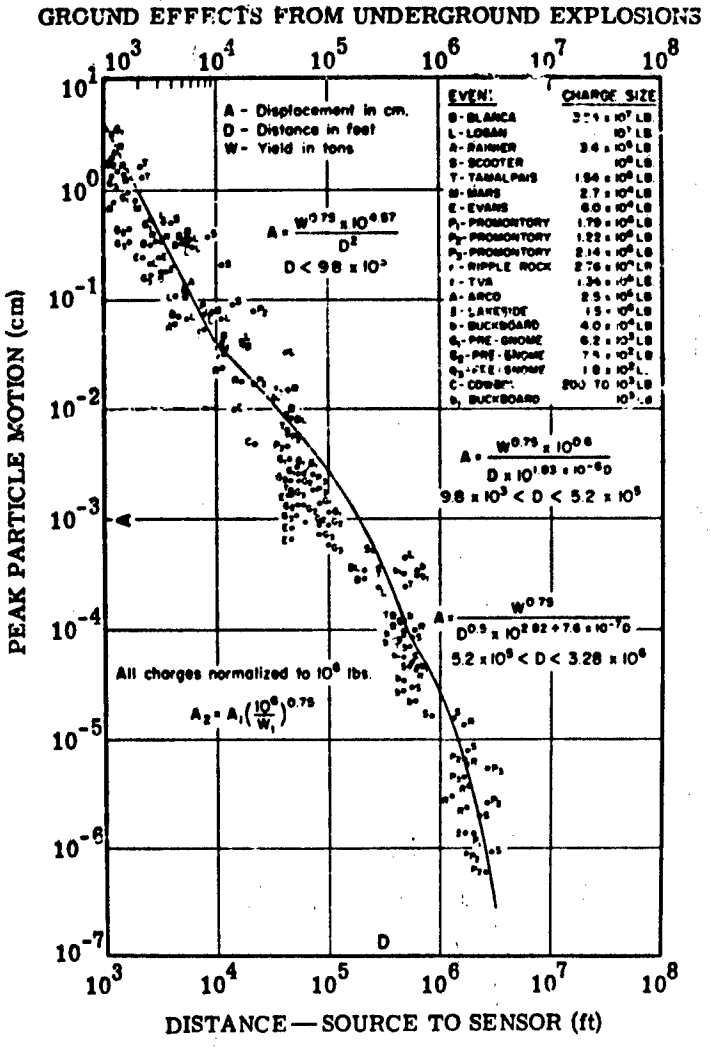

FIGURE 30. PEAK PARTICLE DISPLACEMENT VS. DISTANCE NORMALIZED TO A 10^6-LB YIELD BY THE $W^{-0.75}$ SCALING FUNCTION (After Carder and Mickey)

and Geodetic Survey result. Adams et al. show that this result is not consistent with free-field scaling based on $W^{1/3}$ scaling of length.

On the other hand, the displacement data are found to fit point-source scaling laws much more closely. Each of the three components was found to fit a relationship $A = mW^n r^{-p}$, with slightly different values for the constants. For the vertical component, n was found to be 0.69 and p to be 1.14. The corresponding values for the radial component were 0.94 and 1.68. If the exponent of r is inserted into the scaling relationship for displacement, $A = kW^{(n+1)/3} r^{-n}$, the resulting exponent for W is quite close to the observed value. The authors feels that this follows, in spite of the poor agreement for acceleration, from the fact that the displacment is associated with longer periods and is not so greatly affected by the presence of interfaces.

The exponent of the yield is close to that of the Coast and Geodetic Survey for the vertical and transverse component, and somewhat closer to unity for the radial component. It will be recalled that an exponent of 4/3 or 1.0 was called for at the low-frequency part of the spectrum in the theoretical development, depending on the pulse shape. Peet predicts a value of 0.67 near the maximum of the spectrum. It may be seen from these results that the observed relations fall in the expected range, but that the experimental data are not precise enough to verify the theory. This is not surprising, in view of the nature of explosions and earth materials.

Willis and Wilson [73] have found that the maximum vertical displacement increases as the first power of the yield. This conclusion is based on observations of 13 quarry blasts, two large excavation blasts, and two underground nuclear explosions. It is well known that correlation of signal strengths from quarry blasts are highly variable [74], and depend on such factors as the spacing and burden of the shot and the location of the shot in a given quarry.

On scaling all their data to 1.7 kilotons (RAINIER yield) by means of this $W^{1.0}$ relation, these same authors have found empirical amplitude-yield relations (for r between 1 and 200 km) as follows: $A = (0.65 \pm 0.15) r^{-3/2}$, where A = maximum vertical amplitude (normalized to 1.7 kilotons) in cm, and r = distance in km.

Between 100 and 1000 km,

$$A = (0.013 \pm 0.003) \exp[-(00.72 \pm 0.0003)r] r^{-1/2}$$

64% of the data fall within the envelopes of these equations; the data and empirical curve are shown in Figure 31.

Additional attempts at evolving amplitude-yield-distance equations are also to be found in Berg and Cook [50], Gaskell [75], Habberjam and Whetton [76], Ito [77], Lampson [30], Murphey [36], Obert and Duvall [78], O'Brien [7], and Thoenen and Windes [79]. Some of these are ap-

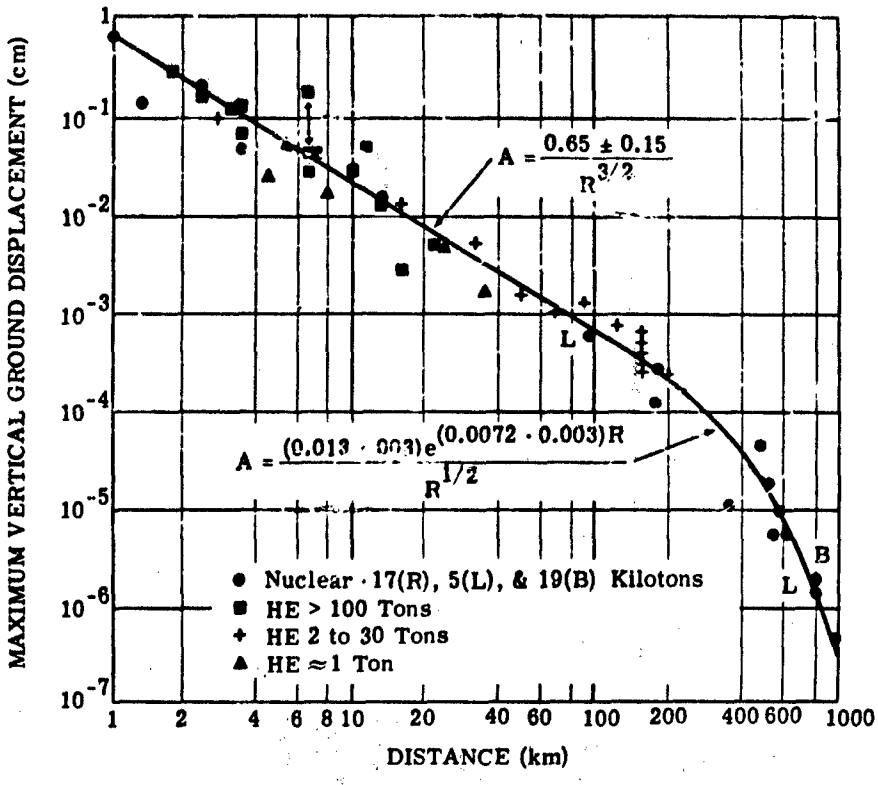

FIGURE 31. PEAK VERTICAL GROUND DISPLACEMENTS FOR EXPLOSIVE BLASTS NORMALIZED TO THE RAINIER EVENT BY THE $W^{1.0}$ SCALING FUNCTION (After Willis and Wilson)

plicable to specific media, e.g., Lampson's work on soils and Murphey's in salt. Others are primarily concerned with quarry blasts, e.g., the pioneering work of Thoenen and Windes, and the studies of Habberjam and Whetton.

Fundamental studies on stress-wave generation are described in a long series of papers by investigators at the U. S. Bureau of Mines. In addition to the report of Obert and Duvall cited above, work by Nicholls [28] and by Fogelson et al. [80] contain data on strain propagation in rocks. References to earlier Bureau of Mines studies may be found in these papers.

There seems little value in recounting here in detail the specific formulas at which these many investigators arrived, since an evaluation of their pertinence requires a full description of the experimental procedures and conditions as well as the methods of analysis. Both O'Brien and Ito present summaries of some of these studies in addition to their original data. Yield de-

pendencies ranging from the 0.4 power to the 1.1 power have been found. O'Brien finds that, for those studies in which $\omega a/c$ (see Section 6.1) is known to be less than 1.0, the first power dependency seems to hold.

Although empirical relations of signal strength and range can be found, any study which ignores attenuation resulting from inelastic behavior of the medium is an oversimplification.

8
SUMMARY AND CONCLUSIONS: THE STATE OF THE ART

The study of explosion-generated seismic waves is still primarily an empirical science. In the absence of a complete theory of the processes that result in the radiated wave, progress in further understanding of the subject is dependent on well designed experiments. Unfortunately, the complex properties of earth materials and geologic structure in which full-scale tests must be carried out make the design of experiments difficult.

It has been seen that the analytic tools needed to develop the theory are known, and seem to be adequate. Numerical techniques exist for evaluating solutions that cannot readily be put into closed form. The greatest need is for additional experimental evidence concerning the nature of the processes involved, so that the theoretical development can be guided along realistic lines. This is particularly true for the terminal nonlinear region. Although both experimental and theoretical work in this zone are difficult, it is in this region that the answers to many of the outstanding questions lie.

Information is required on the dynamic behavior of earth materials (rocks and soils) over all ranges of stress from the vaporization pressure to the region of infinitesimal strains. These data must be collected for a wide variety of materials. The search for correlations between these dynamic properties and convenient laboratory tests should be carried on vigorously.

In the analysis of data relating amplitude to yield, the effect of the properties of the medium and the explosive material cannot be ignored. This is particularly true for chemical explosives. In addition, it is only recently that the influence of ambient stress level or, equivalently, the depth of burial in a particular test site, has been included in a quantitative manner.

Because the relation between amplitude and yield is diagnostic of processes at the source, detailed measurements should be made at every opportunity. The uncontrollable variability of parameters affecting amplitude will make the result of any single experiment of doubtful value for wide application. The results of many experiments may reveal the correct formula. It seems that problems of instrument placement and departures from homogeneity of the earth

between the source and the instrument may be as much a source of variability as the conditions at the source.

The dependence of the amplitude-yield relation on the part of the spectrum that has been observed on a particular seismogram must not be overlooked. Apparent scale effects in going from small to large yields may be explained in terms of the frequency at which the spectrum reaches its peak value and the passband of the surrounding earth.

Appendix
PRINCIPLES OF SCALING AS APPLIED TO UNDERGROUND EXPLOSIONS

Throughout this report, the use of the cube root of the yield $W^{1/3}$ has been used to fix the scale of the explosion. A brief discussion of the principles underlying scaling procedures will be presented. Several authors have treated modeling and the theory of similitude thoroughly, but two in particular have devoted themselves specifically to the ground-shock problem: Lampson [30] and Parkin [81]. Parkin's paper contains an extensive bibliography.

Parkin's discussion is more comprehensive because he considers scaling from one medium to another as well as scaling from one set of dimensions to another in the same medium. He also includes scaling for visco-elastic and elastic-plastic substances, in addition to elastic media. Only the case in which a single medium is involved will be included here. From another viewpoint, it is assumed that in going from one explosion (treated as a model of all explosions in a given medium) to another, the velocity of elastic wave propagation does not depend on the scale of the experiment.

The scale factor is designated by S, and relates lengths in two experiments by $L_2 = SL_1$. On the assumption that the velocity of propagation is independent of the scale, the time will scale in the same manner; i.e., $T_2 = ST_1$. The third dimension needed to describe the quantities involved in the analysis, mass, is treated by using density as a parameter characterizing the medium, and then $M_2 = \rho S^3 L^3$, or $M_2 = S^3 M_1$.

These fundamental dimensions can be introduced into a dimensional analysis of any of the quantities of interest in order to determine the scaling relations. For example, stress, with dimensions $ML^{-1}T^{-2}$, scales to $S^3 M S^{-1} L^{-1} \cdot T^{-2} L^{-2} = ML^{-1}T^{-2}$, so that at the scaled distance SL, at time ST, the same stress is predicted as was observed at L and T in the original system. A similar result follows for particle velocity. On the other hand, particle displacement u at a distance r would appear as a displacement Su at a distance Sr in the new system. It must be understood that this analysis tells nothing about how the quantities vary with distance; one does not find the value at a distance other than the scaled distance from such considerations.

The choice of the scale factor is arbitrary. In the case of an underground explosion, the scale of the experiment is certainly set by the yield. For a spherical charge of weight W, of constant density, the radius of the explosive charge becomes a length representative of the scale. For this reason, a length numerically equal to the cube root of yield has been selected as the scale length. If charge weight is thought of as equivalent to energy, the cube root of the weight obviously does not have dimensions of length. Actually this is no problem as long as the origin and function of this number are understood. However, in order to remove this

apparent inconsistency, Parkin [27, 81] has suggested dividing the explosive energy W by a quantity having dimensions of stress. A quantity with dimensions of L^3 is obtained. He uses the value of Young's modulus as a characteristic quantity for an elastic medium with the dimensions of stress.

Table II is taken from Lampson [30] and summarizes the manner in which frequently occurring quantities scale. Parkin gives a more general table, valid for going from one medium to another as long as Poisson's ratio is the same in both.

TABLE II. MODEL-LAW RELATIONS

The ratio of scales is S which represents a multiplication of all linear dimensions of the experiment by this factor, where $S = (W_2/W_1)^{1/3}$.

Quantity (1)	Symbol (2)	Dimensions (3)	Dimensions in New System (4)	Scale Factor (5)	Quantity in New System (6)	Quantities Comparable at a Constant Value of r/S (7)
Length	L	L	SL	S	SL	L/S
Mass	M	ρL^3	$\rho S^3 L^3$	S^3	S^3M	M/S^3
Time	T	T	ST	S	ST	T/S
Force	F	MLT^{-2}	S^2LT^{-2}	S^2	S^2F	F/S^2
Energy	E	ML^2T^{-2}	$S^3ML^2T^{-2}$	S^3	S^3E	E/S^3
Pressure	P	$ML^{-1}T^{-2}$	$ML^{-1}T^{-2}$	1	P	P
Velocity	v	LT^{-1}	LT^{-1}	1	v	v
Total Impulse	I'	MLT^{-1}	S^3MLT^{-1}	S^3	S^3I'	I/S^3
Impulse per Unit Area	I	$ML^{-1}T^{-1}$	$SML^{-1}T^{-1}$	S	SI	I/S
Displacement		L	SL	S	SD	D/S
Acceleration	a	LT^{-2}	$S^{-1}LT^{-2}$	S^{-1}	$S^{-1}a$	Sa

REFERENCES

1. G. C. Werth, R. F. Herbst, and D. L. Springer, "Amplitudes of Seismic Arrivals from the M Discontinuity," Jour. Geophys. Res., 1962, Vol. 67, No. 4, pp. 1587-1610.
2. W. M. Adams et al., "Summary Report of Strong-Motion Measurements, Underground Nuclear Detonations," Jour. Geophys. Res., 1961, Vol. 66, No. 3, pp. 903-942.
3. J. A. Sharpe, "The Production of Elastic Waves by Explosion Pressures, I," Geophysics, 1942, Vol. 18, No. 2, pp. 144-154.
4. W. I. Duvall, "Strain-Wave Shapes in Rock Near Explosions," Geophysics, 1953, Vol. 18, No. 2, pp. 310-323.
5. F. G. Blake, Jr., "Spherical Wave Propagation in Solid Media," Jour. Acoust. Soc. Amer., 1952, Vol. 24, No. 2, pp. 211-215.
6. G. Morris, "Some Considerations of the Mechanism of the Generation of Seismic Waves by Explosives," Geophysics, 1950, Vol. 15, No. 1, pp. 61-69.
7. P. N. S. O'Brien, "Seismic Energy from Explosions," Geophys. Jour., 1960, Vol. 3, pp. 29-44.
8. H. Linsser, "The Generation of Seismic Waves by Explosions," Early Papers and History of the Eur. Assoc. of Explor. Geophys., 1961, pp. 54-64.
9. B. F. Howell and E. K. Kaukonen, "Attenuation of Seismic Waves Near an Explosion," Bull. Seis. Soc. Amer., 1954, Vol. 44, No. 3, pp. 481-492.
10. H. Aoki, "Seismic Waves in the Region Near Explosive Origin," Jour. Earth Sciences, Nagoya Univ., 1960, Vol. 8, No. 2, pp. 120-173.
11. L. E. Fugelso, Analytic Study of Early Deformation from an Underground Explosion, Semi-Annual Tech. Report MR1167, Amer. Mach. and Found., 1962.
12. V. Cushing and D. Reily, Characteristic Emissions from an Underground Explosion, First Semi-Annual Report, Engineering Physics Company Proj. No. 109, 1962.
13. R. H. Bishop, "Theory of Wave Propagation from Spherical Explosions," Part IV of Close-In Phenomena of Buried Explosions, Second Semi-Annual Report, Contr. No. DASA-EO-300-60, Sandia Corporation, 1962, pp. 39-149.
14. R. H. Cole, Underwater Explosions, Princeton University Press, Princeton, 1948.
15. M. A. Cook, The Science of High Explosives, Reinhold, New York, 1958.
16. H. Jones and A. R. Miller, "The Detonation of Solid Explosives: the Equilibrium Conditions in the Detonation Wave Front and the Adiabatic Expansion of the Products of Detonation," Proc. Roy. Soc. London, 1948, Series No. 194, pp. 480-507.
17. M. H. Rice, R. G. McQueen, and J. M. Walsh, "Compression of Solids by Strong Shock Waves," Solid State Physics, 1958, Vol. 6, pp. 1-64.
18. M. A. Chaszeyka and F. B. Porzel, Study of Blast Effects in Soil, Final Report of Project No. D119, Illinois Inst. Tech. Armour Res. Found., 1958.

19. F. B. Porzel, "Close-In Shock Time-of-Arrival Measurements and Hydrodynamic Yield," Proc. Second Plowshare Symposium, Part I, 1959, U. of Calif., Livermore, Lawrence Radiation Lab., UCRL-5675, pp. 28-49.

20. O. K. Ehlers and A. F. Grum, Theoretical Background and Derivation of Selected Equations from the Report "Study of Blast Effects in Soil," Tech. Rept. 1573-TR, U. S. Army Engineer Res. and Dev. Labs., 1959.

21. G. Taylor, "The Formation of a Blast Wave by a Very Intense Explosion, I," Proc. Roy. Soc. London, 1950, Series A, No. 201, pp. 159-174.

22. M. A. Chaszeyka, Studies of Surface and Underground Nuclear Explosions, Final Report on Contr. No. DA-44-009-ENG-3998, Illinois Inst. Tech., Armour Res. Found, 1961.

23. J. H. Nuckolls, "A Computer Calculation of Rainier," Proc. Second Plowshare Symposium, Part I, 1959, U. of Calif., Livermore, Lawrence Radiation Lab., UCRL-5675, pp. 28-49.

24. W. E. Peet, "A Shock Wave Theory for the Generation of the Seismic Signal Around a Spherical Shot Hole," Geophys. Prosp., 1960, Vol. 8, No. 41, pp. 509-533.

25. J. W. Tukey, "Phase Compensation," Annex A to Appendix 9, The Need for Fundamental Research in Seismology, Rept. of Panel on Seismic Improvement, U. S. Dept. State, pp. 80-87, 1959.

26. H. L. Brode, Cavity Explosion Calculations for the COWBOY Program, RM-2624-AEC, The RAND Corporation, 1960.

27. B. R. Parkin, Elastic Wave Calculations for the COWBOY Program, RM-3105-AEC, The RAND Corporation, 1962.

28. Harry R. Nicholls, "Coupling Explosive Energy to Rock," Geophysics, 1962, Vol. 27, No. 3, pp. 305-316.

29. D. H. Clewell and R. F. Simon, "Seismic Wave Propagation," Geophysics, 1950, Vol. 15, No. 1, pp. 50-60.

30. C. W. Lampson, Final Report on Effects of Underground Explosions, Office of Scientific Research and Development, Rept. No. 6645, 1946.

31. J. C. Jaeger, Elasticity, Fracture and Flow, John Wiley, New York, 1956.

32. N. V. Zvolinskii, "On the Radiation of an Elastic Wave from a Spherical Explosion in the Ground," Prikladniya Matemat. Mekhan., 1960, Vol. 24, pp. 126-133.

33. N. A. Haskell, "A Static Theory of the Seismic Coupling of a Contained Underground Explosion," Jour. Geophys. Res., 1961, Vol. 66, No. 9, pp. 2937-2944.

34. D. B. Lombard, The Hugoniot Equation of State of Rocks, U. of Calif., Livermore, Lawrence Radiation Lab., UCRL-6311, 1961.

35. W. M. Adams and L. M. Swift, "The Effect of Shotpoint Medium on Seismic Coupling," Geophysics, 1961, Vol. 26, No. 6, pp. 765-771.

36. B. F. Murphey, "Particle Motions Near Explosions in Halite," Jour. Geophys. Res., 1961, Vol. 66, No. 3, pp. 947-958.

37. C. Kisslinger, E. J. Mateker, and T. V. McEvilly, "SH Motion From Explosions in Soil," Jour. Geophys. Res., 1961, Vol. 66, No. 10, pp. 3487-3496.

38. J. K. Wright and E. W. Carpenter. "The Generation of Horizontally Polarized Shear Waves by Underground Explosions," Jour. Geophys. Res., 1962, Vol. 67, No. 5, pp. 1957-1963.

39. J. Vanek, "A Contribution to the Theory of Elastic Waves Produced by Shock," Czech. Jour. Phys., 1953, Vol. 3, pp. 97-119.

40. J. Vanek, "On the Magnitude of the Transitional Zone for Elastic Waves Produced by Different Shock-Exciting Functions," Transactions of the Geophysical Institute of the Czechoslovak Academy of Sciences, No. 25, Geofysikalni Sbornik, 1955.

41. J. Vanek, "Transitional Zone in the Classical Region for Explosions in Solid Materials, Czech. Jour. Phys., 1954, Vol. 4, pp. 247-248.

42. W. M. Adams, and D. C. Allen, "Seismic Decoupling for Explosions in Spherical Underground Cavities," Geophysics, 1961, Vol. 26, No. 6, pp. 772-799.

43. R. F. Herbst, G. C. Werth, and D. L. Springer, "Use of Large Cavities to Reduce Seismic Waves from Underground Explosions," Jour. Geophys. Res., 1961, Vol. 66, No. 3, pp. 959-978.

44. A. L. Latter et al., "A Method of Concealing Underground Nuclear Explosions," Jour. Geophys. Res., 1961, Vol. 66, No. 3, pp. 943-946.

45. E. W. Carpenter, R. A. Savill, and J. K. Wright, "The Dependence of Seismic Signal Amplitudes on the Size of Underground Explosions," Geophys. Jour., 1962, Vol. 6, No. 4, pp. 426-440.

46. A. L. Latter, E. A. Martinelli, and E. Teller, "A Seismic Scaling Law for Underground Explosions," Phys. of Fluids, 1959, Vol. 2, No. 3, pp. 280-282.

47. D. E. Weston, "The Low Frequency Sealing Laws and Source Levels for Underground Explosions and Other Disturbances," Geophys. Jour. Roy. Astr. Soc., 1960, Vol. 3, No. 2, pp. 191-202.

48. G. C. Werth, and R. F. Herbst, Comparison of Amplitudes of Seismic Waves from Nuclear Explosions in Four Media, U. of Calif., Livermore, Lawrence Radiation Lab., UCRL-6962, 1962.

49. B. F. Howell and D. Budenstein, "Energy Distribution in Explosion-Generated Seismic Pulses," Geophysics, 1955, Vol. 20, No. 1, pp. 33-52.

50. J. W. Berg, Jr., and K. L. Cook, "Energies, Magnitudes, and Amplitudes of Seismic Waves from Quarry Blasts at Promontory and Lakeside, Utah," Bull. Seis. Soc. Amer., 1961, Vol. 51, No. 3, pp. 389-400.

51. D. T. Griggs and F. Press, "Probing the Earth with Nuclear Explosions," Jour. Geophys. Res., 1961, Vol. 66, No. 1, pp. 237-258.

52. F. Press and C. Archambeau, "Release of Tectonic Strain by Underground Nuclear Explosions," Jour. Geophys. Res., 1962, Vol. 67, No. 1, pp. 337-344.

53. K. Aki, "Study of Earthquake Mechanism by a Method of Phase Equalization Applied to Rayleigh and Love Waves," Jour. Geophys. Res., 1960, Vol. 65, No. 2, pp. 729-740.

54. J. De Noyer, D. E. Willis, and J. T. Wilson, "Observed Asymmetry of Amplitudes from a High Explosive Source," Bull. Seis. Soc. Amer., 1962, Vol. 52, No. 1, pp. 133-138.

55. D. S. Carder and W. K. Cloud, "Surface Motions from Large Underground Explosions," Jour. Geophys. Res., 1959, Vol. 64, No. 10, pp. 1471-1487.

56. N. M. Short, Fracturing of Rock Salt by a Contained High Explosive, U. of Calif., Livermore, Lawrence Radiation Lab., UCRL-6054. 1960.

57. L. Knopoff, and F. Gilbert, "First Motion from Seismic Sources," Bull. Seis. Soc. Amer., 1960, Vol. 50, No. 1, pp. 117-134.

58. M. Ewing, W. Jardetsky, and F. Press, "Elastic Waves in Layered Media," McGraw-Hill, New York, 1957.

59. L. G. Howell, N. F. Neuenschwander, and A. L. Pierson, "Gulf Coast Surface Waves," Geophysics, 1953, Vol. 15, No. 1, pp. 41-53.

60. M. B. Dobrin, R. F. Simon, and P. L. Lawrence, "Rayleigh Waves from Small Explosions," Trans. Amer. Geophys. Union, 1951, Vol. 32, No. 6, pp. 822-832.

61. G. V. Keller, "Dispersion of Seismic Waves Near a Small Explosion," Trans. Amer. Geophys. Union, 1955, Vol. 36, No. 6, pp. 1035-1043.

62. J. W. C. Sherwood and T. W. Spencer, "Signal-to-Noise Ratio and Spectra of Explosion-Generated Rayleigh Waves," Bull. Seis. Soc. Amer., 1962, Vol. 52, No. 3, pp. 573-594.

63. O. W. Nuttli, and J. D. Whitmore, "An Observational Determination of the Variation of the Angle of Incidence of P Waves with Epicentral Distance," Bull. Seis. Soc. Amer., 1961, Vol. 51, No. 21, pp. 269-276.

64. E. Stengel, Effect of Shot Depth on the Generation of Seismic Energy, Tech. Rept. 2, ONR Proj. NRO81-12, Penn. State Univ., 1955.

65. B. F. Howell, "Ground Vibrations Near Explosions, II," Earthquake Notes, 1957, Vol. 28, No. 4, pp. 21-28.

66. Y. Rocard, "Effect of Depth or Height of an Explosion on Seismic Signals," Acad. Sci. Paris Compt. Rend., 1962, Vol. 254, No. 13, pp. 2404-2406.

67. N. A. Ricker, "The Form and Laws of Propagation of Seismic Wavelets," Geophysics, 1953, Vol. 15, pp. 10-40.

68. G. R. Pickett, "Seismic Wave Propagation and Pressure Measurements Near Explosions," Quart. Colo. School Mines, 1955, Vol. 50, No. 4, pp. 1-78.

69. C. Kisslinger, Seismic Waves Generated by Chemical Explosions, Semi-Annual Tech. Report No. 1, Contr. AF 19(604)-7402, St. Louis University, 1961.

70. D. S. Hughes and R. G. McQueen, "Density of Basic Rocks at Very High Pressures," Trans. Amer. Geophys. Union, 1958, Vol. 39, No. 5, pp. 959-966.

71. I. Ito, M. Terada, and T. Sakurai, "Stress Waves in Rocks and Their Effects on Rock Breakage," Mem. Fac. Eng., Kyoto Univ., 1960, Vol. 22, No. 1, pp. 12-29.

72. D. S. Carder, and W. V. Mickey, "Ground Effects from Underground Explosions," Bull. Seis. Soc. Amer., 1962, Vol. 52, No. 1, pp. 67-76.

73. D. E. Willis and J. T. Wilson, "Maximum Vertical Displacement of Seismic Waves Generated by Explosive Blasts," Bull. Seis. Soc. Amer., 1960, Vol. 50, No. 3, pp. 455-460.

74. J. B. Macelwane, et al., The Variability of Vibrations from Quarry Blasts, St. Louis Univ., Inst. of Tech., 1948.

75. T. E. Gaskell, "The Relation Between Size of Charge and Amplitude of Refracted Wave," Geophys. Prosp., 1956, Vol. 4, No. 2, pp. 185-193.

76. G. M. Habberjam and J. T. Whetton, "On the Relationship Between Seismic Amplitude and Charge of Explosive Fired in Routine Blasting Operations," Geophysics, 1952, Vol. 17, No. 1, pp. 116-128.

77. I. Ito, "On the Relationship Between Seismic Ground Amplitude and the Quantity of Explosives in Blasting," Mem. Fac. Eng., Kyoto Univ., 1953, Vol. 15, No. 2, pp. 79-87.

78. L. Obert and W. I. Duvall, Generation of Strain Waves in Rock, Part I, U. S. Bur. Mines, Rept. of Invest., No. 4683, 1950.

79. J. R. Thoenen and S. L. Windes, Seismic Effects of Quarry Blasting, U. S. Bur. Mines, Bull. 442, 1942.

80. E. E. Fogelson, T. C. Atchison, and W. I. Duvall, "Propagation of Peak Strain and Strain Energy for Explosion-Generated Strain Pulses in Rock," Third Symposium on Rock Mechanics, Quart. Colo. Sch. Mines, 1959, Vol. 54, No. 3, pp. 271-284.

81. B. F. Parkin, A Review of Similitude Theory in Ground Shock Problems, RM-2173, The RAND Corporation, 1958.

BIBLIOGRAPHY

Båth, M., and E. Tryggvason, "Amplitudes of Explosion-Generated Seismic Waves. Part I: Icelandic Explosions in 1959 and 1960," Geofisica Pura e Applicata, 1962, Vol. 51, pp. 91-99

Ben-Menahem, A., and H. Cisternas, The Dynamic Response of an Elastic Half-Space to an Explosion in a Spherical Cavity, Contr. No. 1098, Div. Geol. Sci., Cal. Inst. Tech., 1962

Brinkley, S. R., and J. G. Kirkwood, "Theory of Propagation of Shock Waves," Phys. Rev., 1947, Vol. 71, No. 9, pp. 606-611

Carder, D. S., "Seismic Investigations of Large Explosions," Jour. Coast & Geod. Survey, 1948, No. 1, pp. 71-73

Carder, D. S., W. V. Mickey, L. M. Murphy, W. K. Cloud, J. N. Jordan, and D. W. Gordon, Seismic Waves from an Underground Explosion in a Salt Bed, Project GNOME, U. S. Coast and Geod. Survey Internal Report, 1962.

Diment, W. H., S. W. Stewart, and J. C. Roller, "Maximum Ground Acceleration Caused by Nuclear Explosions at Distances of 5 to 300 Kilometers," U. S. Geol. Survey, Prof. Paper 400B: B160-B161, 1960

Dix, C. H., "The Mechanism of Generation of Long Waves from Explosions," Geophysics, 1955, Vol. 20, No. 1, pp. 87-103

Dobyns, D. R., "A Study of Seismic Character and Energy Return from Shooting High and Low Velocity Explosives," Geophysics, 1947, Vol. 12, No. 4, pp. 618-638

Duvall, G. E., "Concepts of Shock Wave Propagation," Bull. Seism. Soc. Amer., 1962, Vol. 52, No. 4, pp. 869-894

Fugelso, L. E., "Analytic Study of Early Deformation from an Underground Explosion," DASA Report No. 1297, Final Technical Report MR1167, American Mach. and Found., 1962

Grine, D. R. and G. R. Fowles, "The Attenuation of Shock Waves in Solid Materials with Seismic Applications," Third Symposium on Rock Mechanics, Quart. Colo. Sch. Mines, 1959, Vol. 54, No. 3, pp. 251-269

Grossling, B. F., "Seismic Waves from the Underground Atomic Explosion in Nevada," Bull. Seism. Soc. Amer., 1959, Vol. 49, No. 1, pp. 11-32

Hamada, H. (Editor), "Symposium on the Equation of State for Earth Materials," SWC TDR 62-126, Air Force Special Weapons Center, Kirkland AFB, N. M., 1962

Howell, B. F., Jr., "Energy Represented by Seismic Waves from Small Explosions," Publications de Bureau Central Seismologique International, Serie A, Travaux Scientifiques, Fasc. 20, 1957

Howell, B. F., "Ground Vibrations Near Explosions," Bull. Seism. Soc. Amer., 1949, Vol. 39, No. 4, pp. 284-310

Hudson, D. E., I. L. Alford, and W. D. Iwan, "Ground Accelerations Caused by Large Quarry Blasts," Bull. Seism. Soc. Amer., 1961, Vol. 51, No. 2, pp. 191-202

Ikegami, R., "On Ground Vibrations Caused by Explosions," Bull. Earthq. Res. Inst. Tokyo Univ., 1951, Vol. 29, No. 1, pp. 197-208

Inst. Fiz. Zemli im. O. Yu. Shmidta, "Seismic Effect of Underground Explosions," Trudy No. 15(182), Akad. Nauk USSR, 1960

Johnson, G. W., G. H. Higgins, and C. E. Violet, "Underground Nuclear Detonations," Jour. Geophys. Res., 1959, Vol. 64, No. 10, pp. 1457-1479

Lamb, G. L., Jr., Some Seismic Effects of Underground Explosions in Cavities, Rept. LA-2405, Los Alamos Scientific Lab., 1960

Langefors, U., H. Westerberg, and B. Kihlstrom, "Ground Vibrations in Blasting," Parts I, II, III, Water Power, Sept., Oct., Nov., 1958

Latter, A. L., E. A. Martinelli, J. Mathews, and W. G. McMillan, "The Effect of Plasticity on Decoupling of Underground Explosions," Jour. Geophys. Res., 1961, Vol. 66, No. 9, pp. 2929-2936

Leet, L. D., "Blasting Vibration Effects," Part I, II, III, Explosives Engineer, 1950-1951, Vol. 28, No. 6, p. 176; Vol. 29, No. 1, p. 12; Vol. 29, No. 2, p. 42

Lombard, D. B., and D. V. Power, Close-in Shock Studies, Preliminary Report, Project GNOME, UCRL, March 22, 1962

McKeown, F. A. and D. D. Dickey, "Some Relations Between Geology and Effects of Underground Nuclear Explosions at Nevada Test Site, Nye County, Nevada," U. S. Geol. Survey, Prof. Paper 400B, pp. B415-418, 1960

McReady, H. S., "Shot Hole Characteristics in Reflection Seismology," Geophysics, Vol. 5, No. 4, pp. 373-380

Meecham, W. C., and J. DeNoyer, "Azimuthal Asymmetry of a Point Source in a Cylindrical Low Velocity Medium," Bull. Seis. Soc. Amer., 1962, Vol. 52, No. 1, pp. 139-144

Nash, H. E. and J. M. Martin, "Significance of Some Fundamental Properties of Explosives with Special Reference to Geophysical Prospecting," Geophysics, 1936, Vol. 1, pp. 239-251

O'Brien, P. N. S., "The Relationship Between Seismic Amplitude and Weight of Charge," Geophys. Prosp., 1957, Vol. 5, No. 3, pp. 349-352

Richard, H. and H. Pieuchot, "Seismic Efficiency of Explosives," Geophys. Prosp., 1956, Vol. 4, No. 2, pp. 167-184

Romney, C., "Amplitudes of Seismic Body Waves from Underground Nuclear Explosions," Jour. Geophys. Res., 1959, Vol. 64, No. 10, pp. 1489-1498

Shock, L., "The Progressive Detonation of Multiple Charges in a Single Seismic Shot," Geophysics, 1950, Vol. 15, No. 2, pp. 208-218

Taylor, J., G. Morris, and T. C. Richards, "The Effect of Velocity of Detonation on the Efficiency of Explosives used in Seismic Prospecting," Geophysics, 1946, Vol. 11, No. 3, pp. 350-361

Willis, D. E., A Study of Seismic-Wave Propagation and Detection, U. of Mich., Inst. of Sci. and Tech., IST Rept. No. 2945-19-F, 1960

Willis, D. E. and J. T. Wilson, "Effects of Decoupling on Spectra of Seismic Waves," Bull. Seis. Soc. Amer., 1962, Vol. 52, No. 1, pp. 123-131

Wright, J. K., E. W. Carpenter, and R. A. Savill, "Some Studies of the P Waves from Underground Nuclear Explosions," Jour. Geophys. Res., 1962, Vol. 67, No. 3, pp. 1155-1160

Yoshikawa, Soji, "The Ground Motion Near Explosion," Disaster Prevention Research Institute, Bull. No. 49, November 1961

DISTRIBUTION LIST

Advanced Research Projects Agency, The Pentagon, Washington 25, D. C.

ATTN: Dr. Charles C. Bates

Air Force Cambridge Research Laboratory, Headquarters, L. G. Hanscom Field, Bedford, Massachusetts

ATTN: Capt. Robert A. Gray, USAF, CRZGW (5)

Air Force Office of Scientific Research, Washington 25, D. C.

ATTN: SRPG, Major William J. Best, USAF (5)

Air Force Technical Applications Center, Washington 25, D. C.

ATTN: TD-1, Lt. Col. Rideaour (5)

Allied Research Associates, Incorporated, Virginia Road, Concord, Massachusetts

ATTN: Mr. Arnold Glaser

Armed Services Technical Information Agency, Arlington Hall Station, Arlington 12, Virginia (20)

Armour Research Foundation, Illinois Institute of Technology, Technology Center, Chicago 16, Illinois

ATTN: Mr. Andrew Unger

Army Engineer Research and Development Laboratories, U. S., Fort Belvoir, Virginia

ATTN: Mine Detection Branch

Roland F. Beers, Incorporated, P. O. Box 23, Alexandria, Virginia

ATTN: Roland F. Beers

Bell Telephone Laboratories, Murray Hill, New Jersey

ATTN: Dr. Bruce P. Bogert

Bell Telephone Laboratories, Room 1A-218, Murray Hill, New Jersey

ATTN: Dr. John W. Tukey

Bell Telephone Laboratories, Whippany, New Jersey

ATTN: Dr. R. A. Walker

Bell Telephone Laboratories, Western Electric Company, Whippany, New Jersey

ATTN: C. F. Wolbush

Bureau of Mines, U. S., Applied Physics Research Laboratory, College Park, Maryland

ATTN: Dr. Leonard Obert

Bureau of Ships, U. S., Code 689 D, Washington 25, D. C.

ATTN: Mr. A. H. Sabol

California Institute of Technology, Seismological Laboratory, 220 North San Rafael Avenue, Pasadena, California

ATTN: Dr. Hugo Benioff

California Institute of Technology, Seismological Laboratory, 220 North San Rafael Avenue, Pasadena, California

ATTN: Dr. L. Knopoff

California Institute of Technology, Seismological Laboratory, 220 North San Rafael Avenue, Pasadena, California

ATTN: Dr. Frank Press

University of California, Lawrence Radiation Laboratory, Livermore, California

ATTN: Dr. Roland F. Herbst, Dr. Charles E. Violet (2)

University of California, Scripps Institute of Oceanography, La Jolla, California

ATTN: Dr. Walter Munk

University of California, Seismographic Station, Berkeley 4, California

ATTN: Professor P. Byerly

Carnegie Institution of Washington, Department of Terrestrial Magnetism, 5241 Broad Branch Road, N. W., Washington, D. C.

ATTN: J. S. Steinhart

Century Geophysical Corporation, P. O. Box C, Admiral Station, Tulsa 15, Oklahoma

ATTN: R. A. Broding

Century Geophysical Corporation, P. O. Box C, Admiral Station, Tulsa 15, Oklahoma

ATTN: J. E. A. T. Woodburn

U. S. Coast and Geodetic Survey, Camp Mercury, Nevada

ATTN: T. H. Pierce

Department of Commerce, Coast and Geodetic Survey, Geophysics Division, Washington 25, D. C.

ATTN: Dr. Dean S. Carder

Department of Commerce, U. S. Coast and Geodetic Survey, Geophysics Division, Washington 25, D. C.

ATTN: Mr. J. Jordan

Department of Commerce, Coast and Geodetic Survey, Geophysics Division, Washington 25, D. C.

ATTN: Mr. Leonard Murphy

Continental Oil Company, P. O. Drawer 293, Ponca City, Oklahoma

ATTN: Dr. John M. Crawford

Defense Atomic Support Agency, Field Command Commander, Sandia Base, Albuquerque, New Mexico

Defense Atomic Support Agency, Headquarters, Washington 25, D. C.

ATTN: John O. Lewis

Dresser Electronics, SIE Division, P. O. Box 32187, Houston 27, Texas

ATTN: Mrs. Mildred Beaman, Librarian (2)

Edgerton, Germeshausen and Grier, Director of Research, 160 Brookline Avenue, Boston, Massachusetts

ATTN: Clyde Dobbie

Edgerton, Germeshausen and Grier, Incorporated, 160 Brookline Avenue, Boston, Massachusetts

ATTN: P. T. Strabala

Electro-Mechanics Company, P. O. Box 8612, Austin 64, Texas

ATTN: Dr. Fred N. Morris

Engineer Research and Development Laboratory, Mines Detection Branch, Fort Belvoir, Virginia

ATTN: Mr. S. E. Dworak

Engineering-Physics Company, 8515 Randolph Street, Rockville, Maryland

ATTN: Mr. Vincent Cushing

General Atronics Corporation, One Bala Avenue, Bala-Cynwyd, Pennsylvania

ATTN: Mr. Joseph T. Underwood, III

General Geophysical Company, 750 Houston Club Building, Houston, Texas

ATTN: Dr. Lewis M. Mott-Smith

Geophysical and Polar Research Center, 8021 South Highland Road, Madison 8, Wisconsin

ATTN: Professor George Woollard, Director

Geophysical Service, Incorporated, P. O. Box 35044, Dallas 35, Texas

ATTN: Dr. Don Saunders

Geotechnical Corporation, WMSO, P. O. Box 2071, Lawton, Oklahoma (2)

Geotechnical Corporation, P. O. Box [illegible], Dallas 26, Texas

ATTN: Dr. W. Heroy, Jr. (10)

Graduate Research Center, P. O. Box 8178, Dallas 5, Texas

ATTN: Dr. Lloyd Berkner (2)

Gulf Research and Development Division, Geophysical Research Division, P. O. Drawer 2038, Pittsburgh 30, Pennsylvania

ATTN: Dr. T. J. O'Donnell, Director

University of Hawaii, Hawaii Institute of Geophysics, Honolulu 14, Hawaii

ATTN: Dr. Doak Cox, Department of Earth Sciences

University of Illinois, Department of Mining, Urbana, Illinois

ATTN: Dr. A. Scheidegger

Department of Interior, Branch of Crustal Studies, U. S. Geological Survey, 7580 West 10th Street, Lakewood 15, Colorado

ATTN: Dr. George Keller

Department of Interior, Branch of Crustal Studies, U. S. Geological Survey, 7580 West 10th Street, Lakewood 15, Colorado

ATTN: Louis C. Pakiser

Department of Interior, U. S. Geological Survey, Denver Federal Center, Denver 25, Colorado

ATTN: Dr. H. Resch

Itek Laboratories, Lexington 73, Massachusetts

ATTN: Mr. Robert Fleming

Jersey Production Research Company, 1133 North Lewis Avenue, Tulsa 10, Oklahoma

ATTN: Mr. P. Jacobson

John Carroll University, Cleveland 18, Ohio

ATTN: Rev. H. F. Birkenhauer, S.J.

John Carroll University, Cleveland 18, Ohio

ATTN: Dr. Edward Walter

Lamont Geological Observatory, Columbia University, Palisades, New York

ATTN: Dr. Maurice Ewing

Lamont Geological Observatory, Columbia University, Palisades, New York

ATTN: Dr. K. L. Hunkins

Lamont Geological Observatory, Columbia University, Palisades, New York

ATTN: Dr. Jack E. Oliver

Massachusetts Institute of Technology, Department of Earth Sciences, Cambridge 39, Massachusetts

ATTN: Professor S. M. Simpson

Melpar, Incorporated, Applied Science Division, 11 Galen Street, Watertown 72, Massachusetts

ATTN: Mrs. Lorraine Massara, Librarian

Melpar, Incorporated, Technical Information Center, 3000 Arlington Boulevard, Falls Church, Virginia

ATTN: P. D. Vashon

University of Minnesota, Institute of Technology, School of Mines and Metallurgy, Minneapolis 14, Minnesota

ATTN: Professor Harold M. Mooney, Geophysics

Mississippi Industrial and Technological Research Commission, P. O. Box 1037, Jackson 5, Mississippi

ATTN: Mr. C. J. McLeod

National Engineering Science Company, 1711 South Fair Oaks, Pasadena, California

ATTN: Dr. S. F. Hook

National Science Foundation, 1951 Constitution Avenue, N. W., Washington, D. C.

ATTN: Dr. Roy E. Hansen

Department of Navy, Office of Naval Research, Washington 25, D. C.

ATTN: James W. Winchester

Navy Electronics Laboratory, U. S. Director, San Diego 52, California

ATTN: Mr. J. McMillen

Navy Radiological Defense Laboratory, Director, San Francisco 24, California

ATTN: Dr. Eugene Cooper

Navy Radiological Defense Laboratory, Hunters Point, Building 815, San Francisco, California

ATTN: Dr. L. Governtsen

Navy Radiological Defense Laboratory, Director, San Francisco 24, California

ATTN: Mr. Ken Shmitt

Oregon State College, Department of Oceanography, Corvallis, Oregon

ATTN: Dr. Joe Berg

Oregon State College, Department of Oceanography, Corvallis, Oregon

ATTN: Dr. P. Dehlinger

The University of Oklahoma, Research Institute, Norman, Oklahoma

ATTN: Dr. Norman Ricker

Pennsylvania State University, Department of Geophysics and Geochemistry, 220 Mineral Sciences Building, University Park, Pennsylvania

ATTN: Dr. B. F. Howell, Jr.

Radio Corporation of America, Camden 2, New Jersey

ATTN: Mr. G. W. K. King

Radio Corporation of America, David Sarnoff Research Center, Princeton, New Jersey

ATTN: Dr. D. S. McCoy

Rand Corporation, The, 1700 Main Street, Santa Monica, California

ATTN: Dr. Richard Latter

Rensselaer Polytechnic Institute, Troy, New York

ATTN: Dr. Samuel Katz

University of Rhode Island, Kingston, Rhode Island

ATTN: Professor Kane

Rice University, Houston 1, Texas

ATTN: Professor J. Cl. DeBremaecker, Department of Geology

Rome Air Development Center, Headquarters, Griffiss AFB, New York

ATTN: 1st Lt. John N. Entsminger, USAF (2)

Sandia Corporation, Division 7000, Sandia Base, Albuquerque, New Mexico

ATTN: Mr. G. A. Fowler

Sandia Corporation, Division 5112, Sandia Base, Albuquerque, New Mexico

ATTN: Mr. M. L. Merritt

Sandia Corporation, Division 7231, Sandia Base, Albuquerque, New Mexico

Sandia Corporation, Sandia Base, Albuquerque, New Mexico

ATTN: William R. Perret

Sandia Corporation, Division 7251, Sandia Base, Albuquerque, New Mexico

ATTN: A. D. Thornbrough

Shell Development Company, P. O. Box 481, Houston 1, Texas

ATTN: Dr. Sidney Kaufman

Southern Methodist University, Department of Geology, Dallas, Texas

ATTN: Dr. Eugene T. Morris

Space-General Corporation, 777 Flower Street, Glendale 1, California

ATTN: Mr. A. P. Albrecht

Space-General Corporation, 777 Flower Street, Glendale 1, California

ATTN: Dr. Glenn L. Brown

Space-General Corporation, 777 Flower Street, Glendale 1, California

ATTN: Dr. R. N. Ghose

Stanford Research Institute, Menlo Park, California

ATTN: C. M. Ablow

Stanford Research Institute, Menlo Park, California

ATTN: Dr. David Bernstein

Stanford Research Institute, Menlo Park, California

ATTN: Dr. George E. Duvall

Stanford Research Institute, Poulter Laboratories, Menlo Park, California

ATTN: Dr. John O. Erkman

Stanford Research Institute, Menlo Park, California

ATTN: Dr. Richard M. Fosco

Stanford Research Institute, Menlo Park, California

ATTN: F. R. Grine

Stanford Research Institute, Palo Alto, California

ATTN: Dr. Allen Peterson

Stanford Research Institute, Poulter Laboratories, Menlo Park, California

ATTN: Dr. Thomas C. Poulter, Director

Stanford Research Institute, Menlo Park, California

ATTN: L. M. Swift

Stanford Research Institute, Building 108, Menlo Park, California

ATTN: Dr. Robert B. Valle, Jr., Director, Physics Division

Stanford University, High Energy Physics Laboratory, Stanford, California

ATTN: Dr. Wolfgang K. H. Panofsky

St. Louis University, The Institute of Technology, 3621 Olive Street, St. Louis 8, Missouri

ATTN: Dr. Carl Kissinger

St. Louis University, The Institute of Technology, 3621 Olive Street, St. Louis 8, Missouri

ATTN: Dr. S. R. Heinrich

St. Louis University, Department of Geophysics, 3621 Olive Street, St. Louis 8, Missouri

ATTN: Dr. William Stauder, S.J.

Texas Instruments Incorporated, P. O. Box 5474, Dallas 35, Texas

ATTN: R. A. Arnett (7)

University of Texas, Austin 12, Texas

ATTN: Professor W. T. Muehlberger, Department of Geology

United Earth Sciences Division, P. O. Box 344, Alexandria, Virginia

ATTN: Mr. F. B. Coker (5)

United ElectroDynamics, Incorporated, 200 Allendale Road, Pasadena California

ATTN: Mrs. Dorothy A. Allen (1)

United ElectroDynamics, Incorporated, 200 Allendale Road, Pasadena, California

ATTN: C. B. Forbes

United ElectroDynamics, Incorporated, 200 Allendale Road, Pasadena, California

ATTN: Mr. Allen M. Rugg, Jr.

U. S. Geological Survey, 345 Middlefield Road, Menlo Park, California

ATTN: Librarian

University of Utah, Department of Geophysics, Mines Building, Salt Lake City, Utah

ATTN: Professor Ken Cook

Weston Observatory, Weston 93, Massachusetts

ATTN: Reverend Daniel Linehan, S.J.

University of Wisconsin, Geophysics and Polar Research Center, 21344 University Avenue, Madison 5, Wisconsin

Xavier University, Cincinnati 7, Ohio

ATTN: Reverend E. A. Bradley, S.J.

Adam, 16 Rue Claude Bernard, Paris V, France

ATTN: Professor Y. Rocard

Arctic Institute of North America, 3458 Redpath Street, Montreal 25, P. Q., Canada

ATTN: Mr. John C. Reed, Executive Director

Jean Lebel, Alpena, 16 Rue Claude Bernard, Paris V, France

University of Saskatchewan, Saskatoon, Saskatchewan, Canada

ATTN: Dr. James Mawdsley

Seismological Laboratory, Uppsala, Sweden

ATTN: Dr. Markus Båth

University of Toronto, Department of Physics, Toronto 5, Canada

ATTN: Professor J. T. Wilson (2)

Weismann Institute of Science, P. O. Box 26, Rehovoth, Israel

ATTN: Professor C. L. Pekeris

University of Witwatersrand, Institute of Bernard Price, Geophysical Research, Johannesburg, South Africa

ATTN: Dr. A. L. Hales

Advanced Research Projects Agency
The Pentagon, Washington 25, D. C. (5

Advanced Research Projects Agency
The Pentagon, Washington 25, D. C.
ATTN: Mr. Russell Baird

Advanced Research Projects Agency
The Pentagon, Washington 25, D. C.
ATTN: Mr. R. Black

Advanced Research Projects Agency
The Pentagon, Washington 25, D. C.
ATTN: Mr. Donald Clements

Advanced Research Projects Agency
The Pentagon, Washington 25, D. C.
ATTN: Mr. Maj. R. Harris

Advanced Research Projects Agency
The Pentagon, Washington 25, D. C.
ATTN: Dr. Jack Ruina

AD Div. 2/10

Inst. of Science and Technology, U. of Mich., Ann Arbor THE GENERATION OF THE PRIMARY SEISMIC SIGNAL BY A CONTAINED EXPLOSION by Carl Kisslinger. VESIAC State-of-the-Art report. Apr. 63. 81 p. incl. illus., tables, 81 refs., bibl.
(Rept. no. 4410-48-X)
(Contract SD-78) Unclassified report

In order to analyze the mechanism by which buried explosions generate seismic waves, the region around the detonation is divided into three zones: (1) a strong-shock (hydrodynamic) zone, (2) a transitional, nonlinear zone, and (3) the elastic region. Experimental equation-of-state data are used in calculating the history of the propagating stress wave. The theory of shock waves in a fluid is applicable to the close-in region, and several failure mechanisms have been postulated for the transition region.

(over)

UNCLASSIFIED

I. Title: VESIAC
II. Kisslinger, Carl
III. Advanced Research Project Agency
IV. Contract SD-78

Armed Services Technical Information Agency
UNCLASSIFIED

AD Div. 2/10

Inst. of Science and Technology, U. of Mich., Ann Arbor THE GENERATION OF THE PRIMARY SEISMIC SIGNAL BY A CONTAINED EXPLOSION by Carl Kisslinger. VESIAC State-of-the-Art report. Apr. 63. 81 p. incl. illus., tables, 81 refs., bibl.
(Rept. no. 4410-48-X)
(Contract SD-78) Unclassified report

In order to analyze the mechanism by which buried explosions generate seismic waves, the region around the detonation is divided into three zones: (1) a strong-shock (hydrodynamic) zone, (2) a transitional, nonlinear zone, and (3) the elastic region. Experimental equation-of-state data are used in calculating the history of the propagating stress wave. The theory of shock waves in a fluid is applicable to the close-in region, and several failure mechanisms have been postulated for the transition region.

(over)

UNCLASSIFIED

I. Title: VESIAC
II. Kisslinger, Carl
III. Advanced Research Project Agency
IV. Contract SD-78

Armed Services Technical Information Agency
UNCLASSIFIED

AD Div. 2/10

Inst. of Science and Technology, U. of Mich., Ann Arbor THE GENERATION OF THE PRIMARY SEISMIC SIGNAL BY A CONTAINED EXPLOSION by Carl Kisslinger. VESIAC State-of-the-Art report. Apr. 63. 81 p. incl. illus., tables, 81 refs., bibl.
(Rept. no. 4410-48-X)
(Contract SD-78) Unclassified report

In order to analyze the mechanism by which buried explosions generate seismic waves, the region around the detonation is divided into three zones: (1) a strong-shock (hydrodynamic) zone, (2) a transitional, nonlinear zone, and (3) the elastic region. Experimental equation-of-state data are used in calculating the history of the propagating stress wave. The theory of shock waves in a fluid is applicable to the close-in region, and several failure mechanisms have been postulated for the transition region.

(over)

UNCLASSIFIED

I. Title: VESIAC
II. Kisslinger, Carl
III. Advanced Research Project Agency
IV. Contract SD-78

Armed Services Technical Information Agency
UNCLASSIFIED

AD Div. 2/10

Inst. of Science and Technology, U. of Mich., Ann Arbor THE GENERATION OF THE PRIMARY SEISMIC SIGNAL BY A CONTAINED EXPLOSION by Carl Kisslinger. VESIAC State-of-the-Art report. Apr. 63. 81 p. incl. illus., tables, 81 refs., bibl.
(Rept. no. 4410-48-X)
(Contract SD-78) Unclassified report

In order to analyze the mechanism by which buried explosions generate seismic waves, the region around the detonation is divided into three zones: (1) a strong-shock (hydrodynamic) zone, (2) a transitional, nonlinear zone, and (3) the elastic region. Experimental equation-of-state data are used in calculating the history of the propagating stress wave. The theory of shock waves in a fluid is applicable to the close-in region, and several failure mechanisms have been postulated for the transition region.

(over)

UNCLASSIFIED

I. Title: VESIAC
II. Kisslinger, Carl
III. Advanced Research Project Agency
IV. Contract SD-78

Armed Services Technical Information Agency
UNCLASSIFIED

AD

The objective of the analysis is the determination of the stress waveform at the inner boundary of elastic behavior. The peak amplitude and spectral content depend on the yield, the type of medium, and the ambient stress (depth of burial). The experimental determination of the shortest range at which elastic behavior begins is difficult in principle, because solutions valid at great distances are not applicable.

Experimental determinations of the amplitude-yield relationship must take into account (1) the combined effect of the shift of the spectral peak to lower frequencies as the yield increases and (2) the low-pass filtering properties of the earth. Empirical studies of the effect of the shot-point medium are influenced by the properties of the explosive material. The effect of source depth is difficult to isolate because in most test sites the medium changes with depth.

UNCLASSIFIED

DESCRIPTORS

Explosion effects
Shock waves
Underground explosions
Seismic waves
Seismology

UNCLASSIFIED

AD

The objective of the analysis is the determination of the stress waveform at the inner boundary of elastic behavior. The peak amplitude and spectral content depend on the yield, the type of medium, and the ambient stress (depth of burial). The experimental determination of the shortest range at which elastic behavior begins is difficult in principle, because solutions valid at great distances are not applicable.

Experimental determinations of the amplitude-yield relationship must take into account (1) the combined effect of the shift of the spectral peak to lower frequencies as the yield increases and (2) the low-pass filtering properties of the earth. Empirical studies of the effect of the shot-point medium are influenced by the properties of the explosive material. The effect of source depth is difficult to isolate because in most test sites the medium changes with depth.

UNCLASSIFIED

DESCRIPTORS

Explosion effects
Shock waves
Underground explosions
Seismic waves
Seismology

UNCLASSIFIED